A review on overcoming challenges and pioneering advances

MXene-based materials for energy storage applications

Jangra, Sahil; Kumar, Bhushan; Sharma, Jaishree; Sengupta, Shilpi; Das, Subhankar; Brajpuriya, R. K.; Ohlan, Anil; Mishra, Yogendra Kumar; Goyat, M. S.

Go to publication entry in University of Southern Denmark's Research Portal

Download date: 10. Jan. 2025

Review article

A review on overcoming challenges and pioneering advances: MXene-based materials for energy storage applications

Sahil Jangra [a], Bhushan Kumar [b], Jaishree Sharma [a], Shilpi Sengupta [c], Subhankar Das [b,*],
R.K. Brajpuriya [a], Anil Ohlan [d], Yogendra Kumar Mishra [e], M.S. Goyat [a,e,**]

[a] Department of Applied Science, School of Advanced Engineering, UPES, Dehradun 248007, India
[b] Department of Mechanical Engineering, School of Advanced Engineering, UPES, Dehradun 248007, India
[c] Electrochemical Energy Storage Laboratory, Department of Chemistry, SRM Institute of Science and Technology, Tamil Nadu 603203, India
[d] Department of Physics, Maharshi Dayanand University, Rohtak 124001, India
[e] Mads Clausen Institute, NanoSYD, University of Southern Denmark (SDU), Denmark

A R T I C L E I N F O

Keywords:
Energy storage
MXene
Composites
Supercapacitors
Batteries

A B S T R A C T

Two-dimensional (2D) MXene-based materials have attracted considerable attention because of their distinctive physical and chemical properties, rendering them relevant in diverse domains like energy storage, catalysis, sensing, electronics and environmental remediation. Over the years, numerous high-quality review papers on MXene have been published, highlighting its synthesis methods, properties, and applications. However, there is hardly any review paper available on systematic study of synthesis-structure-mechanism-application-expansion aspects of MXene. The current review article provides an in-depth investigation of most used synthesis approaches of MXenes, structural, stability, electrical, hydrophilic and mechanical properties. Additionally, applications of MXenes as supercapacitors and electrode materials for batteries are covered in this article. However, MXenes have some limitations such as restacking, oxidation, and others which results in their low electrochemical performance. To overcome such limitations, various materials such as carbon, metal oxides, and conducting polymers were incorporated into the MXenes layers to improve their electrochemical performance. The article also addresses the challenges and potential solutions for MXene based materials for energy storage applications. Overall, the article provides valuable insights and various opportunities in supercapacitors and batteries to novices and the research community.

1. Introduction

Energy is fundamental to the growth of human civilization, yet fossil fuel-based energy production has significant negative impacts on the global economy and environment [1]. The depletion of fossil fuels and the escalating issues of climate change are major global concerns. To address the growing energy demand, it is crucial to develop sustainable, efficient, and affordable energy production and storage technologies. Unlike geothermal energy, which is location-specific, tidal power and wave energy are more predictable and abundant due to their reliance on constant flows [2]. However, the collection and transmission of energy from these sources present significant challenges. Renewable energy sources like wind and solar are often inconsistent, but energy storage technologies can capture excess energy during favourable conditions for

later use [3]. Researchers are thus focused on developing efficient energy storage systems with high capacities and excellent cyclic performance. Advanced supercapacitors and batteries are expected to become essential power sources in daily life, powering portable electronic devices such as smartphones, laptops, and cameras. They will also enhance the capabilities of hybrid and plug-in hybrid vehicles and facilitate the development of smart grid systems [4–8]. This ongoing research is crucial for building a sustainable energy future.

Commercially available materials have so far failed to fully meet the demanding requirements of supercapacitors and batteries, particularly in achieving both high energy density and high-power density [9]. Activated carbon (AC) is widely used in commercial supercapacitors due to its straightforward synthesis process, cost-effectiveness, porous structure with a high surface area, reasonable electrical conductivity,

and satisfactory electrochemical stability [10]. However, the high contact resistance and slow ion transport associated with AC result in inadequate capacitances and low energy densities. Similarly, graphite, which is used as the anode material in commercial lithium-ion batteries (LIBs), has a limited theoretical capacity of 372 mAh·g^{-1} and a working potential of 0.05 V vs Li$^+$/Li. These limitations hinder the development of high-energy-density LIBs [11–13]. Therefore, there is a pressing need for new materials and innovative approaches to overcome these challenges and enhance the performance of energy storage systems.

Recently, two-dimensional (2D) materials have attracted significant attention from researchers worldwide because of their exceptional electrical and electronic properties, which distinguish them from their bulk counterparts [14]. Currently, graphene is the most extensively studied 2D material, celebrated for its remarkable mechanical stability, high intrinsic mobility, and excellent electrical conductivity [15]. These properties make graphene an ideal candidate for flexible electronics, energy conversion, and storage devices. In addition to graphene, there has been substantial research on other 2D materials over the past few years, including transition metal dichalcogenides (TMDs), hexagonal boron nitride and phosphorene [16–18]. These materials are also being explored for their potential in various advanced technological applications due to their unique properties.

MXenes, a novel family of 2D early transition metal carbides and/or nitrides, were discovered nearly a decade ago by Yury Gogotsi and colleagues at Drexel University in the United States [19]. The chemical formula for MXenes is $M_{n+1}X_nT_x$, where M signifying an early transition metal, X denoting carbon and/or nitrogen, and Tx representing surface functional groups like —O, -OH, —F, or —Cl (Fig. 1a) [20–22]. MXenes are synthesized through the chemical etching of the A element from their 3D precursor, known as the MAX phase [23,24]. In the MAX phase, M-X bonds are significantly stronger than M-A bonds. A schematic diagram illustrating the structure of both the MAX phase and MXene is shown in Fig. 1(b). Despite many synthesis routes have been developed since the first inception of MXene, the synthesis of MXene is generally more expensive than other 2D materials due to complex and hazardous etching processes. Researchers are actively working on making MXene synthesis more economical by exploring alternative less expensive etching methods that reduce or eliminate the need for hazardous

Fig. 1. (a) MAX phases comprise the elements of $M_{n+1}AX_n$ shown in periodic table; (b) structure of MAX phases and associated MXenes; (c) the number of journal publications concerning MXenes for supercapacitor and battery applications, identified through keyword searches "MXene Supercapacitor" and "MXene battery". Source: (http://apps.webofknowledge.com, 2015 to 2023). (a) Reprinted with permission from Ref. [20], Ceramics International, © 2019 Elsevier. (b) Reprinted with permission from Ref. [41], Advanced materials, Copyright © 2014, Wiley-VCH).

chemicals like HF acid [25]. Researchers are also investigating scalable production techniques, such as using milder etchants and optimizing the synthesis process to reduce waste and energy consumption. Additionally, efforts are being made to find more cost-effective raw materials and to improve the efficiency of post-synthesis treatments, all aimed at lowering the overall production cost while maintaining the quality and properties of MXenes [26].

The most prominent characteristics of MXenes are, metal like conductivity, notable theoretical capacities (e.g., approximately 448 mAh·g^{-1} for single layered Ti_3C_2 MXene in lithium storage) [11], high mechanical strength, numerous redox reaction, high metallic conductivity (around 25,000 S·m^{-1}) and tunable hydrophilicity. Due to these outstanding properties, MXenes have demonstrated substantial potential in various applications, including electrochemical energy storage

[27–32], electromagnetic shielding [33,34], sensors [35–37], biomedical applications [38], and photocatalysis dye degradation [39]. Over the past, MXenes, have gained significant interest in both supercapacitors and batteries, as illustrated by the annual publication figures depicted in Fig. 1(c).

Fig. 2(a) shows the annual growth of publications, highlighting the progressive establishment of MXene-based energy storage research. Numerous studies on MXenes in this field have been published. The research landscape can be visualized using VOSviewer, a free tool for constructing bibliometric networks. Relevant keywords significantly impact document search efficacy. Our keyword analysis identified MXene, performance, and nanosheets as the top keywords. Fig. 2(b) illustrates a network of keyword occurrences.

This review article provides a systematic investigation of MXene-

Fig. 2. (a) Number of Publications on topic "MXene energy storage". Source: (http://apps.webofknowledge.com) (data accessed on 18 Sept. 2023). (b) An illustration of co-occurrence of keywords.

based materials for energy storage application. It covers diverse synthesis approaches, and a variety of properties like structural stability, electronic characteristics, hydrophilicity, and mechanical strength. This review article majorly focused on the MXenes based materials for rechargeable batteries and supercapacitors, leveraging their remarkable electrochemical performance driven by large surface area, high electrical conductivity, and interlayer spacing for efficient charge storage and fast ion diffusion. However, MXenes have some limitations such as restacking, oxidation, and others which results in their low electrochemical performance. To overcome such limitations, various materials such as carbon, metal oxides, and conducting polymers were incorporated into the MXenes layers to improve their electrochemical performance. Furthermore, a bibliometric analysis from 2012 to 2023 was conducted using VOSviewer software to reveal the trends in MXene-based energy storage globally. The bibliometric analysis offered insights into collaborative research patterns and prospects. Opportunities and challenges in MXene-based energy storage solutions are discussed, alongside strategies for improving stability, scalability, and performance. Overall, the review serves as a comprehensive guide for future research directions to address energy and sustainability challenges.
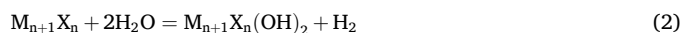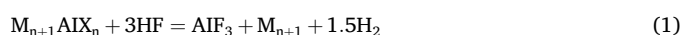
2. Most commonly used techniques for synthesis of MXene

The first MXene ($Ti_3C_2T_x$) was discovered in 2011 through the selective removal of aluminum from Ti_3AlC_2 using aqueous HF at room temperature, which led to the substitution of aluminum atoms with oxygen, hydroxyl, and/or fluorine atoms [42]. Following this discovery, researchers sought alternative synthesis methods to reduce the risks associated with HF. Various techniques have been developed to produce MXenes, including fluoride-salt etching, molten salt etching, fluoride-free etching, electrochemical etching, chemical vapor deposition (CVD), and the template method, as shown in Fig. 3 [43]. These techniques can be broadly categorized into two groups: top-down and bottom-up approaches. Top-down synthesis methods involve breaking down bulk materials into nanoscale structures through mechanical, chemical, or thermal processes, such as HF etching, fluoride-salt etching, which serves as a safer alternative to HF, molten salt etching, which occurs at high temperatures and can produce distinct structural and surface properties, and fluoride-free etching, which eliminates the use of fluoride entirely, reducing potential hazards [44–46]. These methods allow for precise control over the size, shape, and surface characteristics of MXenes, making them ideal for applications in energy storage, catalysis, and electronics. Conversely, bottom-up synthesis methods involve assembling nanomaterials from atomic or molecular precursors,

allowing for the construction of MXenes with tailored properties for specialized applications [47]. Methods like chemical vapor deposition (CVD), where gaseous precursors react or decompose on a substrate to form thin films or nanostructures, and the template method, which uses pre-existing templates to guide the assembly of MXene layers or structures, are key examples of this approach [48,49]. Both approaches are crucial for MXene synthesis, with each offering unique advantages depending on the desired application. Moving forward, efforts should focus on optimizing these methods to enhance the stability, environmental friendliness, cost-effectiveness, scalability, simplicity, and quality of MXene production.

2.1. HF etching

HF etching is commonly carried out by incorporating MAX into a solution of hydrofluoric acid while maintaining continuous agitation [50]. Following this step, the resulting mixture requires multiple wash with deionized water until its pH stabilizes within the range of 6–7. The residual products (AlF_3) and water undergo reactions with additional MXenes, resulting in the formation of termination groups such as —F, -OH, and —O. The following reactions (1)–(3) are involved for the synthesis of MXenes using HF etching [51].

$$M_{n+1}AIX_n + 3HF = AIF_3 + M_{n+1} + 1.5H_2 \qquad (1)$$

$$M_{n+1}X_n + 2H_2O = M_{n+1}X_n(OH)_2 + H_2 \qquad (2)$$

$$M_{n+1}X_n + 2HF = M_{n+1}X_nF_2 + H_2 \qquad (3)$$

HF etching method is considered especially when synthesis of MXenes needed at low or even room temperature. This type of etching often endorsed for its simplicity and ease of implementation. However, fully fluorine terminated MXenes exhibit significant resistance to oxidation and thereby offers better stability compared to the MXenes with other terminated groups. Furthermore, HF aqueous etching provides various advantages, including the complete removal of the Al layer from the MAX phase and improvements in morphology and yield [52,53]. Because of these benefits, researchers predominantly employed this approach to produce of MXenes and their derivatives. The duration of etching also varies depending on the type of Metal (M) atom. The M atom possessing a greater number of valence electrons needs more robust etching. For instance, Nb_2AlC demands a stirring time three times longer than $Ti_3C_2T_x$ [54].

While HF etching of MXenes produces better results compared to alternative chemical synthesis methods, but it poses significant hazards
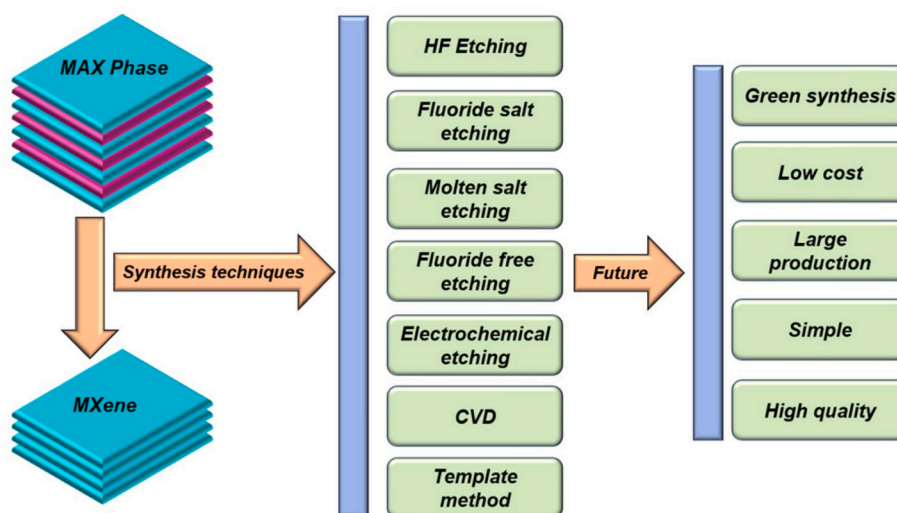

Fig. 3. An illustration depicting various typical techniques for producing MXenes.

due to highly toxic and corrosive properties of HF. Additionally, HF etching generates H_2 gas as a byproduct, which is highly flammable and can readily disperse into the surrounding environment. The synthesis of MXene Ti_3C_2 from MAX Phase Ti_3AlC_2 using HF etching treatment is shown in Fig. 4(a) [51]. SEM images of MAX phase Ti_3AlC_2 (Fig. 4b) and MXenes after HF treatment shows layered structure of MXene are depicted in (Fig. 4c) [51].

Theoretically, elevated temperatures and higher concentrations of HF are advantageous for MXene synthesis [55]. Various literature reports indicate that Ti_3C_2 MXene can be synthesized using different reaction times of HF etching such as 2 h [56], 24 h [57], 72 h [58]. However, the reaction for 2 h duration was found inefficient for complete exfoliation of Ti_3AlC_2. But, the increase in reaction processing time up to 24 h duration leads to the complete exfoliation of Ti_3AlC_2 and its transformation into MXene [59].

However, due to corrosive and toxic nature of HF, its direct utilization is constrained. MXenes fabricated through this process typically exhibit elevated fluorine levels, which present challenges, particularly in photocatalytic reactions and biomedical applications. Such disadvantages forced the researchers to find alternative safe and less hazardous methods [60].

2.2. Fluoride salts etching

Comparatively safer alternative to HF etching has been devised by the researchers and named as Fluoride salts etching [61]. Acid/fluoride salt etching serves as an in-situ HF etching, offering the benefit of reduced chemical hazards and energy consumption during the etching process. This method utilizes an etchant comprising a fluoride salt solution (such as LiF, NH_4F, KF or NaF) and HCl for the synthesis of MXene [62]. The synthesis can be elucidated by the following reactions (4) and (5) [63]:

$$LiF + HCl = HF + LiCl \tag{4}$$

$$NH_4F + H_2O = NH_3 \cdot H_2O + HF \tag{5}$$

The synthesis of MXene utilizing HCl-LiF etching is depicted in Fig. 4 (d) [64]. Various studies have illustrated the preparation of MXenes, such as $Ti_3C_2T_x$ films [24] and Mo_2CT_x [65] nanosheets, through the reaction between MAX Phase materials like Ti_3AlC_2 and Mo_2Ga_2C, and LiF-HCl etchants, resulting in MXenes with low defects.

In another study, Ti_3C_2 MXene was synthesized through the etching of Ti_3AlC_2 MAX Phase using various fluoride salts in a hydrochloric acid (HCl) solution. Optimal conditions for preparing Ti_3C_2 MXene using a 4 mol/L etching solution were identified as follows: 24 h at 50 °C using LiF, 48 h at 40 °C using NaF, 48 h at 40 °C using KF, and 24 h at 30 °C using NH_4F [66].

Although fluoride-based etching of MXene offers certain advantages, it poses significant hazards due to its potential toxicity and corrosivity, and it can adversely affect the specific capacitance in supercapacitors
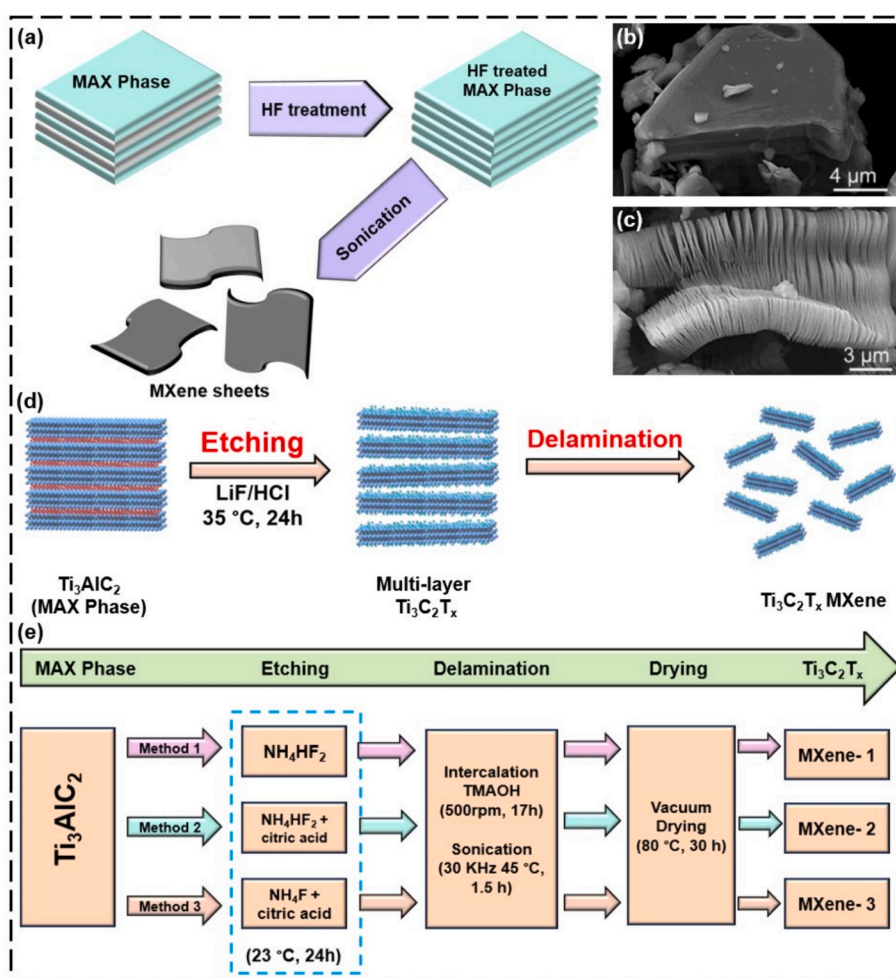

Fig. 4. (a) Illustration of the exfoliation process of MAX phases leading to the formation of MXenes. SEM images (b) Ti_3AlC_2 (MAX Phase), (c) Ti_3C_2 MXene, (d) synthesis $Ti_3C_2T_x$ MXene nanosheets using In-situ HF etching, (e) synthesis of $Ti_3C_2T_x$ MXenes utilizing fluorinated salts.
(a–c) (Reprinted with permission from Ref. [51], ACS Nano, © 2012 American Chemical Society). (d) (Reprinted with permission from Ref. [64], ACS Nano, © 2021 American Chemical Society). (e) (Reprinted with permission from Ref. [69], FlatChem, © 2023 Elsevier).

[67]. Moreover, this method may induce structural damage, compromising the integrity of the MXene layers. The process also fails to eliminate grain boundaries in the MAX phase, leaving behind residual MAX phase particles and unetched MXenes, which leads to a low yield [68].

Over the years, various salts have been explored to enhance the yield of MXene, including bifluoride salts such as NH_4HF_2, $NaHF_2$, and KHF_2. These milder etchants offer a safer approach for the synthesis of MXenes. NH_4HF_2 is commonly utilized for etching Ti_3AlC_2 powder to produce $Ti_3C_2T_x$ MXene using a range of temperature starting from room temperature to elevated temperatures for different duration in hours. The synthesis of $Ti_3C_2T_x$ MXenes using NH_4HF_2, NH_4HF_2 and citric acid combination, and NH_4F with citric acid is illustrated in Fig. 4(e) [69]. Table 1 outlines the various synthesis methods for MXene and its applications in various energy storage systems.

In situ HF etching significantly enhances MXene quality, facilitating the production of high-conductivity MXene films of any size, which are ideal for energy storage applications. This technique enables the creation of MXene ink that can be directly deposited onto substrates without the need for sonication for delamination. It produces large quantities of MXene with minimal energy consumption [71]. Additionally, introducing metal cations between MXene layers increases interlayer spacing and aids in separation. This approach improves reaction stability, surface area, and the number of redox-active sites, allowing for direct delamination through fluoride ion intercalation [60].

2.3. Molten salt etching

The molten salt method is a novel and efficient approach that addresses many of the challenges associated with MXene synthesis. In this technique, a MAX phase precursor is treated with molten salt at elevated temperatures for a shorter duration, enabling the production of MXenes with tunable surface groups and inter-layer spacing [72]. The molten salt selectively removes specific elements from the precursor, resulting in the formation of MXene layers. Compared to traditional fluoride-based etching, this method offers several advantages, including higher purity MXenes and the avoidance of hazardous fluoride compounds, making it both safer and more environmentally friendly [73,74]. MXenes can also be synthesized through high temperature etching of MAX phases. For instance, a recent experiment demonstrated that treating Ti_4AlN_3 MAX phase in a molten fluoride salt mixture at 550 °C within an argon atmosphere successfully produced Ti_4N_3Tx MXene [75]. In another study, the Ti_3AlC_2 MAX phase was combined with HCl and LiF solutions, then heated at 400 °C for approximately 45 h, followed by washing to adjust the pH. This process yielded a clay-like paste that could be formed into an expandable film with enhanced volumetric conductivity. Consequently, the molten-salt etching technique for MXene synthesis is a promising approach, offering significant potential for the development of new technologies and their diverse applications [76]. However, it also has limitations, including the requirement for high operational temperatures, which can be energy-intensive and risk degrading the MXene structure. Additionally, achieving uniform and consistent etching is challenging, potentially leading to non-uniform material properties, and the scalability of the method is complex due to the need for maintaining uniform temperature and salt composition over large-scale reactions. Disposal of used salts and environmental impact are also critical concerns [77].

2.4. Fluoride-free etching process

The fluoride-free etching process for MXene synthesis is needed to avoid the high toxicity and environmental hazards of fluoride salts, resulting in a safer, more environmentally friendly production of MXenes with potentially fewer structural defects [78]. Traditional

Table 1
A summary of synthesis routes and applications of MXene in energy storage domain.

MAX phase	Materials	Synthesis approach	Morphology of MXene	Application	Ref.
Ti_3AlC_2	$Ti_3C_2T_x$	HF etching	Single layer	SCs	[105]
$(Mo_{2/3}Sc_{1/3})_2AlC$	$Mo_{1.3}CT_x$	HF etching	Nanosheets	SCs	[106]
Ta_4AlC_3	$Ta_4C_3T_x$	HF etching	Layered morphology	SCs	[107]
Ti_2AlC	Ti_2CT_x	HF etching	Nanosheets	Symmetric SCs	[108]
Ti_3AlC_2	$Ti_3C_2T_x$	HCl + LiF etching	Nanosheets	Flexible SCs	[109]
V_2AlC	ZrO_2-V_2CT_x	Hydrothermal method	Nanosheets	SCs	[110]
Ti_3AlC_2	$Ti_3C_2T_x$MXene/carbon nanofiber	Electrospinning	Single layer	SCs	[111]
Ti_3AlC_2	Zn@ Ti_3C_2	Deposition	Multilayer	SCs	[112]
Ti_3AlC_2	$Ti_3C_2T_x$/CNTs	Electrostatic self-assembly	Single layer	SCs	[113]
Ti_3AlC_2	Ti_3C_2/AgNWs	Vacuum-assisted filtration	Single layer	SCs	[114]
Ti_3AlC_2	$Ti_3C_2T_x$ -rGO	Electrostatic self-assembly	Single layer	SCs	[115]
Ti_3AlC_2	MoS_2/$Ti_3C_2T_x$	Hydrothermal method	Single layer	SCs	[116]
Ti_3AlC_2	$Ti_3C_2T_x$	Hydrothermal method	Single layer	Flexible SCs	[117]
Ti_3AlC_2	$NiCo_2Se_4$/MXene	Hydrothermal method	Single layer	SCs	[118]
Ti_3AlC_2	MXene/carbon dots	Evaporate and vacuum drying	Nanosheets	SCs	[119]
Ti_3AlC_2	MXene-CNT/PANI	Electrophoretic deposition	Nanosheets	SCs	[120]
Ti_3AlC_2	MXene/rGO aerogels	Self-assembly	Nanoflakes	SCs	[121]
Ti_2AlC	Ti_2C/activated carbon	HF etching	Nanosheets	SCs	[122]
Ti_3AlC_2	MXene/$MoSe_2$	Hydrothermal method	Nanosheets	Asymmetric SCs	[123]
Ti_3AlC_2	$Ti_3C_2T_x$//activated carbon	HCl + LiF etching	Accordion-like layered structure	Micro- SCs	[124]
Ti_3AlC_2	Ti_3C_2/graphene	Wet-spinning process	Nanosheets	Flexible SCs	[125]
V_2AlC	V_2CT_x	HF etching	Layered morphology	Li-ion battery	[126]
Nb_2AlC	Nb_2CT_x	HF etching	Layered morphology	Li-ion battery	[126]
Nb_4AlC_3	$Nb_4C_3T_x$	HF etching	Multilayered	Li-ion battery	[127]
Nb_2AlC	Nb_2CT_x	Hydrothermal etching	Nanosheets	Li-ion battery	[128]
Ti_3AlC_2	MXene/Ag	Self-reduction	Multilayer	Li-ion battery	[129]
Ti_3AlC_2	Ti_3C_2/graphene oxide	Freeze-drying	Single layer	Li-ion battery	[130]
Ti_3AlC_2	LTO (lithiophilic)/Ti_3C_2	Electrochemical deposition	Multilayer	Li-ion battery	[131]
Ti_3AlC_2	Sb_2O_3/$Ti_3C_2T_x$	Facile solution-phase method	Few-layered	Na-ion battery	[123]
Ti_3AlC_2	PANI/$Ti_3C_2T_x$	Electrostatic self-assembly	Single layer	Na-ion battery	[132]
Ti_3AlC_2	$Ti_3C_2T_x$ (nanodots)/P (red phosphorous)	Ball milling	Quantum dot	Na-ion battery	[133]
Ti_3AlC_2	$Ti_3C_2T_x$ nanodots	Hydrothermal method	Quantum dot	Li–S battery	[134]
Ti_3AlC_2	Ti_3C_2 nanoribbon	Alkali treatment	Nanoribbon	Li–S battery	[135]
Ti_3AlC_2	h-Ti_3C_2/CNTs	Alkali treatment	Nanoribbon	Na-O_2 batteries	[136]

methods often result in the attachment of numerous fluorine groups to MXene surfaces, which negatively impacts their electrochemical performance [79]. To overcome these challenges, various approaches have been developed to eliminate the use of fluoride ions in MXene fabrication. Efforts are also being made to expand the range of MAX precursors to fully exploit the potential of MXenes. Consequently, researchers are focusing on developing fluorine-free methods for MXene synthesis. Alternative methods such as molten salt Lewis acid etching, electrochemical etching, chemical vapor deposition (CVD), and the template method have been proposed to synthesize MXenes without using fluorine [46].

2.4.1. Etching via molten salt Lewis's acid

The discovery of molten salt Lewis acidic etching marks a significant breakthrough, providing a fluorine-free method that enables etching from a wide variety of MAX precursors and allows for the modification of MXene surface chemistry [81,82].

For instance, Ti_3ZnC_2 MXene was synthesized by etching of Ti_3AlC_2 with $ZnCl_2$ molten salt at 550 °C under N_2 atmosphere. During this process, Zn^{2+} ions interact with the aluminum layers and fill the aluminum atom sites within Ti_3AlC_2 and yields Ti_3ZnC_2. However, Ti_3ZnC_2 can be converted into $Ti_3C_2Cl_2$ MXene by introducing additional $ZnCl_2$ molten salt. Such methodology can be extended to other precursor materials such as Ti_2AlC, Ti_2AlN, and V_2AlC, with a similar synthesis mechanism [81]:

$$Ti_3AlC_2 + 1.5ZnCl_2 = Ti_3ZnC_2 + 0.5\,Zn + AlCl_3 \tag{6}$$

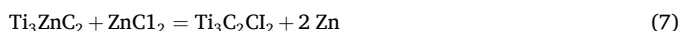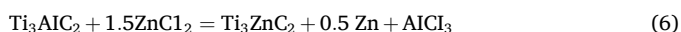$$Ti_3ZnC_2 + ZnCl_2 = Ti_3C_2Cl_2 + 2\,Zn \tag{7}$$

Fig. 5(a) depicts a graphical depiction of the molten salt Lewis's acid synthesis procedure. Once the reaction concluded, the resultant product underwent purification using deionized water to remove residual salts. Furthermore, the product was subjected to treatment with HCl to eliminate the Zn particles from the MXene [81].

There are tremendous possibilities for creating tailored termination groups for MXenes through substitution and elimination reactions [84]. For instance, using $CdBr_2$ as a Lewis acid, the etching of MAX phase produces MXenes with Br termination groups. These terminations can undergo surface exchange reactions with various halide ions and functional groups like –NH, —S, —Se, and —Te and thereby enhancing MXene properties beyond structural and chemical modifications [85]. This synthesis method facilitates the investigation of MXene characteristics, particularly based on the termination groups.

2.4.2. Electrochemical etching

Electrochemical etching is an efficient method for producing fluoride-free MXenes, where a potential difference is applied between an MXene sample and a counter/reference electrode submerged in an electrolyte solution, as illustrated in Fig. 5(b) [83].

This technique allows for precise control over parameters such as voltage, current, time, and temperature. Electrochemical etching enables the selective removal of specific MXene layers, resulting in tailored properties [86]. By applying an electric field to the MXene surface, ions are prompted to intercalate and modify the surface chemistry, which can enhance charge storage capacity and electrode performance [87,88].

The process involves adjusting the electrochemical potential of MXene and is adaptable to various electrolytes. For example, the Ti_2AlC
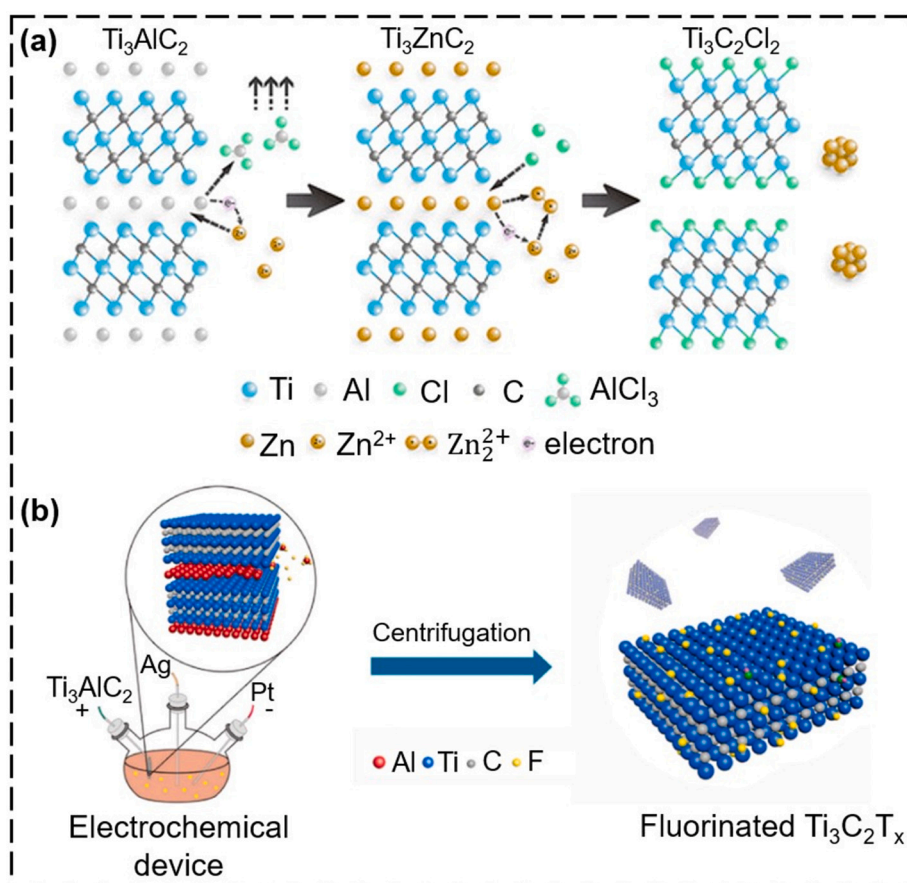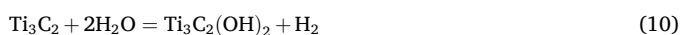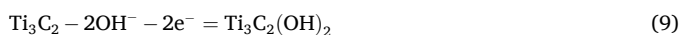

Fig. 5. (a) A diagram illustrating the mechanism of the element replacement technique and the consequent production of $Ti_3C_2Cl_2$. (b) Diagram illustrating the synthesis setup and exfoliation process of Ti_3AlC_2 using the electrochemical etching method.
(a) (Reprinted with permission from Ref. [81], Journal of American Chemical Society Copyright © 2019 American Chemical Society). (b) (Reprinted with permission from Ref. [83], Ceramics International, © 2021 Elsevier).

MAX phase electrode was utilized in a diluted HCl solution to generate Ti_2CT_x MXenes. This method did not involve the use of fluoride ions, resulting in MXenes with only -OH, —Cl, and —O groups, differing from those produced by chemical etching methods that use HF or LiF/HCl [46,89].

To prevent over-etching and control the size of MXenes, it is crucial to maintain the potential difference within a specific range during the reaction between the "A" and "M" layers in the MAX structure. Controlling the potential window and reaction time is essential. Various electrolytes such as H_2SO_4, HNO_3, NaOH, NH_4Cl, and $FeCl_3$ have been tested for their effectiveness in etching the "A" layer. Electrolytes containing chlorine (Cl) have been found to improve etching yields due to their strong bonding with the "A" element. The combination of NH_4Cl and TMAOH electrolytes optimized ion accessibility and increased etching yield by expanding the interlayer spacing in the MAX phase [89]. The proposed etching reaction is outlined as follows [89]:

$$Ti_3AlC_2 - 3e^- + 3Cl^- = Ti_3C_2 + AlCl_3 \tag{8}$$

$$Ti_3C_2 - 2OH^- - 2e^- = Ti_3C_2(OH)_2 \tag{9}$$

$$Ti_3C_2 + 2H_2O = Ti_3C_2(OH)_2 + H_2 \tag{10}$$

In another investigation, researchers focused on different MAX precursors and the toxicity of intercalants. They aimed to enhance product yield through a thermo-assisted electrochemical etching method. This method provides a straightforward, gentle, and environmentally friendly approach, requiring minimal energy input. MXenes produced via electrochemical etching can achieve an accordion-like morphology

through precise parameter control and the absence of fluorine terminations [90,91]. Despite its advantages, the electrochemical etching method faces challenges in achieving commercially viable production due to its low yield [46].

2.5. Chemical vapor deposition (CVD)

The bottom-up chemical vapor deposition (CVD) technique offers a versatile method for systematically producing high-quality MXenes, enabling the creation of monolayered carbide MXenes with unique properties that are not achievable through traditional etching methods. This technique provides several advantages, including the omission of the MAX phase, scalability, and precise process control [92–94]. For instance, in the synthesis of ultrathin Mo_2C, methane served as the carbon source, while a Cu foil on a Mo foil acted as the substrate at temperatures exceeding 1085 °C. The resulting Mo_2C single layer measured approximately 3 nm in thickness, with a lateral size exceeding 100 μm, yielding a substantial surface area. Experimental factors such as reaction temperature, duration, and the type of metal foil substrate can modify the size and defect density of the morphology. Additionally, changing the metal foil can lead to the production of ultrathin WC and TaC crystals with enhanced crystalline quality [92].

A single-step synthesis of a two-dimensional Mo_2C layer on a graphene substrate was achieved via chemical vapor deposition CVD, using molten copper as the catalyst. The schematic representation of the growth process is depicted in Fig. 6(a) [95].

In another study, Ti-based MXenes were effectively fabricated using CVD. This process involves the reaction between methane or nitrogen
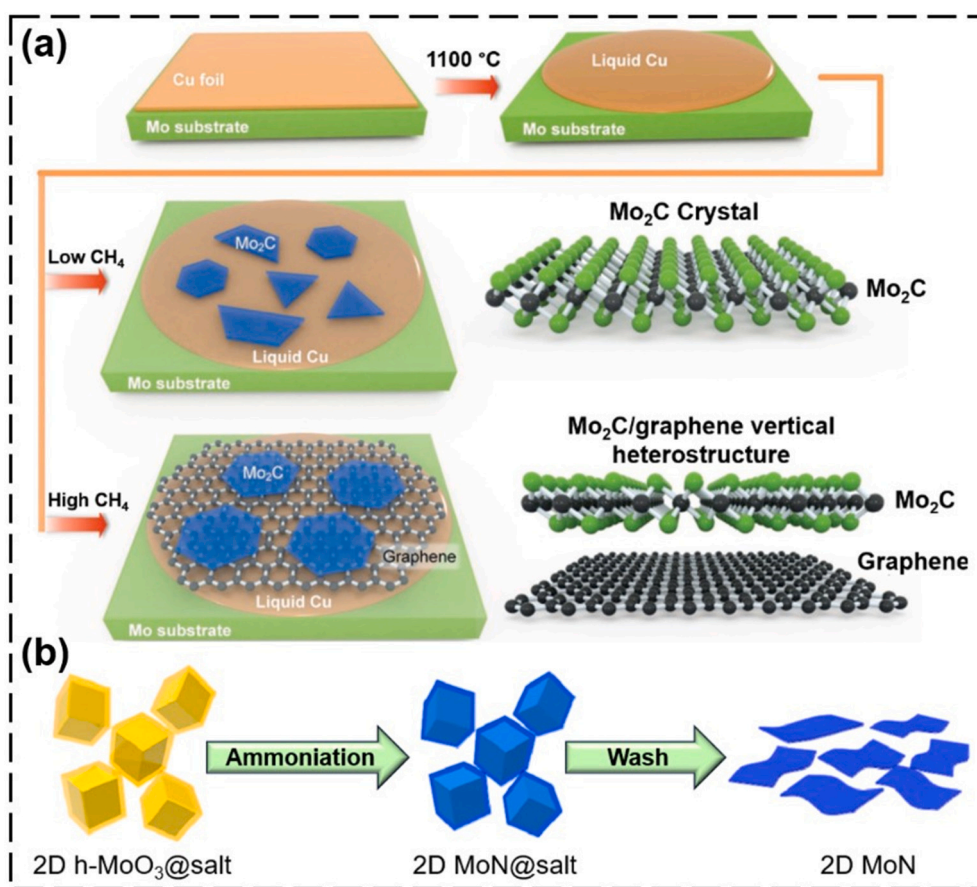

Fig. 6. (a) Diagram showing the growth of Mo_2C products under varying flow rates of CH_4 gas, both high and low; (b) fabrication of two-dimensional MoN using the salt template method.
(a) (Reprinted with permission from Ref. [95], Advanced materials, Copyright © 2017, Wiley-VCH). (b) (Reprinted with permission from Ref. [99], ACS Nano, © 2017 American Chemical Society).

gas and TiCl$_4$ on a Ti metal substrate, leading to the creation of chlorine terminated Ti$_2$CCl$_2$ or Ti$_2$NCl$_2$, respectively. Subsequently, the MXene layers vertically develop from the metal surface and detach, exposing the surface for subsequent reactions. This indicates the potential for producing large quantities of MXene sheets given sufficient precursor amounts. The proposed CVD approach presents an opportunity for scaling up MXene production commercially and exploring novel phases and structures of MXenes [48]. For instance, the Ti$_2$NCl$_2$ produced marked the first report of a chloride-terminated nitride MXene [96].

Additionally, a 3D hybrid nanocomposite was created featuring ultrafine platinum nanoparticles decorated on reduced graphene oxide and MXene nanosheets. This resulting nanocomposite demonstrated prolonged stability and elevated catalytic performance, exhibiting remarkable electrocatalytic properties for the oxidation of methanol [97].

Controlling morphology of MXene in CVD involves controlling of several key parameters, including precursor selection, flow rates, substrate temperature, and chamber pressure. Precursors affect deposition rates and uniformity, while substrate temperature influences nucleation and growth kinetics, impacting film smoothness and grain size [98]. Additionally, chamber pressure and gas composition can alter deposition rates and film characteristics, allowing for tailored material properties and structures.

However, this method is not typically used for MXene preparation because it produces thin layers rather than single layers. Consequently, the chemical vapor deposition (CVD) approach is not suitable for MXene production. Instead, a top-down method is employed, but this alternative method is expensive and results in low production rates, highlighting the need for further optimization to improve the efficiency and cost-effectiveness of MXene preparation.

2.6. Template method

The concept of salt-templated synthesis was introduced as a novel method for producing molybdenum nitride (MoN) as shown in Fig. 6(b). This process involved four main stages: (i) Initially, a 2D template was prepared using a Mo precursor to obtain MoO$_3$. (ii) In next step, the template was coated with salt by heating MoO$_3$ with NaCl in an argon environment. (iii) later on, ammonization was performed, where heating the MoO$_3$-coated NaCl to 650 °C in an NH$_3$ atmosphere produced MoN. (iv) Finally, the template was removed by rinsing with deionized water to eliminate the salt. This innovative approach offered a promising strategy for the controlled synthesis of MoN and potentially other materials [99].

A modified version of the template method has been employed to arrange two dimensional MXene layers into three dimensional MXenes, In the process of assembling 3D MXenes, a template comprising MXene solution coated with a polymer, such as polystyrene, that is compatible with the MXene material. This polymer then can be eliminated by heating the up to 450 °C in an inert atmosphere. Crucially, the transformation involves reconstructing 2D metal carbide into 3D MXene, highlighting the essence of the method [100,101]. Table 1 summarised different synthesis methods used for energy storage application.

In analyzing MXene synthesis, key characterization techniques were categorized and compared across structural, morphological, and compositional analyses. X-ray diffraction (XRD) confirmed MXene formation through a shift in the (002) peak shifts towards a lower angle and the removal of the Al peak, indicates the increased interlayer spacing and the etching of the Al layer, respectively [102]. Scanning electron microscopy (SEM) provided visual evidence of the layered nanosheet structure, with variations in the "accordion" morphology linked to different etching method [103]. Energy-dispersive X-ray spectroscopy (EDS) confirmed the elemental composition but was limited in assessing surface terminations. By correlating XRD's structural data with SEM's morphological insights and EDS's compositional analysis, the impact of synthesis parameters on MXene's final structure was comprehensively

understood [104].

3. Properties of MXene

Materials based on MXene exhibit remarkable properties, due to their layered structure, high surface area, variable surface chemistries, and hydrophilic surfaces [137,138]. These properties include exceptional electrical conductivity, with Ti$_3$C$_2$T$_x$ MXene reaching its highest recorded value of 25,000 S cm^{-1} [139]. Sc$_2$CF$_2$ MXene demonstrates impressive thermal conductivity as 722 W/m^{-1} K^{-1} [140]. Additionally, MXenes showcase outstanding mechanical properties, such as a tensile strength of up to 570 MPa [141] and a Young's modulus of 333 ± 13 GPa for Ti$_3$C$_2$T$_x$ [142]. Pristine Ti$_3$CNT$_x$ MXene offers EMI shielding effectiveness as 116 dB [143], while delaminated Ti$_3$C$_2$ MXene electrodes exhibit a high specific capacitance of up to 654 F g^{-1} at 1 A g^{-1} [144], along with excellent cycling stability as illustrated in Fig. 7. These properties collectively underscore MXene's potential as a promising electrode material for practical applications.

3.1. Structural and stability property

Advanced computational modeling is frequently utilized to assess the structural properties of newly developed stable materials like MXene. The investigation has revealed six different arrangements of MXenes, as illustrated in Fig. 8. These configurations include solid solutions, individual metal elements, double metal elements with out-of-plane ordering where transition metals are positioned in the outer layer, in-plane ordering, structured vacancies, and randomly distributed vacancies [20,145,146].

The stability and properties of MXenes can be modified by altering their terminal groups. Computational research has shown that M$_2$XT$_2$ structures, characterized by six bonds between X and M atoms, exemplify the signature six-coordination of transition metals. Analysis of the positions of terminal T$_x$ atoms relative to X and M atoms has revealed that various configurations often demonstrate optimal stability. In certain MXenes, placing T$_x$ elements above X atoms has been found to improve their electrical interface. Experimental results have confirmed that termination groups in V$_2$CT$_x$ and Ti$_3$C$_2$T$_x$ MXenes exhibit a random distribution, consistent with predictions from density functional theory (DFT) calculations [147,148].
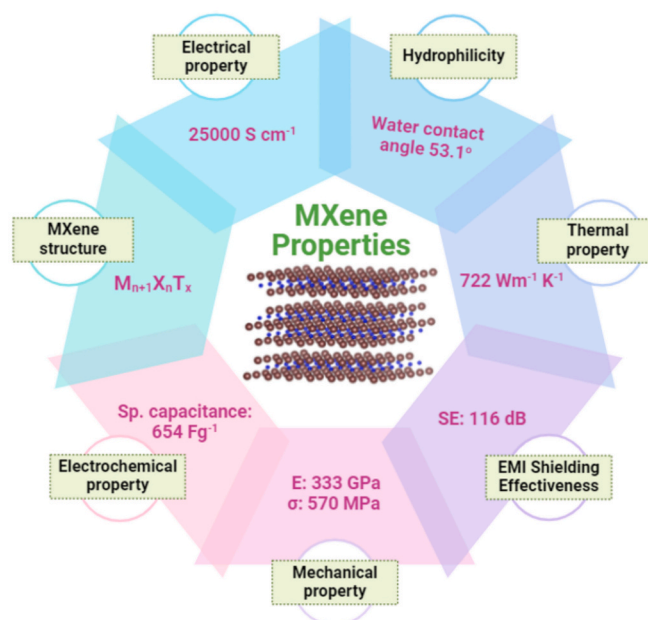

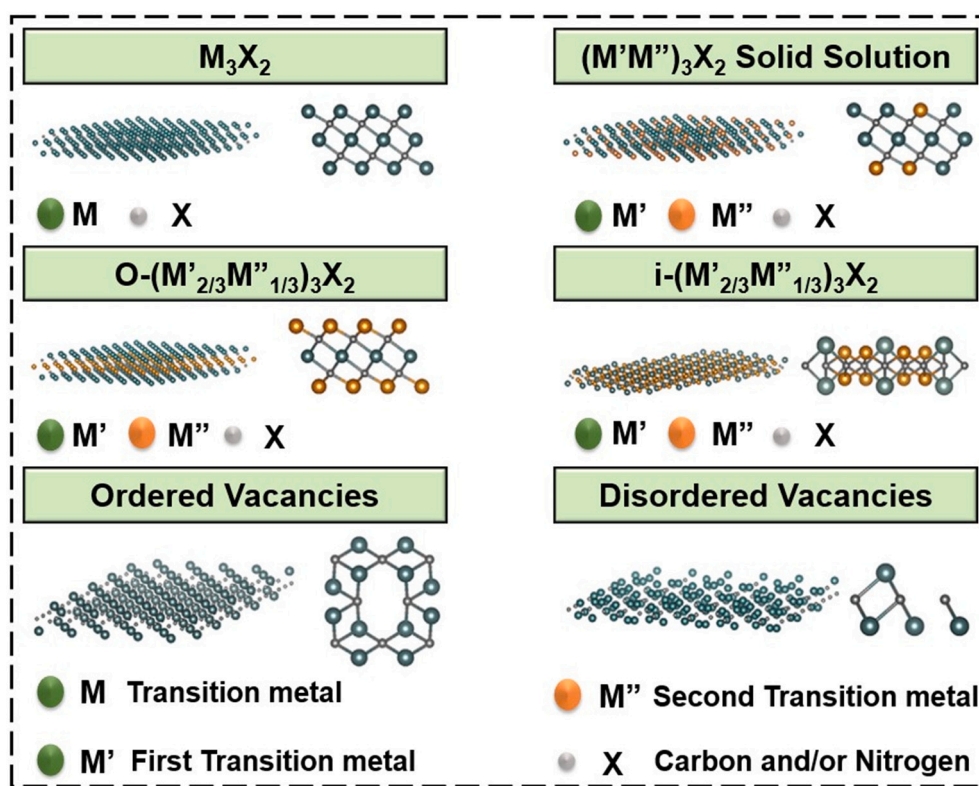**Fig. 7.** Summary of diverse properties of MXene.

Fig. 8. Various configurations of MXene structures (a).
(Reprinted with permission from Ref. [20], Ceramics International, © 2019 Elsevier).

The potential degradation of MXenes can happen upon exposure to moisture or higher temperatures, highlighting the importance of assessing their durability during storage and usage. Experimental findings indicate that the initial conductivity of $Ti_3C_2T_x$ can be reduced by 20 % when exposed to air for >70 h [149].

Therefore, to maintain the stability of MXene over an extended period, it is recommended to store them in an oxygen-free environment, apply protective coatings, and regularly monitor the stability of MXene samples using advance characterization techniques like STM, TEM, XPS, NMR, XRD, FTIR, etc. [150,151]. Furthermore, the stability of MXene can be enhanced by employing optimized etching techniques to minimize the presence of adatoms on its surface [20,153].

3.2. Electrical properties

MXenes serve as a preferred choice for electrical and optoelectronic devices as they offer exceptional electrical conductivity and hydrophilicity. The metallic nature contributes to their very high electrical conductivity. Interestingly, the conductivity of MXenes can vary significantly from 1 S cm^{-1} to >25,000 S cm^{-1}. That usually depends on various factors such as precursors of MAX phase, synthesis techniques, type and combination of surface termination groups and post-synthesis conditions [20,155].

The electrical conductivity of MXenes can be improved by modifying their surface functional groups or their elemental composition. The studies revealed that the metallic conductivity of $Ti_{n+1}C_n$ MXenes without surface functional groups decreases with the increase in value of 'n' [156].

The electrical conductivities of $Ti_3C_2T_x$ MXene depends on several factors such as surface functionality, d-spacing between MXene particles, lateral dimensions, and the yield of delamination resulting from the etching technique [157]. Experimentally measured electrical conductivity can go up to 2.4×10^5 S/m for pure $Ti_3C_2T_x$ films and 2.2×10^4 S/m for $Ti_3C_2T_x$/PVA composite film [158].

Additionally, the electrical conductivity of functional group-terminated $Ti_3C_2T_x$ MXenes was can go up to 4600 S cm^{-1} [159]. However, in another research, high conductivity of 3000 S cm^{-1} has been shown by an aramid nanofiber@MXene coaxial fiber [160].

Both the theoretical and experimental calculations revealed that the majority of functionalized MXenes tend to exhibit metallic characteristics or a metallic appearance or semiconductor MXenes (relatively rare). Due to the non-terminated nature of MXenes, the outermost layer of transition metal elements often exhibits a notable density of states at the Fermi surface. The density of states in proximity to the Fermi surface is largely influenced by the d-electrons of transition metals, while the energy bands are formed by the p-electrons of X atoms, typically situated approximately −3 eV to −5 eV below the Fermi surface level [157,161,162].

The work functions (WFs) of both bare MXenes and surface functionalized MXenes tend to be metallic. Notably, the calculated WFs of metallic MXenes can vary from 1.8 eV to 8 eV, as illustrated in Fig. 9(a). This variability in WF is closely linked to the surface chemistry of the MXenes. For a given MXene, the presence of OH (O) groups generally decreases (increases) its work function compared to the bare surface, while the effect of F decoration varies depending on the specific material. It is noteworthy that all MXenes terminated with OH groups demonstrate remarkably low work functions (below 2.8 eV), even lower than that of Scandium (Sc), which is one of the lowest among all elemental metals. Conversely, certain MXenes terminated with O groups exhibit work functions even greater than that of Platinum, which has the highest work function among elemental metals. The work functions of MXenes terminated with F typically lie between those of OH- and O-terminated counterparts. The alteration in work function due to surface functionalization arises from changes in the surface dipole moment induced by the functionalization process [163,164].
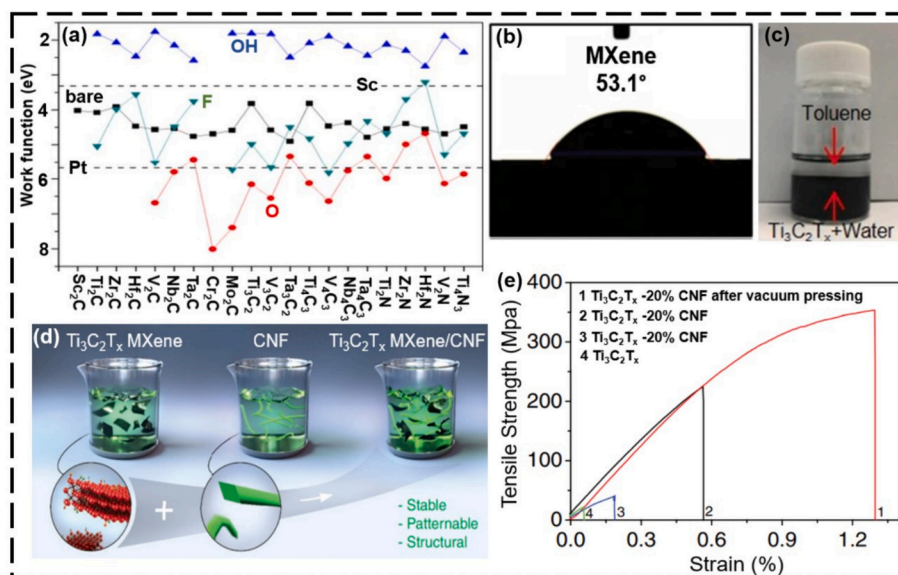
Fig. 9. (a) Displays the work functions of MXenes with different terminations. Bare MXenes are represented by black squares, while O-terminated, OH-terminated, and F-terminated MXenes are denoted by red circles, blue up-triangles, and cyan down-triangles, respectively. Additionally, dashed lines indicate the work functions of Sc and Pt for comparison; (b) illustrates the contact angle of pristine MXene; (c) demonstrates the dispersion test of pristine MXene in water and toluene; (d) a schematic representation of the dispersion of MXene-CNF hybrids (e) displays the stress-strain curves of MXene-CNF nanocomposite films both before and after vacuum pressing.

(a) (Reprinted with permission from Ref. [163], Journal of American Chemical Society Copyright © 2016 American Chemical Society). (b–c) (Reprinted with permission from Ref. [165], Advanced Materials Interfaces, Copyright © 2020, Wiley-VCH). (d–e) (Reprinted with permission from Ref. [166], Advanced materials, Copyright © 2019, Wiley-VCH).

3.3. Hydrophilicity property

The term "hydrophilicity" refers to a surface property where the water contact angle between a liquid droplet and the surface is <90° [167]. $Ti_3C_2T_x$ MXene is typically produced through acid etching in a water-based environment, leading to the generation of numerous polar terminal groups like -OH (hydroxyl) or —O (oxygen) on its surface. These terminations reveal highly hydrophilic nature of $Ti_3C_2T_x$ nanosheets, an important characteristic extensively utilized in various applications such as energy storage, photocatalytic pollutant breakdown and biomedical [168]. The hydrophilicity of MXene can be controlled by its synthesis route and subsequent delamination agent [169].

The hydrophilicity of pristine MXene (Ti_3C_2) was evaluated by measuring the contact angles of water droplets. As shown in Fig. 9(b), the contact angle for pristine MXene is 53.1°, indicating its hydrophilic nature due to the presence of surface terminal groups. Additionally, the functional groups (such as = O, –OH, and —F) on the surface of pristine MXene flakes enable them to disperse in polar organic solvents and water (Fig. 9(c)) [165]. Alternatively, a hydrophobic surface for $Ti_3C_2T_x$, tailored for specific environments, can be achieved by modifying its surface functional terminations or incorporating it into composite materials with other functionalities [170].

Moreover, a hydrophobic porous foam based on Ti_3C_2 was developed by encapsulating a Ti_3C_2 film between two ceramic wafers. These wafers were coated with 80 % hydrazine monohydrate followed by calcination at 90 °C. In contrast to the hydrophilic Ti_3C_2 films, which have a contact angle of 59.5°, the Ti_3C_2-based foam exhibited hydrophobic characteristics, with a contact angle of 94°. This distinct hydrophobicity endowed the Ti_3C_2 foam with excellent resilience in humid conditions and enhanced stability in water [171].

In another study, a combination of MXene and polyvinyl alcohol (PVA) was used to produce a nanofiber film, resulting in a PVA/MXene composite with a water contact angle of 24.5°, while pristine MXene exhibited contact angle as 35.7° respectively. This composite demonstrated improved hydrophilicity compared to pristine MXene [172].

The synthesis technique and subsequent delamination agent affect the hydrophilicity of MXene [169]. Additionally, treating MXene with alkaline solutions increased the oxygen-fluorine ratio within its functional groups, notably increasing the presence of -OH groups. This treatment significantly enhanced the hydrophilicity of MXenes [173].

3.4. Mechanical properties

MXene demonstrates outstanding physicochemical properties, exceptional strength, and elongation, owing to its multilayered structure, making it well-suited for diverse energy applications such as Li-ion batteries and supercapacitors. Its tensile stiffness, ranging from 81.71 to 561.4 N/m, surpasses that of conventional 2D materials like graphene [174].

The mechanical properties of MXene significantly impact its electrochemical performance in energy storage applications. Experimental results show that incorporating polyvinyl alcohol (PVA) between MXene flakes enhances flexibility and cationic intercalation, resulting in a capacitance of 530 F/cm³ for the MXene/PVA–KOH composite film at a scan rate of 2 mV s^{-1} [175,176].

Additionally, the mechanical properties of Ti_3C_2 nanosheets are influenced by the interaction forces between the individual layers. For example, a $Ti_3C_2T_x$ film with a thickness of 940 nm exhibits a tensile strength of 570 MPa and a Young's modulus of approximately 20.6 GPa [177].

The Hybrid dispersions of MXene/CNF are created by blending delaminated (d- $Ti_3C_2T_x$) MXene flakes with carboxymethylated cellulose nanofibers (CNFs) at various mass ratios, as shown in Fig. 9(d). After vacuum pressing, the resulting nanocomposite films exhibit a significant enhancement in tensile strength to 341 MPa and Young's modulus to 42.8 GPa. This improvement, 1.6 times greater than the initial MXene-CNF films, is due to stronger interconnections and a denser structure, effectively reducing voids, as illustrated in Fig. 9(e) [166].

Furthermore, to enhance intelligent technology, reducing product

thickness while maintaining mechanical stability is crucial for flexible electronics. Ti_3C_2 MXene nanosheets achieve a tensile strength of 670 MPa at 40 nm thickness and a Young's modulus of 120–140 GPa perpendicular to the orientation. However, increasing defect concentration from 2 % to 8 % decreases the ultimate tensile strength from 21.6 to 18.9 GPa [178]. Additionally, a biopolymer based on MXene-phenyl phosphonic diaminohexane demonstrated exceptional mechanical and physicochemical properties [179]. Table 2 depicted the mechanical performance of MXenes with other conventional 2D materials.

4. MXene based materials for energy storage

Global climate change and greenhouse gas emissions have been caused by the widespread consumption of fossil fuels in recent decades [187]. Therefore, with the objective of diminishing their dependence on fossil fuels, numerous nations have invested substantial resources into the advancement of sustainable renewable energy [188,189]. However, the majority of renewable energy sources, such as tidal, wind, and solar energy, exhibit intermittency and rely on environmental conditions for power generation [190]. Hence, in order to store natural energy and transform it into electricity that can be utilized by the consumers when needed, power storage units are required. Energy storage units, such batteries, are currently being employed in electric cars in an attempt to lower greenhouse gas emissions [191,192]. Furthermore, to ensure a consistent energy supply, advanced smart electrical grids necessitate characteristics such as robust and high specific energy and power capabilities, along with exceptional long-term performance [193,194]. MXenes exhibit remarkable physical and chemical attributes, including exceptional mechanical strength, outstanding electrical conductivity, diverse surface terminations, hydrophilic properties, superior specific surface area, and the capability to accommodate intercalants. These qualities render MXenes highly suitable for energy storage applications [195–197]. We delve into the most recent developments in nanoengineering aimed at improving the efficiency of 2D MXenes and their derivatives in energy storage applications, including supercapacitors and batteries, in the upcoming sections [198].

4.1. MXenes based composite materials for supercapacitors

The inexpensive maintenance costs, longer cycling life, and high power density of supercapacitors (SCs) are attributed to them, making them unique electrochemical energy storage devices [199–201]. Pseudocapacitive, or battery-type materials and Electric double layer capacitive (EDLC, which are among the primary classifications of electrode materials in supercapacitors. They distinguish between rapid surface ionic charge accumulation in polarized electrodes for EDLC, and Faradic charge storage for pseudocapacitive materials. The choice of electrode material, which affects structural stability and charge conduction, is the primary factor affecting SCs [202].

The effectiveness of 2-D materials as electrode materials for energy storage arises from their significant surface area, improved conductivity,

and rapid ion diffusion kinetics [203]. Recent advancements, particularly in MXenes, have significantly improved the durability and electrochemical energy storage capacity of supercapacitors. The performance of supercapacitors (SCs) depends on factors such as electrode material, electrolyte selection, and potential window size [204]. Among these, the electrode material significantly influences electrochemical performance. MXene electrodes exhibit swift surface redox reactions, inducing pseudocapacitive behavior in supercapacitors. MXene's behavior is influenced by the type of electrolyte utilized [205]. For example, in acidic electrolytes (e.g., H_2SO_4), MXene shows redox pseudocapacitive behavior due to reactions with surface terminal groups. In neutral electrolytes (e.g. Na_2SO_4), it exhibits electric double-layer capacitance (EDLC) due to interactions between metal ions and water molecules. [206].

MXenes are being explored as a valuable material for creating composite materials in energy storage applications. MXene based composites usually consists of carbon-based substances or metal oxides or conducting polymers to boost their performance. Fig. 10 illustrates the schematic structure of the materials used for the fabrication of MXene based composites. The carbon-based substances or metal oxides or conducting polymers enhance electronic conductivity, increase surface area, and stabilize active material structures. Active components prevent MXene restacking, acting as spacers to facilitate fast ion transport and improve ion accessibility. This synergy yields superior electrochemical properties, especially in supercapacitor applications [207].

4.1.1. MXene/carbon based materials composite for supercapacitors

Highly conductive carbon materials, including Graphene, carbon nanotubes (CNTs), and activated carbon, are esteemed for their expansive surface area and exceptional conductivity. These materials are extensively employed in energy storage applications due to their significant specific surface area and superior electronic conductivity, facilitating efficient charge storage and electron transfer, ultimately leading to enhanced rate capability [208].

To overcome challenges like self-restacking, and structural instability during cycling, MXenes are combined with carbon materials. This blending helps manage volume expansion and collaboratively improves the electrochemical and mechanical properties of MXene-based supercapacitors [11].

Carbon fiber materials derived from natural biomaterials have garnered significant interest due to their vast availability, cost-effectiveness, exceptional electrical conductivity, and environmental benefits. Recently, a novel hierarchical porous structure, called "skin/ skeleton"-like MXene/biomass-derived carbon fibers (MXene/CF) heterostructure, has been developed via a one-step pyrolysis process. When employed as a self-supporting electrode in supercapacitors, this MXene/ CF heterostructure demonstrates a significant capacitance of 7.14 F cm^{-3}, with impressive rate capability and exceptional cyclic stability, retaining 99.8 % of its capacitance even after 5000 cycles [209].

Activated carbon's affordability, porous structure, extensive surface area, and strong electrical conductivity make it an excellent choice for

Table 2
Mechanical performance of MXenes and other 2D materials.

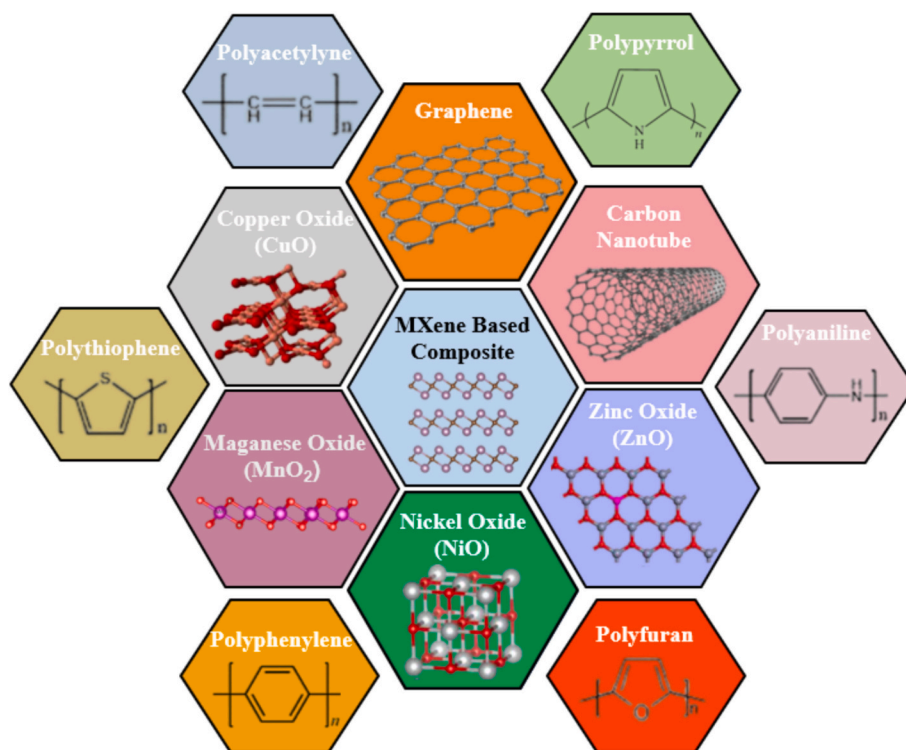| Material	Type	Thickness (nm)	Tensile strength (GPa)	Young's modulus (GPa)	Measurement technique	Ref.
$Ti_3C_2T_x$	Monolayer	0.98	15.4	483.5	AFM deflection	[180]
$Ti_3C_2T_x$	Monolayer	1.6	17.3 ± 1.6	333 ± 30	AFM deflection	[142]
$Nb_4C_3T_x$	Monolayer	1.26	–	386 ± 13	AFM deflection	[181]
Graphene	Monolayer	0.335	130	1000	AFM deflection	[182]
MOS_2	Monolayer	0.65	–	270 ± 100	AFM deflection	[183]
Boron nitride (BN)	Monolayer	0.65	–	865 ± 7.3	AFM deflection	[184]
Tungsten disulfide (WS_2)	Monolayer	0.62	47 ± 8.6	302.4 ± 24.1	AFM deflection	[185]
Tungsten diselenide (WSe_2)	Monolayer	0.65	38 ± 6	258.6 ± 38.3	AFM deflection	[185]
Tungsten ditelluride (WTe_2)	Monolayer	0.71	6.4 ± 3.3	149.1 ± 9.4	AFM deflection	[185]
Tungsten nitride (WN)	Few layer	4.5	–	390 ± 10	AFM deflection	[186]
Tungsten nitride (WN)	Few layer	12	–	390 ± 10	AFM deflection	[186]

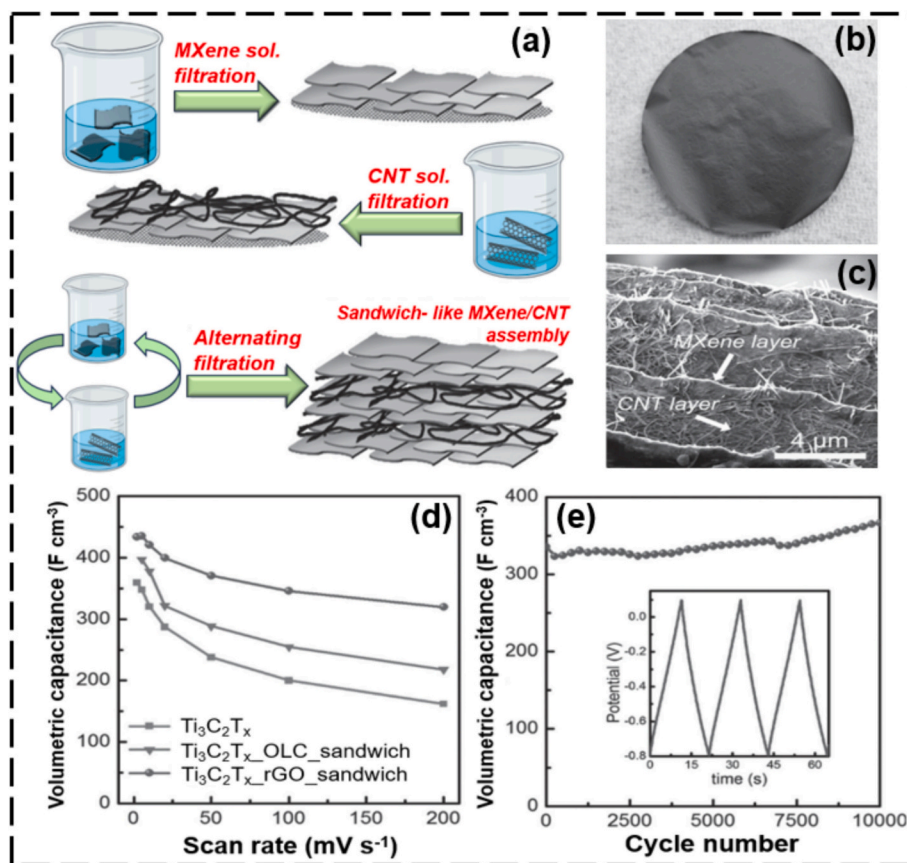**Fig. 10.** MXene based composite materials.

Fig. 11. (a) Schematic illustrating the synthesis process of the sandwich-like MXene/CNT papers (b) digital images displaying a flexible and free-standing layered structure composed of MXene and carbon nanotubes (CNTs) paper (c) SEM images of $Ti_3C_2T_x$/MWCNT paper (d) volumetric capacitances measured at various scan rates for $Ti_3C_2T_x$ and $Ti_3C_2T_x$/CNT electrodes (e) $Ti_3C_2T_x$/MWCNT electrode cycling stability at 10 A g^{-1}.
Reprinted with permission from Ref. [214], Advanced materials, Copyright © 2014, Wiley-VCH.

supercapacitors. Investigating further, a composite of MXene and activated carbon (AC) was thoroughly studied, showcasing remarkable performance. It exhibited a notable capacitance of 126 F g^{-1} and impressive stability, retaining 57.9 % capacitance even at a high current density of 100 A g^{-1} in an organic electrolyte [210].

Moreover, an electrode structure formed by acid-activated carbon and MXene materials can create a three-dimensional conductive network. These electrodes demonstrate a high specific capacity of 378 F g^{-1} at 0.5 A/g and maintain good capacitance, with 88.9 % retention at 30 A/g [211].

In a separate study, Carbon-encapsulated Ti$_3$C$_2$T$_x$ (Ti$_3$C$_2$T$_x$@C) was synthesized via a hydrothermal process and utilized in inkjet printing for flexible micro-supercapacitors. Agarose served as a carbon source, facilitating the formation of phenolic carbon on Ti$_3$C$_2$T$_x$ sheets during heating. This method prevented oxidation and aggregation of Ti$_3$C$_2$T$_x$ while increasing active sites and enhancing ion diffusion. Consequently, the MXene sheets exhibited a capacitance of 736 F·g^{-1} at 2 A·g^{-1} [212].

For the production of a 3D hybrid foam called MGC for solid-state supercapacitors, a simple template method was employed. This structure enhances both electron and ion transport. The MGC electrode achieved a capacitance of 276 F·g^{-1} at 0.5 A·g^{-1}, owing to the synergistic combination of its components and structure. Furthermore, it maintained structural integrity even under an 80 % compressive strain and displayed remarkable flexibility and stability at various angles [213].

One-dimensional nanostructured materials like carbon nanotubes (CNTs) have been extensively studied for energy storage due to their exceptional properties. To capitalize on this, sandwich-like MXene/CNT composite electrodes were synthesized (Fig. 11(a)). Upon separation from filter membranes, these electrodes form substantial, self-supporting sheets with thicknesses ranging from 2 to 3 µm (Fig. 11 (b)). The sandwich-like structure of MXene and CNT layers is evident (Fig. 11(c)). Notably, sandwich-like Ti$_3$C$_2$T$_x$/rGO sheets exhibit superior capacitive and rate performances, achieving a high volumetric capacitance of 435 F cm^{-3} at 2 mV s^{-1}, with excellent cyclic stability over 10,000 cycles (Fig. 11(d, e)) [214].

Furthermore, aiming for both high performance and cost-effectiveness, a Ti$_3$C$_2$T$_x$/SCNT self-assembled composite electrode was synthesized via vacuum filtration. This electrode demonstrates remarkable electrochemical properties, including a high areal capacitance of 220 mF cm-2 and 95 % capacitance retention after 10,000 cycles [215].

Graphene, with stronger interlayer van der Waals forces compared to carbon nanotubes (CNTs), offers superior durability as an electrode material. In recent research, reduced graphene oxide (rGO) nanosheets were incorporated between MXene layers via electrostatic interaction (Fig. 12a). The measured interlayer spacing (1.51 nm) aligns with TEM observations (Fig. 12(b)). Galvanostatic charge/discharge curves of the MXene/rGO electrode (Fig. 12(c)) indicate its pseudocapacitive nature, achieving a volume capacitance of 1040 F cm^{-3} at 2 mV s^{-1} (Fig. 12(d)), with 61 % capacitance retention and extended cycle life at 1 V s^{-1}. These findings drive interest in MXene/carbon composites for portable supercapacitors [216].

Furthermore, current research aims to enhance supercapacitor electrode performance by employing Ti$_3$C$_2$T$_x$/graphene composites. Electrochemical assessments showed that capacitors incorporating graphene exhibited over 1.5 times higher capacitance compared to those without graphene [217].

4.1.2. MXene/metal oxide for supercapacitors

Transition metal oxides exhibit superior electrical conductivity potential, synergistic effects, and the ability to undergo multiple valence changes in comparison to bimetallic transition metal oxides. Examples like MnO$_2$, MoO$_3$, NiO, CuO, ZnO SnO$_2$, WO$_3$ and RuO$_2$ display exceptionally high pseudocapacitance compared to carbon materials [218]. Intercalating pseudocapacitive materials into MXene improves areal capacitance and prevents self-restacking. Hybridizing Metal Oxides with MXene shows promise for high-performance supercapacitors, but the right combination is crucial for optimal results. This enhances energy density and cycle stability, overcoming inherent limitations of supercapacitors [176,219].

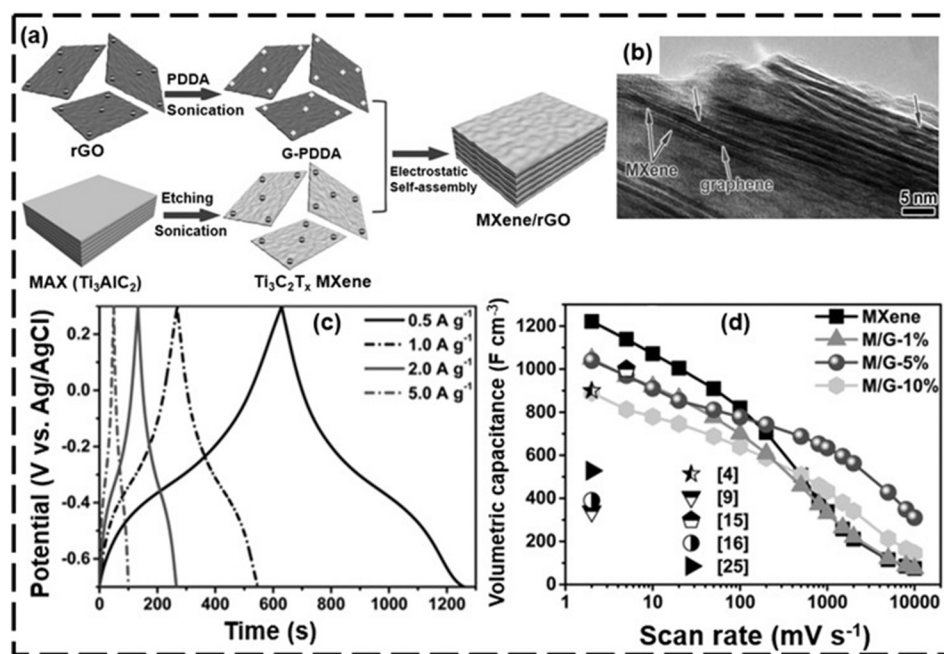In the past few years, a TiO$_2$-decorated Ti$_3$C$_2$ MXene based composite

Fig. 12. (a) Diagram depicting the process of synthesizing MXene/rGO hybrids, (b) Transmission Electron Microscopy (TEM) photographs showcasing the MXene/rGO-hybrid composite, (c) Galvanostatic Charge-Discharge (GCD) plots displaying the performance of the MXene/rGO-hybrid composite electrode across various current densities, and (d) evaluation of volumetric capacitance and cycling stability under different current densities.
(Reprinted with permission from Ref. [216], Advanced Functionals Materials, Copyright © 2017, Wiley-VCH).

has been explored for supercapacitor electrode material. In a research study, this hybrid composite displayed a specific capacitance of 143 F g^{-1} at a rate of 5 mV s^{-1}, outperforming pure MXene by 1.5 times in terms of capacitance. Furthermore, it demonstrated excellent cycling stability, retaining 92 % of its capacitance even after 6000 cycles [220].

Further, research work has been extended to enhance the performance of supercapacitor electrode by utilizing a sandwich-like structure of ZnO nanoparticles decorated on Ti_3C_2. It was found that specific capacitance enhanced by of 120 F g^{-1} at 2 mV s^{-1} and excellent cycling stability, retaining 85 % of its capacitance after 10,000 cycles at 5 A/g. The outcome of the study demonstrated that the Ti_3C_2/ZnO composite could be employed for supercapacitor applications [221].

Additionally, the other metal oxides were also investigated by the worldwide researchers. In one of the studies MnO_2 directly onto s-MXene/CC have been examined to improve the overall electrochemical traits of the composite compare to the existing one. Fig. 13(a) depicted the synthesis of MXene using HF etching followed by deposition on MnO_2 directly onto s-MXene/CC, as illustrated in Fig. 13(b). The three-layer structure of the composite and a rod-like morphology of MnO_2 were confirmed by SEM analysis shown in Fig. 13(c). Remarkably, the MMC as shown in Fig. 13(d) demonstrated an exceptional retention rate of 83 % after 10,000 charge-discharge cycles, indicating its remarkable stability and long cycle life [222].

In continuation a new type of pseudocapacitive material $W_{18}O_{49}$/$Ti_3C_2T_x$ was prepared. This heterostructure displayed superior supercapacitor performance, achieving a capacitance of 696.2 F g^{-1} at 1 A g^{-1}, along with outstanding cyclic retention of 99.7 % over 6000 cycles [223].

In another research, a series of NiO_2/MXene hybrids was developed by varying compositions, including 5 %, 10 %, 15 %, and 20 % nickel oxide content. Among these, the 15 % NiO_2/MXene composite electrode exhibited the highest capacitance of 1542 F g^{-1} at a current density of 6 mA cm^{-2} in a 1 M KOH electrolyte. The study suggests that the 15 % NiO_2/MXene composite holds promise as an anode material for all-solid-state supercapacitor applications [224].

Furthermore, a new method for fabricating flexible electrodes for

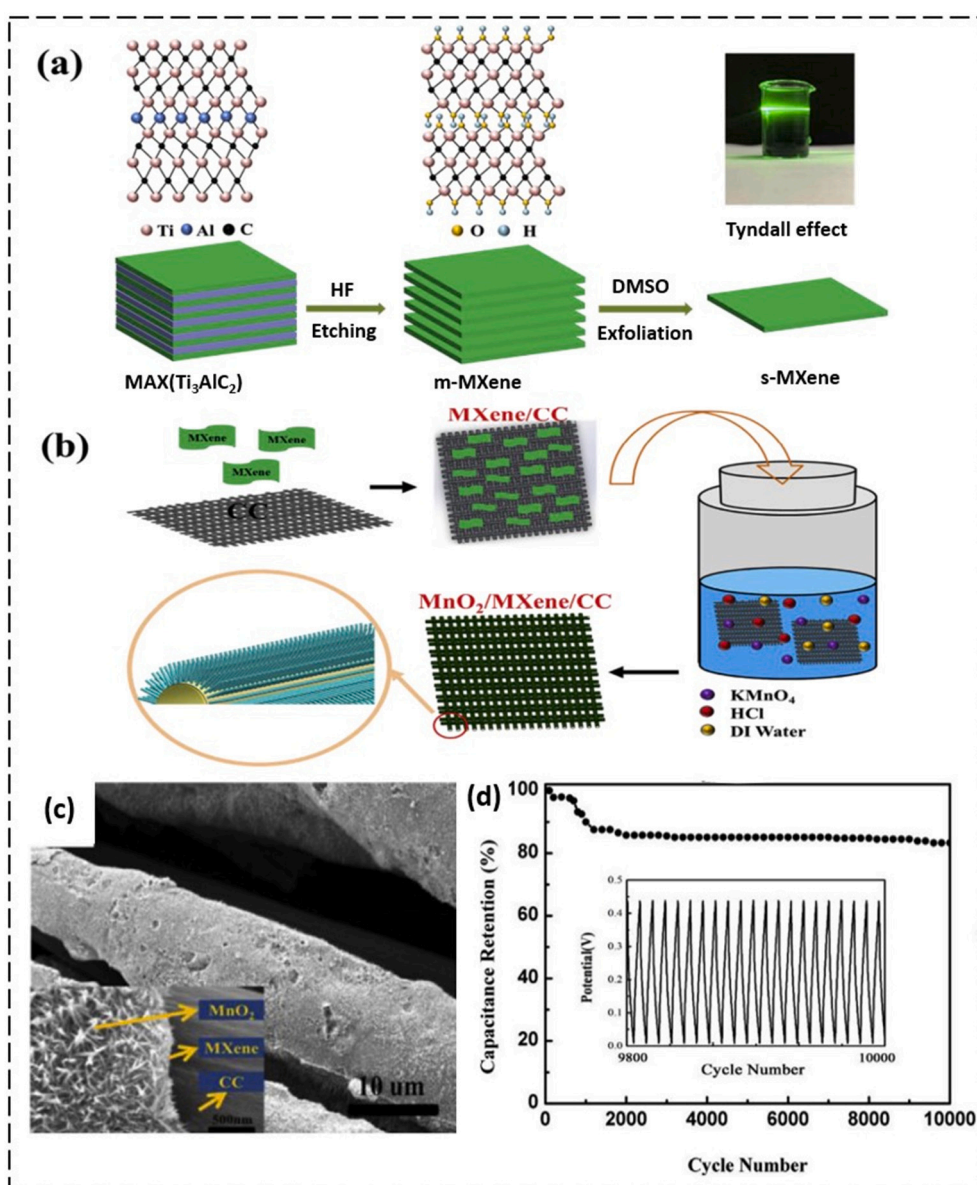**Fig. 13.** (a) Illustrates the synthesis process of s-MXene. (b) The preparation of MnO_2/MXene/CC composite. (c) SEM images in depict the structure of the MnO_2 nanorods/MXene/CC composite. (d) The cycling performance of the device over 10,000 cycles.
(Reprinted with permission from Ref. [222], Journal of Alloys and compounds, © 2019 Elsevier).

supercapacitors using ascorbic acid-treated MXene/SnO$_2$ hetero-structures. Their material exhibited a notable specific capacitance of 643 F g^{-1} and displayed excellent electrochemical stability, retaining 98 % of its capacitance after 1000 cycles. Furthermore, the MXene/SnO$_2$ composite demonstrated high resistance to environmental humidity [225].

4.1.3. MXene/conducting polymer for supercapacitors

Conducting polymers offer unique advantages for wearable super-capacitors compared to other pseudocapacitive materials, due to their inherent flexibility and conductivity [226]. MXene, a promising elec-trode material for high-performance applications in supercapacitors, faces challenges typical of other two-dimensional materials, notably restacking, which hinders ion transport within the electrode [227]. This restrains specific capacitance and rate capability. MXene/conducting polymer composites, much like conducting polymers, can achieve high capacitance in acidic electrolytes. Currently, various conducting poly-mers, including polyaniline (PANI) [228], (PEDOT) [228], Polypyrrole (PPy) [229], PDA [230], and polyfluorene derivatives (PFDs) [231], have been combined with MXenes to create hybrids with outstanding electrochemical performance.

PEDOT, renowned for its outstanding chemical and electrochemical durability, high conductivity, and fast redox reactions, is extensively researched as a conducting polymer for supercapacitors. A flexible composite film of aligned Mo$_{1.31}$C MXene and PEDOT: PSS was pro-duced using vacuum co-filtration on a mixture solution, followed by treatment with concentrated H$_2$SO$_4$. This process resulted in a flexible film exhibiting a high volumetric capacitance of 1310 Fcm^{-3} in a 1 M H$_2$SO$_4$ electrolyte [228].

In an additional investigation, researchers examined the impact of mass loading by creating a composite electrode film of Ti$_3$C$_2$T$_x$/PANI. This resulted in a specific capacitance of around 383 F g^{-1} at a scan rate of 20 mV s^{-1} in a 3 M H$_2$SO$_4$ electrolyte [228].

Furthermore, to enhance performance, organ-like nanocomposites of Ti$_3$C$_2$T$_x$/PPy were created through a low-temperature chemical oxida-tion process, polymerizing pyrrole monomers directly onto Ti$_3$C$_2$T$_x$ nanosheets. This method resulted in well-dispersed polypyrrole, as shown in Fig. 14(a, b) with Ti$_3$C$_2$T$_x$ nanosheets acting as a framework to control PPy growth and prevent self-aggregation, thereby enhancing composite stability. The uniform PPy nanoparticles expanded the interlayer spacing within Ti$_3$C$_2$T$_x$ nanosheets (Fig. 14(c)). The optimized Ti$_3$C$_2$T$_x$/PPy composite electrode achieved a specific capacitance of 184.36 F g^{-1} at a scan rate of 2 mV s^{-1} and maintained 83.33 % of its initial capacitance after 4000 charge-discharge cycles at a current den-sity of 1 A g^{-1} (Fig. 14(d)). This method is cost-effective and scalable for producing Ti$_3$C$_2$T$_x$/PPy composites [229].

MXene-based composites are being more frequently employed in the production of supercapacitors because of their elevated specific capac-itance, strong mechanical properties, and improved conductivity [232]. As illustrated in Table 3, MXene/Carbon Composites are highly regarded for supercapacitor electrodes due to their excellent electrical conduc-tivity, good cyclic stability, and high surface area. These features make them ideal for applications demanding long-term stability and high-

Table 3
Advantages and disadvantages associated with different MXene based composites.

MXene based composites	Advantages	Disadvantages	Ref.
MXene/carbon based composite	• High electrical conductivity • High surface area for charge storage • Good Cyclic stability • Enhanced mechanical strength	• Limited pseudocapacitance • High cost • Potential for aggregation of carbon materials	[236,237]
MXene/metal oxides based composite	• High Pseudocapacitance • High energy density • Good structural stability	• Lower electrical conductivity compared to carbon materials	[234,238]
MXene/conducting polymers based composite	• Good flexibility and mechanical strength • Enhanced capacitance	• Stability issues • Moderate electrical conductivity	[239,240]

Fig. 14. (a) A schematic illustrating the fabrication process of Ti$_3$C$_2$T$_x$/PPy composites. (b) A scanning electron microscopy (SEM) image displaying Ti$_3$C$_2$T$_x$/PPy. (c) A comparison of specific capacitance among Polypyrrole, Ti$_3$C$_2$, and Ti$_3$C$_2$/Polypyrrole at different scan rates. (d) Cycling performance curves at 1 A g^{-1}. (Reprinted with permission from Ref. [229], Ceramics International, © 2019 Elsevier).

power density [205,233]. However, for applications that prioritize higher energy density over slightly reduced conductivity and cyclic stability, MXene/Metal Oxides Composites may be more appropriate because of their superior pseudocapacitance [234]. If flexibility is required, MXene/Conducting Polymers Composites might be a better choice, despite their stability issues [235].

Overall, MXene/Carbon Composites offer a well-balanced performance, combining the strengths of both MXene and carbon materials. They provide a good mix of high conductivity, stability, and capacitance, making them suitable for a variety of supercapacitor applications. Their future outlook involves propelling energy storage innovations through the creation of resilient, high-capacity supercapacitors, thereby fostering the evolution of effective and eco-friendly energy solutions [176,207]. Table 4 shows the electrochemical performance of MXene based supercapacitors.

4.2. MXene based materials as an electrode material for batteries

MXene batteries, recognized for their exceptional performance and rapid charging abilities, stand ready to revolutionize portable electronics and electric vehicles due to their dependable operation and effectiveness [56]. MXenes exhibit a layered structure that provides numerous remarkable advantages for the storage of electrochemical energy i.e.:

i) Its unique layered structure enables low diffusion energy barrier and fast ion diffusion
ii) Fast electron transport becomes possible by its high electrical conductivity
iii) Its surface has a large number of functional groups, which facilitate the formation of a strong and adequate bond with other materials
iv) large surface area

These features enabled MXenes for high-performance electrochemical energy storage devices, including metal-ion batteries and SCs [206]. These developments address various requirements across different types of batteries, from lithium-ion batteries for electric

vehicles to emerging alternatives like Na^+, K^+, Zn^{2+}, Mg^{2+}, and Al^{3+}-ion batteries, reflecting a growing interest in cost-effectiveness and high-safety battery substitutes [267]. Fig. 15(a) illustrates significant
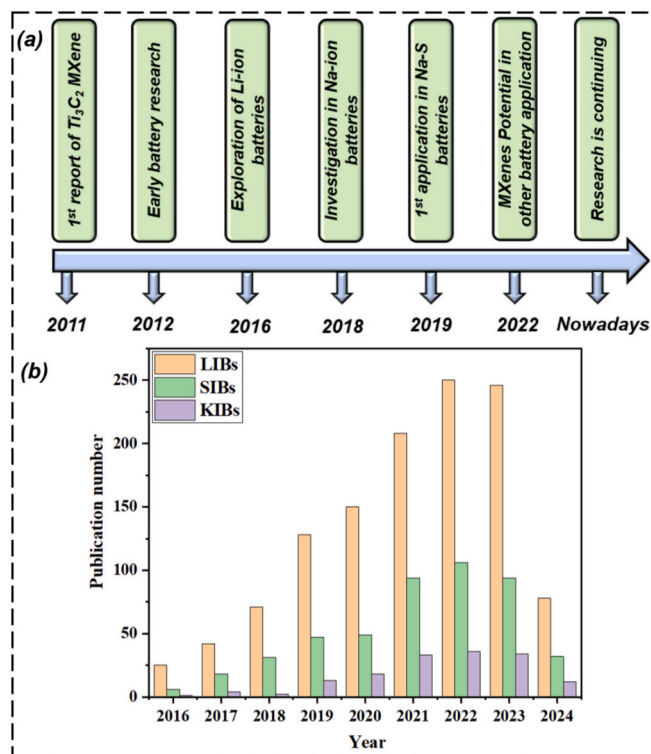

Fig. 15. (a) Illustrates a schematic timeline depicting the significant milestones achieved through in situ growth engineering on 2D MXenes for rechargeable batteries. (b) Number of journal publications on MXenes for LIBs, SIBs and KIBs batteries applications, searched with keywords "MXene Supercapacitor" and "MXene battery".
Source: (http://apps.webofknowledge.com, 2016 to 2024).

Table 4
MXene and its composites for use in supercapacitors.

MXene-based composites	Material	Electrolyte	Specific capacitance (F g^{-1})	Cycles	Capacity retention (%)	Ref.
	Ti_3C_2	KOH	124	6000	87 %	[241]
	$N–Ti_3C_2T_x$	1 M H_2SO_4	192	10,000	92 %	[242]
	$Ti_3C_2T_x$ hydrogel	3 M H_2SO_4	226	10,000	97 %	[243]
	Polyaniline/MXene (V_2C)	H_2SO_4/PVA	337.5	10,000	97.6 %	[244]
	$Ti_3C_2T_x$/C	1 M H_2SO_4	364.3	10,000	99 %	[245]
MXene–carbon composite	MXene/graphene	3 M H_2SO_4	335.4	20,000	100 %	[246]
	MXene/AC	1 M Et_4NBF_4/AN	126	10,000	92.4 %	[247]
	$Ti_3C_2T_x$/CDs	1 M H_2SO_4	144	10,000	101.1 %	[248]
	d- $Ti_3C_2T_x$/CNT	1 M $MgSO_4$	150	10,000	100 %	[214]
	$Ti_3C_2T_x$/CNT	1 M Na_2SO_4	167	10,000	89 %	[249]
	MnO_2/MXene/CNT	1.0 M Na_2SO_4	181.8	5000	91 %	[250]
	MXene/MnO_2/polyaniline	1 M Na_2SO_4	216	5000	74 %	[251]
	Fe_2O_3/$Ti_3C_2T_x$	3 M H_2SO_4	584	13,000	121 %	[252]
	MXene/V_2O_5 film	1 M H_2SO_4	319.1	5000	70.4 %	[253]
	MoO_3/D-$Ti_3C_2T_x$	1 M H_2SO_4	545	5000	90 %	[254]
	MnO_2/$Ti_3C_2T_x$	1 M Na_2SO_4	130.5	1000	100 %	[255]
MXene–metal oxide composite	MXene/Ag NWs/cellulose	PVA/H_2SO_4	505	500	90.9 %	[256]
	MnO_2 @MXene/CNTF	1 M Na_2SO_4	181.8	5000	91 %	[250]
	WO_3–Ti_3C_2	0.5 M H_2SO_4	566	5000	92.33 %	[258]
	$Ti_3C_2T_x$/AuNPs	1 M H_2SO_4	278	10,000	95 %	[260]
	MXene/MnO_2/CC	3 M KOH	511.2	10,000	83 %	[261]
	MXene/PANI	1 M H_2SO_4	661	10,000	91.2 %	[262]
	$Ti_3C_2T_x$/PPy	1 M Na_2SO_4	184	4000	83.33 %	[229]
MXene–polymer composites	$Ti_3C_2T_x$/PANI-NTs	1 M H_2SO_4	597	5000	87.5 %	[263]
	AC//MXene/PANI	7 M KOH	262	10,000	90.82 %	[264]
	PPy/$Ti_3C_2T_x$ film	PVA/H_2SO_4 gel electrolyte	420.2	10,000	86 %	[265]
	PANI@TiO_2/$Ti_3C_2T_x$	1 M KOH	188.3	9000	94 %	[266]

progress in in-situ growth engineering for 2D MXenes in rechargeable battery applications [268]. Fig. 15(b) depicts the annual publication count from 2016 to 2024 for papers concerning MXene-based batteries. Over the past decade, battery research has surged, particularly with the dominance of lithium-ion batteries (LIBs) in the energy storage market. Despite their widespread use, LIBs face limitations in energy density, driving interest towards alternatives like lithium-sulfur (Li—S), sodium, and potassium-based batteries [269,270]. Additionally, there's a focus on developing new anode materials with higher capacities and longer lifetimes. With the rise of electric vehicles, there's a demand for robust power systems, prompting the search for materials like MXenes known for their potential in high-power lithium-ion battery applications [271]. Theoretical computational study suggests that MXenes are highly promising contenders for numerous energy storage applications. MXenes' unique properties make them attractive materials for battery

applications. The theoretical capacity for Li intercalation of bare Ti_3C_2 was predicted to be 320 mA h g^{-1} [272]. On the other hand, the storage capacity of Li^+ is limited by the presence of —F or -OH on the surface of MXene. In actuality, the capacity was only around 130 mA h g^{-1} for $Ti_3C_2F_2$ and 67 mA h g^{-1} for $Ti_3C_2(OH)_2$, as reported [273].

In the past few years, Ti_2C MXene, when subjected to hydrogen peroxide (H_2O_2) treatment, serves as the anode material in lithium-ion batteries (LIBs). MXene sheets increase up as a result of the H_2O_2 treatment, forming TiO_2 nanocrystals on the sheet surface. The MXene treated with H_2O_2 exhibited superior rate capability (150 mA h g^{-1} at 5 A g^{-1}) and an increased discharge specific capacity (389 mA h g^{-1} at 100 mA g^{-1} after 50 cycles) as compared to pure Ti_2C MXenes [274]. A new 2D $Hf_3C_2T_z$ MXene, produced by hydrofluoric acid etching of layered $Hf_3[Al(Si)]_4C_6$, demonstrated a remarkable reversible capacity of 1567 mAh cm^{-3} over 200 cycles at 200 mA g^{-1} for lithium-ion
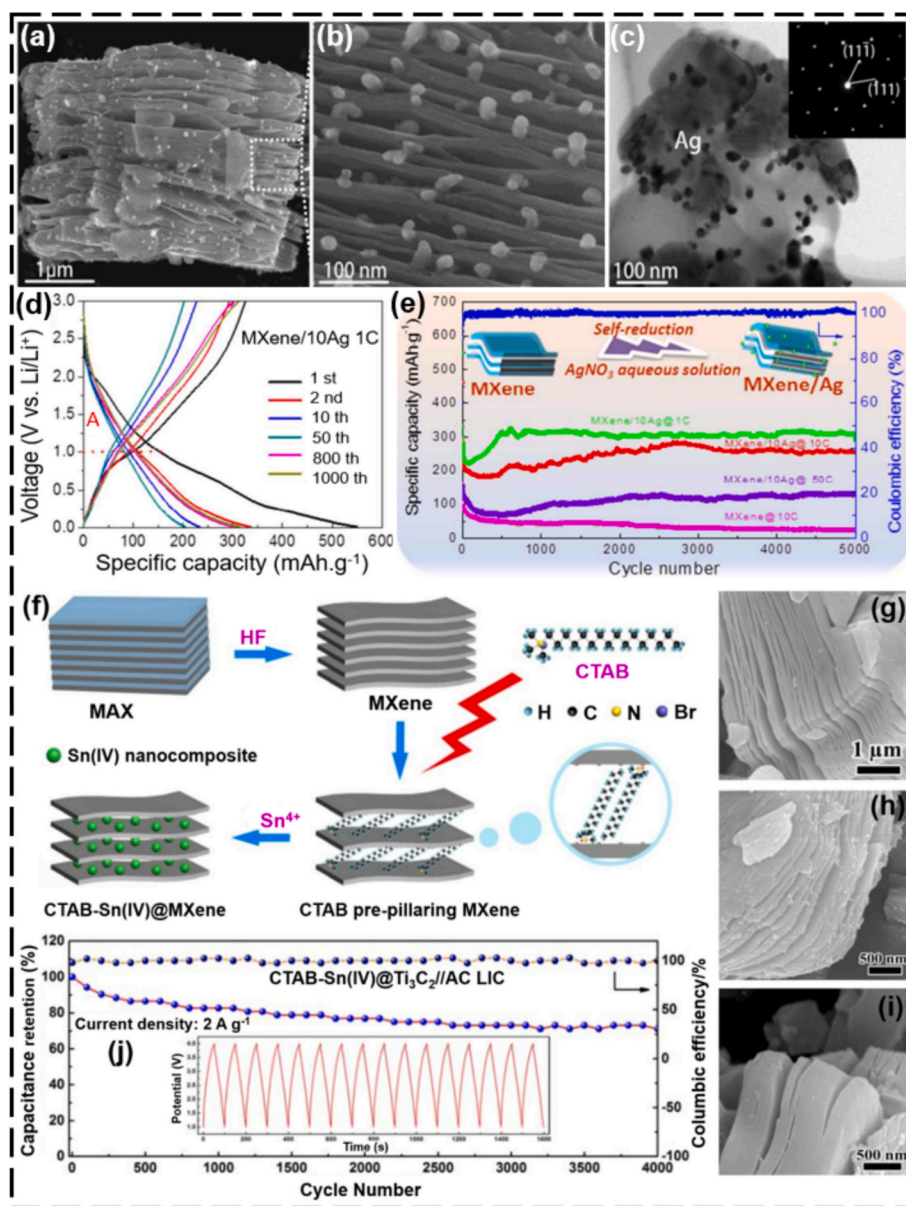

Fig. 16. (a, b) SEM images depicting the layered morphology of the MXene/Ag composite. (c) Transmission electron microscopy image displays the composite. (d) Charge-discharge behavior of the nanocomposite at 1 C. (e) Comparison of rate capacities is presented between the MXene and MXene/Ag composite. (f) Schematic depiction of the synthesis process for cetyltrimethylammonium bromide CTAB-Sn (IV)@ Ti_3C_2. (g–i) SEM images depicting Ti_3C_2, CTAB@ Ti_3C_2, and CTAB-Sn (IV)@ Ti_3C_2. (j) Cycling performance at 2 A g^{-1}.
(a–e) (Reproduced with permission from Ref. [129], ACS Applied Materials & Interfaces Copyright © 2016 American Chemical Society). (f–j) (Reproduced with permission from Ref. [279], ACS Nano Copyright © 2017 American Chemical Society).

batteries (LIBs) [275].

Recent research has investigated the impact of different synthesis methods on Li-ion battery performance. One study compared fluorine-free $Ti_3C_2T_x$ MXene and HF-etched $Ti_3C_2T_x$. The fluorine-free $Ti_3C_2T_x$ showed greater capacity and superior performance, achieving 106.6 mAhg^{-1} at 0.5 Ag^{-1} after 250 cycles with a mass loading of 1.24 mg cm^{-2}, nearly twice that of the HF-etched counterpart. The improved performance was due to a larger c-lattice parameter and the presence of functional groups without fluorine termination [276].

To further enhance battery performance, hybrid Mg^{2+}/Li^+ batteries are being explored for high voltage and capacity. These batteries use a dual-salt electrolyte with Mg^{2+} and Li^+, a dendrite-free Mg metal anode, and a 2D $Ti_3C_2T_x$ MXene with CNT cathode. A flexible $Ti_3C_2T_x$/CNT "paper" electrode achieved about 100 mAh g^{-1} at 0.1 C and around 50 mAh g^{-1} at 10C. After 500 cycles at 1C, it maintained a specific capacity of 80 mAh g^{-1} [277].

MXene-based composite nanosheets demonstrate rapid and reliable lithium storage capabilities. They address challenges such as self-restacking and structural instability during cycling by combining MXenes with other materials. The synergy between MXenes and these additional components enhances overall performance. To address this, Nb_2CT_x/CNT composite electrodes were prepared for LIBs. This composite performed well as an anode material, with a capacity of over 400 mA h g^{-1} at 0.5C and high cyclability [278].

Additionally, MXene/Ag composite composed of stacked MXene sheets and nanosized Ag particles was synthesized. The MXene/10Ag (Fig. 16a, b, and c) with the highest performance was developed based on the quantity of $AgNO_3$ aqueous solution. This sample had an excellent initial specific capacity of around 550 mA h g^{-1} (Fig. 16d). At 1C and 50C, reversible capacities of 310 mA h g^{-1} and 150 mA h g^{-1} were attained (Fig. 16e) [129].

In another work, using a facile liquid-phase approach to synthesize the composite of cetyltrimethylammonium bromide (CTAB)-Sn (IV) @Ti$_3$C$_2$ as shown in Fig. 16(f). The SEM images of Ti$_3$C$_2$, CTAB@Ti$_3$C$_2$ and CTAB-Sn (IV)@Ti$_3$C$_2$ are demonstrated in Fig. 16(g, h, and i). After

4000 cycles at 2 A g^{-1}, the capacity retention of the CTAB-Sn(IV) @Ti$_3$C$_2$//AC Li-ion hybrid capacitor was 71.1 %, demonstrating robust cycling performance as well (Fig. 16j) [279].

Researchers are currently directing their attention towards Rechargeable Sodium-ion Batteries (SIBs) as a compelling alternative to Lithium-ion Batteries (LIBs). This interest stems from sodium's similar low potential to lithium (−2.71 V vs Standard Hydrogen Electrode for sodium and −3.04 V vs SHE for lithium), its cost-effectiveness, and its abundant availability compared to lithium. However, the larger atomic radius of sodium (1.06 Å) compared to lithium (0.76 Å) results in slower sodium ion diffusion kinetics and more significant volume expansion during charging and discharging processes [280,281]. MXenes, with high conductivity, wide interlayer spacing, and low sodium ion diffusion barriers, show promise for flexible SIBs. However, due to the larger size of sodium ions, SIBs have a lower theoretical capacity (315.8 mAh g^{-1}) compared to LIBs. Therefore, developing novel MXene-based flexible materials with optimized interlayer structures is crucial for enhancing sodium ion diffusion and improving SIB performance [282].

In the past years, using the hydrothermal method, three-dimensional flower-like structures of VO_2/MXenes are synthesized as anode materials for sodium-ion batteries. These structures exhibit a reversible capacity of 280.9 mAh g^{-1} after 200 cycles at a current density of 0.1 A g^{-1} [283].

To improve the performance of sodium ion batteries (SIBs), Sulfur-decorated Ti_3C_2 MXenes are produced through a solution soaking technique with electrostatic attraction as shown in Fig. 17(a). Analysis of SEM image from Fig. 17(b) confirms the presence of sulfur-containing materials on the surface of Ti_3C_2 MXenes. As demonstrated in Fig. 17(c), the sulfur-modified Ti_3C_2 MXene, employed as an anode in sodium ion batteries, exhibits a reversible capacity of 135 mAh g^{-1} under a significant current density of 2 A g^{-1} after completing 1000 cycles [284].

Potassium offers a lower reduction potential (−2.93 V vs SHE) and a higher theoretical capacity (687 mAh g^{-1}) compared to sodium, placing it in line with lithium and positioning it as a promising alternative for LIBs. However, its larger ion radius leads to substantial volume

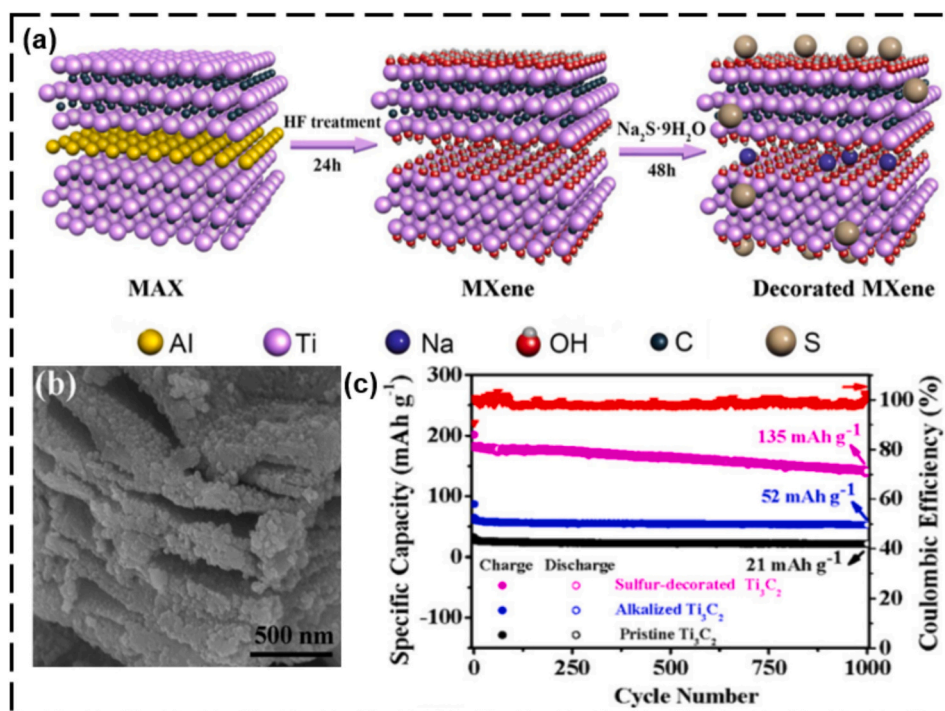**Fig. 17.** (a) A diagram demonstrating the steps involved in the preparation of sulfur-decorated- MXenes (Ti$_3$C$_2$); (b) SEM images of sulfur-decorated Ti$_3$C$_2$ MXenes; (c) the cyclic stability and Coulombic efficiencies of sulfur-modified Ti$_3$C$_2$ MXenes and alkali-decorated Ti$_3$C$_2$ MXenes at a current density of 2 A g^{-1}. (Reprinted with permission from Ref. [284], Chemical Engineering Journal, © 2019 Elsevier).

fluctuations during charging and discharging, constraining the selection of electrode materials for PIBs. Initial calculations indicate that 2D conductive MXenes, with their ample interlayer gaps, can accommodate potassium ions, underscoring their potential as high-capacity anode materials for PIBs [285].

The initial investigation shows, composites of TiO_2/Ti_3C_2 with expanded interlayer spacing demonstrate sustained cyclability, retaining 42 mA h·g^{-1} at a high current density of 200 mA·g^{-1} over 500 cycles [286].

In further research to enhance KIBs' electrochemical performance, researchers produced alkalized (a-Ti_3C_2) MXene nanoribbons through continuous shaking treatment of pristine Ti_3C_2 MXene in a KOH solution (Fig. 18a). SEM and TEM images in Fig. 18(b, c) display a-Ti_3C_2 nanoribbons (MNRs). The a-Ti_3C_2 anodes exhibited outstanding sodium/potassium storage performance, with high reversible capacities of 168 and 136 mA h g^{-1} at 20 mA g^{-1} and 84 and 78 mA h g^{-1} at 200 mA g^{-1} achieved for SIBs and KIBs, respectively. Moreover, a-Ti_3C_2 exhibited substantial long-term cycling performance, maintaining a discharge capacity of approximately 50 mA h g^{-1} at 200 mA g^{-1} over 500 cycles (Fig. 18d) [287]. When employed as an anode material in KIBs, it demonstrates the potential for achieving substantial reversible capacities. Table 5 outlines the performance of MXene-based materials in battery applications. Therefore, the continued development in MXene-based flexible electrodes has been immensely important for enhancing storage capability and cycling stability in battery applications.

5. Challenges and future prospectives

Recently, there has been a surge in interest surrounding a novel class of materials known as MXenes, evoking memories of the exciting advancements seen during the golden age of graphene. MXenes exhibit a remarkable range of physical and chemical properties, presenting promising prospects for various emerging energy applications, notably in heavy-duty energy storage devices [303]. Despite notable advancements in this rapidly evolving field, there remains considerable distance

Table 5
Performances of MXene-based materials in LIBs, NIBs and KIBs.

Battery type	Material	Specific capacity (mAh·g^{-1})	Ref.
Li-ion battery	Ti_3C_2	123.6 mAh g^{-1} @ 1C	[288]
	Nb_2CT_X	170 mAh g^{-1} @ 1C	[289]
	V_2CT_X	260 mAh g^{-1} @ 1C	[289]
	$Ti_3C_2T_X/NiCo_2O_4$	1330 mAh g^{-1} @ 0.1C	[290]
	Nb_2CT_X/CNT	400 mAh g^{-1} @ 0.5C	[278]
	$Fe_3O_4@ Ti_3C_2T_X$	747.4 mAh g^{-1} @ 1C	[291]
	$rGO/Ti_3C_2T_X$	221 mAh g^{-1} @ 50 mAg^{-1}	[292]
	$MoS_2/Ti_3C_2T_X$	656 mAh g^{-1} @ 50 mAg^{-1}	[293]
	$SnS/Ti_3C_2T_X$	412.8 mAh g^{-1} @ 100 mAg^{-1}	[294]
Na-ion battery	V_2CT_x	22 mAh g^{-1} @ 20C	[295]
	Hf_3CT_X	90 mAh g^{-1} @ 10 mAg^{-1}	[296]
	$Ti_3C_2T_X/Sb_2O_3$	472 mAh g^{-1} @ 0.1 Ag^{-1}	[123]
	$Ti_3C_2T_X/VO_2$	280.9 mAh g^{-1} @ 0.1 Ag^{-1}	[283]
	$Ti_3C_2T_X/FeS_2$	563 mAh g^{-1} @ 0.1 Ag^{-1}	[298]
	$Ti_3C_2T_X/TiO_2$	153 mAh g^{-1} @ 0.6 Ag^{-1}	[286]
K-ion battery	Ti_3CNT_x	90 mAh g^{-1} @ 0.01 Ag^{-1}	[299]
	$Ti_3C_2T_X/MoS_2$	290.7 mAh g^{-1} @ 0.05 Ag^{-1}	[300]
	$MoSe_2/MXene @C$	350 mAh g^{-1} @ 0.1 Ag^{-1}	[301]
	Ti_3C_2-Derived Potassium Titanate NRs	105 mAh g^{-1} @ 0.1 Ag^{-1}	[302]

to cover before novel MXene materials can be effectively integrated into practical energy storage devices. MXene-based energy storage technologies, such as rechargeable batteries, supercapacitors, and ion

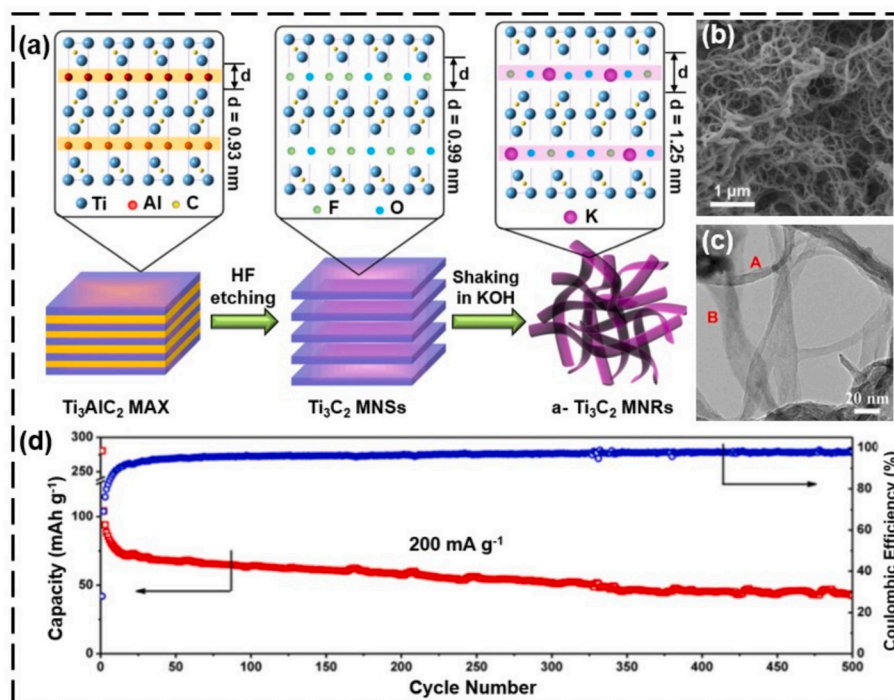**Fig. 18.** (a) Schematic illustrating the synthesis of a-Ti_3C_2 MXene nanoribbons (MNRs). (b) SEM image of a-Ti_3C_2 MNRs. (c) TEM image of a-Ti_3C_2 MNRs. (d) Cycle performance and coulombic efficiency of a-Ti_3C_2 MNRs over a long time at 200 mA g^{-1}.
(a–d) (Reproduced with permission from Ref. [287], Nano Energy, Copyright 2017, Elsevier.)

capacitors, are currently in their early stages of development and require substantial enhancements moving forward [196,304]. MXenes have garnered substantial global research attention and have exhibited considerable promise in energy storage applications due to their layered structure, exceptional hydrophilicity, metallic properties, high mobility of charge carriers, adjustable bandgap, and diverse surface chemistry [305]. Despite the promising electrochemical energy storage performance demonstrated by pure MXenes and MXene-based electrode materials, which have garnered significant achievements through extensive academic and industrial research and applications in energy storage devices, there remains considerable scope for further development [306]. In spite of the superior performance of MXene based materials still there are few challenges associated with this material that hinder the practical utilization in energy storage application [307]. Specifically, the primary obstacles to the production of high-performance energy storage devices based on MXene materials include [308,309]:

- In the realm of acid etching techniques for producing MXenes, there are typically low yields and considerable risks involved. Therefore, it's crucial to establish a synthetic approach that is both controllable and efficient, while also prioritizing environmental friendliness and safety. This approach should enable the synthesis of MXenes with precise layer control, adjustable surface characteristics, expanded interlayer spacing, and exceptional quality. Moving forward, there should be a shift towards exploring fluoride-free and bottom-up methods such as chemical vapor deposition and atomic layer deposition, which offer promising avenues for achieving these goals [310].

- The oxidation of MXene is linked to surface defects resulting from the chemical etching process. This can be reduced by removing dissolved oxygen with dry nitrogen and storing MXenes at lower temperatures. Factors like MXene aggregation and structural properties such as basal spacing and surface chemistry greatly affect the electrochemical charge storage mechanism of MXene-based electrodes. [311].

- MXenes are typically obtained by removing main group elements like Al or Si through etching the MAX phase. Despite using techniques like XRD, EDS, XPS, and NMR, pinpointing precise surface termination groups on MXenes remains challenging. Our understanding of MXenes' surface/interface chemistry is limited, making theoretical simulations essential for correlating performance with structure. However, experimental findings are crucial for validating these theories, especially considering MXenes' importance in energy applications [312].

- Research on MXenes beyond $Ti_3C_2T_x$ is limited. While over 70 % of publications focus on titanium-based MXenes (Ti-MXene), this has laid the foundation for customizable 2D MXene materials. Yet, numerous other transition metals show promise for broader applications. Exploring novel MXenes for energy storage devices holds great potential and is an area ripe for exploration. There's growing interest in using theoretical and computational techniques to explore non-titanium MXenes [313].

- The continuous progress of MXene-based materials encounters hurdles like restacking and instability in oxygen-rich environments. Overcoming this requires strategic structural designs and precise morphological manipulation of electrodes. Creating 3D porous architectures, aerogels, and applying coatings can enhance stability and performance [314].

- Theoretical investigations need to account for the diverse distribution of surface groups and stacked layers in MXenes to provide accurate property predictions and experimental guidance. Incorporating simulations with advanced computational techniques such as machine learning, Density Functional Theory (DFT), and high-throughput computation is crucial for comprehending surface chemistries and interfaces. Further, there's a need for improved theories, predictive models, and computing tools to bridge the gap between predictions and experimental results at a lower cost [315].

- Most of the research on MXene batteries has focused on coin cells, primarily aiming to characterize the electrochemical properties of the active materials. However, there is a growing need to develop and integrate pouch-type batteries and supercapacitors into flexible or wearable electronics in the future. Therefore, it is essential to prepare by expanding the supply of solid-state electrolytes capable of accommodating the exceptional characteristics of MXene-based versatile electrodes [316].

MXene based electrode materials show great promise across various applications due to their unique nanostructures, large surface areas, and customizable compositions. Ether-based electrolytes can boost capacitance and extend cycling life in energy storage devices, while aqueous electrolytes are favoured for their eco-friendly, safe, and scalable characteristics. There's also anticipation for thinner and more stable electrode/electrolyte interfaces to improve storage efficiency and mitigate volume changes. Overcoming these challenges will be pivotal in advancing MXene-based materials in energy storage applications. Despite the challenges mentioned earlier, MXene-based electrode materials offer promising prospects not only in energy storage and conversion but also in catalysis, environmental protection, and biomedicine. Understanding the electrochemical charge storage mechanism of MXene-based materials requires significant efforts, innovative ideas, and advanced research methods.

6. Conclusions

This review offers a comprehensive overview of the latest advancements in MXene-based materials for energy storage applications, with a particular focus on supercapacitors and batteries. The synthesis methods for MXenes, including both top-down and bottom-up approaches including their limitations and future prospects were discussed in detail. The review highlights the notable properties of MXenes, such as structural stability, electronic characteristics, hydrophilicity, and mechanical properties. Emphasis is placed on MXenes' role in energy storage devices, driven by their outstanding electrochemical performance, high specific surface area, excellent electrical conductivity, and unique interlayer spacing, which facilitate efficient charge storage and rapid ion diffusion. The review integrates a data-driven perspective on research trends and explores various composite configurations of MXenes, including those with carbon, metal oxides, and conducting polymers, for their potential in enhancing the performance of supercapacitors and MXene-based electrodes for batteries. It discussed the challenges and future prospects of MXene in energy storage applications, offering practical insights and strategies for enhancing stability, scalability, and overall performance. $Ti_3C_2T_x$ MXene boasts high electrical conductivity (25,000 S cm^{-1}), tensile strength (up to 570 MPa), and a Young's modulus of 333 $\pm$ 13 GPa. Sc_2CF_2 MXene shows remarkable thermal conductivity (722 W/m·K), while Ti_3CNT_x offers EMI shielding effectiveness of 116 dB. Delaminated Ti_3C_2 MXene electrodes deliver a specific capacitance of up to 654 F g^{-1}, highlighting MXene's potential in practical applications. Ultimately, the review serves as a comprehensive analysis of recent research and a guide for future research directions in harnessing MXenes to address global energy and sustainability challenges.

Ethical approval

Not applicable.

CRediT authorship contribution statement

Sahil Jangra: Writing – original draft, Software, Methodology, Data curation, Conceptualization. **Bhushan Kumar:** Writing – original draft,

Data curation. **Jaishree Sharma:** Writing – original draft, Data curation. **Shilpi Sengupta:** Writing – original draft, Data curation. **Subhankar Das:** Writing – review & editing. **R.K. Brajpuriya:** Supervision. **Anil Ohlan:** Writing – review & editing. **Yogendra Kumar Mishra:** Writing – review & editing. **M.S. Goyat:** Supervision.

Declaration of competing interest

The authors declare that they have no known competing financial interests or personal relationships that could have appeared to influence the work reported in this paper.

Data availability

No data was used for the research described in the article.

Acknowledgments

References

[1] K. Poonam, A. Sharma, S.K. Arora, Tripathi, review of supercapacitors: materials and devices, J. Energy Storage 21 (2019) 801–825, https://doi.org/10.1016/j.est.2019.01.010.

[2] M. Asif, Renewable Energy: Technologies, Applications and Trends, in: Handb. Energy Environ. 21st Century, CRC Press, n.d.: pp. 41–65.

[3] M.H. Kabir, S.M.S. Newaz, T. Kabir, A.S. Howlader, Integrating solar power with existing grids: strategies, technologies, and challenges & review, Int. J. Sci. Eng. 1 (2024) 48–62.

[4] X. Zhang, L. Hou, A. Ciesielski, P. Samorì, 2D materials beyond graphene for high-performance energy storage applications, Adv. Energy Mater. 6 (2016), https://doi.org/10.1002/aenm.201600671.

[5] Y. Gogotsi, P. Simon, True performance metrics in electrochemical energy storage, Science (80-.). 334 (2011) 917–918.

[6] P. Simon, Y. Gogotsi, Materials for electrochemical capacitors, Nat. Mater. 7 (2008) 845–854.

[7] F. Bonaccorso, L. Colombo, G. Yu, M. Stoller, V. Tozzini, A.C. Ferrari, R.S. Ruoff, V. Pellegrini, Graphene, related two-dimensional crystals, and hybrid systems for energy conversion and storage, Science (80-.). 347 (2015) 1246501.

[8] D. Larcher, J.-M. Tarascon, Towards greener and more sustainable batteries for electrical energy storage, Nat. Chem. 7 (2015) 19–29.

[9] M. Vijayakumar, A.B. Sankar, G. Elsa, M. Karthik, Fabrication of Supercapacitor Devices and their Applications, in: Mater. Energy Storage, CRC Press, n.d.: pp. 215–232.

[10] C. Zhong, Y. Deng, W. Hu, J. Qiao, L. Zhang, J. Zhang, A review of electrolyte materials and compositions for electrochemical supercapacitors, Chem. Soc. Rev. 44 (2015) 7484–7539.

[11] W. Bi, G. Gao, C. Li, G. Wu, G. Cao, Synthesis, properties, and applications of MXenes and their composites for electrical energy storage, Prog. Mater. Sci. 142 (2024) 101227, https://doi.org/10.1016/j.pmatsci.2023.101227.

[12] S. Chen, J. Ma, C. Song, X. Cai, F. Jiao, H. Du, Template-free synthesis of flower-like hierarchical vanadium nitride/carbon composites for long cycle-life half and full lithium-ion batteries, J. Power Sources 520 (2022) 230924.

[13] P. Li, G. Zhao, X. Zheng, X. Xu, C. Yao, W. Sun, S.X. Dou, Recent progress on silicon-based anode materials for practical lithium-ion battery applications, Energy Storage Mater. 15 (2018) 422–446.

[14] Y. Sun, D. Chen, Z. Liang, Two-dimensional MXenes for energy storage and conversion applications, mater. Today, Energy 5 (2017) 22–36, https://doi.org/10.1016/j.mtener.2017.04.008.

[15] P. Ares, K.S. Novoselov, Recent advances in graphene and other 2D materials, Nano, Mater. Sci. 4 (2022) 3–9.

[16] K.S. Novoselov, A.K. Geim, S. V Morozov, D. Jiang, Y. Zhang, S. V Dubonos, I. V Grigorieva, A.A. Firsov, Electric field effect in atomically thin carbon films, Science (80-.). 306 (2004) 666–669.

[17] E.P. Randviir, D.A.C. Brownson, C.E. Banks, A decade of graphene research: production, applications and outlook, Mater. Today 17 (2014) 426–432.

[18] G.R. Bhimanapati, Z. Lin, V. Meunier, Y. Jung, J. Cha, S. Das, D. Xiao, Y. Son, M. S. Strano, V.R. Cooper, L. Liang, S.G. Louie, E. Ringe, W. Zhou, S.S. Kim, R. R. Naik, B.G. Sumpter, H. Terrones, F. Xia, Y. Wang, J. Zhu, D. Akinwande, N. Alem, J.A. Schuller, R.E. Schaak, M. Terrones, J.A. Robinson, Recent advances in Two-dimensional materials beyond graphene, ACS Nano 9 (2015) 11509–11539, https://doi.org/10.1021/acsnano.5b05556.

[19] Y. Gogotsi, B. Anasori, The rise of MXenes, ACS Nano 13 (2019) 8491–8494.

[20] R.M. Ronchi, J.T. Arantes, S.F. Santos, Synthesis, structure, properties and applications of MXenes: current status and perspectives, Ceram. Int. 45 (2019) 18167–18188, https://doi.org/10.1016/j.ceramint.2019.06.114.

[21] K. Rasool, M. Helal, A. Ali, C.E. Ren, Y. Gogotsi, K.A. Mahmoud, Antibacterial activity of Ti3C2Tx MXene, ACS Nano 10 (2016) 3674–3684, https://doi.org/10.1021/acsnano.6b00181.

[22] M. Pandey, K. Deshmukh, A. Raman, A. Asok, S. Appukuttan, G.R. Suman, Prospects of MXene and graphene for energy storage and conversion, Renew. Sustain. Energy Rev. 189 (2024) 114030.

[23] Z. Otgonbayar, S. Yang, I.J. Kim, W.C. Oh, Recent advances in Two-dimensional MXene for supercapacitor applications: Progress, challenges, and perspectives, Nanomaterials 13 (2023), https://doi.org/10.3390/nano13050919.

[24] M. Alhabeb, K. Maleski, B. Anasori, P. Lelyukh, L. Clark, S. Sin, Y. Gogotsi, Guidelines for synthesis and processing of two-dimensional titanium carbide (Ti3C2T x MXene), Chem. Mater. 29 (2017) 7633–7644.

[25] U.U. Rahman, M. Humayun, U. Ghani, M. Usman, H. Ullah, A. Khan, N.M. El-Metwaly, A. Khan, MXenes as emerging materials: synthesis, properties, and applications, Molecules 27 (2022), https://doi.org/10.3390/molecules27154909.

[26] M.A. Zaed, K.H. Tan, N. Saidur, N. Abdullah, A.K. Pandey, Invited viewpoint: pathways to low-cost MXene synthesis, J. Mater. Sci. 1–20 (2024).

[27] A. Inman, T. Hryhorchuk, L. Bi, R.J. Wang, B. Greenspan, T. Tabb, E.M. Gallo, A. VahidMohammadi, G. Dion, A. Danielescu, Wearable energy storage with MXene textile supercapacitors for real world use, J. Mater. Chem. A 11 (2023) 3514–3523.

[28] S. Pu, Z. Wang, Y. Xie, J. Fan, Z. Xu, Y. Wang, H. He, X. Zhang, W. Yang, H. Zhang, Origin and regulation of self-discharge in MXene supercapacitors, Adv. Funct. Mater. 33 (2023) 2208715.

[29] Y. Wang, Y. Wang, Recent progress in MXene layers materials for supercapacitors: high-performance electrodes, SMARTMAT 4 (2023), https://doi.org/10.1002/smm2.1130.

[30] R. Ma, L. Cao, J. Zhuo, J. Lu, J. Chen, J. Huang, G. Yang, F. Yi, Designed redox-electrolyte strategy boosted with electrode engineering for high-performance Ti3C2Tx MXene-based supercapacitors, Adv. Energy Mater. 13 (2023) 2301229.

[31] T. Bashir, S. Zhou, S. Yang, S.A. Ismail, T. Ali, H. Wang, J. Zhao, L. Gao, Progress in 3D-MXene electrodes for lithium/sodium/potassium/magnesium/zinc/aluminum-ion batteries, Electrochem. Energy Rev. 6 (2023) 5.

[32] M.A.A.M. Abdah, J. Cherusseri, N.A. Dzulkarnain, M. Mokhtar, M.S. Su'ait, Y. S. Tan, M.N. Mustafa, M. Khalid, A. Numan, A. Radwan, Facile synthesis of microwave-etched Ti3C2 MXene/activated carbon hybrid for lithium-ion battery anode, J. Electroanal. Chem. 928 (2023) 117050.

[33] R. Verma, P. Thakur, A. Chauhan, R. Jasrotia, A. Thakur, A review on MXene and its' composites for electromagnetic interference (EMI) shielding applications, Carbon N. Y. 208 (2023) 170–190.

[34] M.S. Irfan, M.A. Ali, T. Khan, S. Anwer, K. Liao, R. Umer, MXene and graphene coated multifunctional fiber reinforced aerospace composites with sensing and EMI shielding abilities, Compos. Part A Appl. Sci. Manuf. 165 (2023) 107351.

[35] Y. Li, S. Huang, S. Peng, H. Jia, J. Pang, B. Ibarlucea, C. Hou, Y. Cao, W. Zhou, H. Liu, Toward smart sensing by MXene, Small 19 (2023) 2206126.

[36] S.M. Majhi, A. Ali, Y.E. Greish, H.F. El-Maghraby, S.T. Mahmoud, V2CTX MXene-based hybrid sensor with high selectivity and ppb-level detection for acetone at room temperature, Sci. Rep. 13 (2023) 3114.

[37] N.H. Solangi, N.M. Mubarak, R.R. Karri, S.A. Mazari, A.S. Jatoi, Advanced growth of 2D MXene for electrochemical sensors, Environ. Res. 222 (2023) 115279.

[38] N.H. Solangi, S.A. Mazari, N.M. Mubarak, R.R. Karri, N. Rajamohan, D.-V.N. Vo, Recent trends in MXene-based material for biomedical applications, Environ. Res. 115337 (2023).

[39] N.H. Solangi, R.R. Karri, S.A. Mazari, N.M. Mubarak, A.S. Jatoi, G. Malafaia, A. K. Azad, MXene as emerging material for photocatalytic degradation of environmental pollutants, Coord. Chem. Rev. 477 (2023) 214965.

[41] M. Naguib, V.N. Mochalin, M.W. Barsoum, Y. Gogotsi, 25th anniversary article: MXenes: a new family of two-dimensional materials, Adv. Mater. 26 (2014) 992–1005, https://doi.org/10.1002/adma.201304famil.

[42] N. Ahmad, S. Rasheed, A. Mohyuddin, B. Fatima, M.I. Nabeel, M.T. Riaz, M. Najam-ul-Haq, D. Hussain, 2D MXenes and their composites; design, synthesis, and environmental sensing applications, Chemosphere 141280 (2024).

[43] J.A. Kumar, P. Prakash, T. Krithiga, D.J. Amarnath, J. Premkumar, N. Rajamohan, Y. Vasseghian, P. Saravanan, M. Rajasimman, Methods of synthesis, characteristics, and environmental applications of MXene: a comprehensive review, Chemosphere 286 (2022) 131607.

[44] Z. Chen, C. Zhao, X. Zhou, L. Xiao, Z. Li, Y. Zhang, A review of top-down strategies for the production of quantum-sized materials, Small Sci. 3 (2023) 2300086.

[45] S. Venkateshalu, A.N. Grace, Synthesis and processing strategies, in, Fundam. Asp. Perspect. MXenes, Springer (2022) 17–36.

[46] S. Siddique, A. Waheed, M. Iftikhar, M.T. Mehran, M.Z. Zarif, H.A. Arafat, S. Hussain, F. Shahzad, Fluorine-free MXenes via molten salt Lewis acidic etching: applications, challenges, and future outlook, Prog. Mater. Sci. 101183 (2023).

[47] G. Murali, J.K. Reddy Modigunta, Y.H. Park, J.-H. Lee, J. Rawal, S.-Y. Lee, I. In, S.-J. Park, A review on MXene synthesis, stability, and photocatalytic applications, ACS Nano 16 (2022) 13370–13429.

[48] D. Wang, C. Zhou, A.S. Filatov, W. Cho, F. Lagunas, M. Wang, S. Vaikuntanathan, C. Liu, R.F. Klie, D. V Talapin, Direct synthesis and chemical vapor deposition of 2D carbide and nitride MXenes, Science (80-.). 379 (2023) 1242–1247.

[49] F. Song, G. Li, Y. Zhu, Z. Wu, X. Xie, N. Zhang, Rising from the horizon: three-dimensional functional architectures assembled with MXene nanosheets, J. Mater. Chem. A 8 (2020) 18538–18559.

[50] K.M. Musthafa, A. Hamzah, O.W. Ling, A.H.A. Rosol, N. Mohamed, M.M. Mafroos, S.W. Harun, Synthesisation, fabrication, and incorporation techniques of MAX

phase and MXene Saturable absorber in passively Q-switched and mode-locked all-fibre laser cavities: a review, J. Adv. Res. Appl. Sci. Eng. Technol. 32 (2023) 119–141.

[51] M. Naguib, O. Mashtalir, J. Carle, V. Presser, J. Lu, L. Hultman, Y. Gogotsi, M. W. Barsoum, Two-dimensional transition metal carbides, ACS Nano 6 (2012) 1322–1331, https://doi.org/10.1021/nn204153h.

[52] M.Z. Abid, K. Rafiq, A. Aslam, R. Jin, E. Hussain, Scope, evaluation and current perspectives of MXene synthesis strategies for state of the art applications, J. Mater. Chem. A (2024) 7351–7395, https://doi.org/10.1039/d3ta06548k.

[53] B. Anasori, M. Naguib, G. Editors, Two-dimensional MXenes, MRS Bull. 48 (2023) 238–244.

[54] M. Rahman, M.S. Al Mamun, Future prospects of MXenes: synthesis, functionalization, properties, and application in field effect transistors, Nanoscale Adv. 6 (2023) 367–385, https://doi.org/10.1039/d3na00874f.

[55] O. Mashtalir, M. Naguib, B. Dyatkin, Y. Gogotsi, M.W. Barsoum, Kinetics of aluminum extraction from Ti3AlC2 in hydrofluoric acid, Mater. Chem. Phys. 139 (2013) 147–152.

[56] M. Naguib, M. Kurtoglu, V. Presser, J. Lu, J. Niu, M. Heon, L. Hultman, Y. Gogotsi, M.W. Barsoum, Two-dimensional nanocrystals produced by exfoliation of Ti3AlC2, Adv. Mater. 23 (2011) 4248.

[57] N.M. Tran, Q.T.H. Ta, J.-S. Noh, Unusual synthesis of safflower-shaped TiO2/ Ti3C2 heterostructures initiated from two-dimensional Ti3C2 MXene, Appl. Surf. Sci. 538 (2021) 148023.

[58] P. Zhang, M. Xiang, H. Liu, C. Yang, S. Deng, Novel two-dimensional magnetic titanium carbide for methylene blue removal over a wide pH range: insight into removal performance and mechanism, ACS Appl. Mater. Interfaces 11 (2019) 24027–24036.

[59] Z. Li, L. Wang, D. Sun, Y. Zhang, B. Liu, Q. Hu, A. Zhou, Synthesis and thermal stability of two-dimensional carbide MXene Ti3C2, Mater. Sci. Eng. B Solid-State Mater. Adv. Technol. 191 (2015) 33–40, https://doi.org/10.1016/j. mseb.2014.10.009.

[60] M. Tahir, A. Sherryna, R. Mansoor, A.A. Khan, S. Tasleem, B. Tahir, Titanium carbide MXene nanostructures as catalysts and cocatalysts for photocatalytic fuel production: a review, ACS Appl. Nano Mater. 5 (2022) 18–54.

[61] A. Gentile, S. Marchionna, M. Balordi, G. Pagot, C. Ferrara, V. Di Noto, R. Ruffo, Critical analysis of MXene production with in-situ HF forming agents for sustainable manufacturing, ChemElectroChem 9 (2022) e202200891.

[62] I. Mubeen, S. Shah, E. Pervaiz, W. Miran, The promising frontier for next-generation energy storage and clean energy production: a review on synthesis and applications of MXenes, Mater. Sci. Energy Technol. 7 (2024) 180–194, https:// doi.org/10.1016/j.mset.2023.10.002.

[63] Y. Yu, Q. Fan, Z. Li, P. Fu, MXene-based electrode materials for supercapacitors: synthesis, properties, and optimization strategies, Mater. Today Sustain. 24 (2023) 100551.

[64] Y. Zhu, J. Liu, T. Guo, J.J. Wang, X. Tang, V. Nicolosi, Multifunctional Ti3C2Tx MXene composite hydrogels with strain sensitivity toward absorption-dominated electromagnetic-interference shielding, ACS Nano 15 (2021) 1465–1474, https:// doi.org/10.1021/acsnano.0c08830.

[65] J. Halim, S. Kota, M.R. Lukatskaya, M. Naguib, M. Zhao, E.J. Moon, J. Pitock, J. Nanda, S.J. May, Y. Gogotsi, Synthesis and characterization of 2D molybdenum carbide (MXene), Adv. Funct. Mater. 26 (2016) 3118–3127.

[66] F. Liu, A. Zhou, J. Chen, J. Jia, W. Zhou, L. Wang, Q. Hu, Preparation of Ti3C2 and Ti2C MXenes by fluoride salts etching and methane adsorptive properties, Appl. Surf. Sci. 416 (2017) 781–789, https://doi.org/10.1016/j. apsusc.2017.04.239.

[67] L.-Y. Xiu, Z.-Y. Wang, J.-S. Qiu, General synthesis of MXene by green etching chemistry of fluoride-free Lewis acidic melts, Rare Met. 39 (2020) 1237–1238.

[68] O.J. Kewate, I. Hussain, N. Tyagi, S. Saxena, K. Zhang, E.G. Rajamansingh, N. Chinnappan, H. Joshi, S. Punniyakoti, Nb-based MXenes: structures, properties, synthesis, and application towards supercapacitors, J. Energy Storage 94 (2024) 112445, https://doi.org/10.1016/j.est.2024.112445.

[69] S. Shah, I. Mubeen, E. Pervaiz, H. Nasir, Facile and efficient synthesis of carboxylic terminated Ti3C2Tx nanosheets using citric acid, FlatChem 41 (2023) 100544, https://doi.org/10.1016/j.flatc.2023.100544.

[71] M. Malaki, A. Maleki, R.S. Varma, MXenes and ultrasonication, J. Mater. Chem. A 7 (2019) 10843–10857.

[72] L. Liu, M. Orbay, S. Luo, S. Duluard, H. Shao, J. Harmel, P. Rozier, P.-L. Taberna, P. Simon, Exfoliation and delamination of Ti3C2T x MXene prepared via molten salt etching route, ACS Nano 16 (2021) 111–118.

[73] X. Wang, Y. Shi, J. Qiu, Z. Wang, Molten-salt etching synthesis of delaminatable MXenes, Chem. Commun. 59 (2023) 5063–5066.

[74] J. Chen, Q. Jin, Y. Li, H. Shao, P. Liu, Y. Liu, P. Taberna, Q. Huang, Z. Lin, P. Simon, Molten salt-shielded synthesis (MS3) of MXenes in air, Energy Environ. Mater. 6 (2023) e12328.

[75] P. Urbankowski, B. Anasori, T. Makaryan, D. Er, S. Kota, P.L. Walsh, M. Zhao, V. B. Shenoy, M.W. Barsoum, Y. Gogotsi, Synthesis of two-dimensional titanium nitride Ti 4 N 3 (MXene), Nanoscale 8 (2016) 11385–11391.

[76] M. Ghidiu, M.R. Lukatskaya, M.-Q. Zhao, Y. Gogotsi, M.W. Barsoum, Conductive two-dimensional titanium carbide 'clay'with high volumetric capacitance, Nature 516 (2014) 78–81.

[77] M. Shen, J. Wang, Guidelines for the molten salt etching of MXenes, Transit. Met. Carbides Nitrides Handb. Synth. Process. Prop. Appl. (2024) 85–108.

[78] G. Ljubek, M. Kralj, M. Kraljić Roković, Fluorine-free mechanochemical synthesis of MXene, Mater. Sci. Technol. 39 (2023) 1645–1649.

[79] J. Chen, M. Chen, W. Zhou, X. Xu, B. Liu, W. Zhang, C. Wong, Simplified synthesis of fluoride-free Ti3C2T x via electrochemical etching toward high-performance electrochemical capacitors, ACS Nano 16 (2022) 2461–2470.

[81] M. Li, J. Lu, K. Luo, Y. Li, K. Chang, K. Chen, J. Zhou, J. Rosen, L. Hultman, P. Eklund, P.O.Å. Persson, S. Du, Z. Chai, Z. Huang, Q. Huang, Element replacement approach by reaction with Lewis acidic molten salts to synthesize Nanolaminated MAX phases and MXenes, J. Am. Chem. Soc. 141 (2019) 4730–4737, https://doi.org/10.1021/jacs.9b00574.

[82] Y. Bai, C. Liu, T. Chen, W. Li, S. Zheng, Y. Pi, Y. Luo, H. Pang, MXene-copper/ cobalt hybrids via Lewis acidic molten salts etching for high performance symmetric supercapacitors, Angew. Chemie 133 (2021) 25522–25526.

[83] T. Yin, Y. Li, R. Wang, O.A. Al-Hartomy, A. Al-Ghamdi, S. Wageh, X. Luo, X. Tang, H. Zhang, Synthesis of Ti3C2Fx MXene with controllable fluorination by electrochemical etching for lithium-ion batteries applications, Ceram. Int. 47 (2021) 28642–28649, https://doi.org/10.1016/j.ceramint.2021.07.023.

[84] V. Kamysbayev, A.S. Filatov, H. Hu, X. Rui, F. Lagunas, D. Wang, R.F. Klie, D. V Talapin, Covalent surface modifications and superconductivity of two-dimensional metal carbide MXenes, Science (80-.). 369 (2020) 979–983.

[85] S. Sardar, A. Jana, Covalent surface alteration of MXenes and its effect on superconductivity, Matter 3 (2020) 1397–1399.

[86] M.P. Bilibana, Electrochemical properties of MXenes and applications, Adv. Sens. Energy Mater. 2 (2023) 100080.

[87] L. Zhang, W. Song, H. Liu, H. Ding, Y. Yan, R. Chen, Influencing factors on synthesis and properties of MXene: a review, Processes 10 (2022) 1744.

[88] G. Manasa, C.S. Rout, Versatile MXenes as Electrochemical Sensors for Heavy Metal Ions and Phenolic Moiety-Containing Industrial Chemicals: Recent Development and Prospects, Mater, Adv, 2024.

[89] W. Sun, S.A. Shah, Y. Chen, Z. Tan, H. Gao, T. Habib, M. Radovic, M.J. Green, Electrochemical etching of Ti 2 AlC to Ti 2 CT x (MXene) in low-concentration hydrochloric acid solution, J. Mater. Chem. A 5 (2017) 21663–21668.

[90] S.-Y. Pang, Y.-T. Wong, S. Yuan, Y. Liu, M.-K. Tsang, Z. Yang, H. Huang, W.-T. Wong, J. Hao, Universal strategy for HF-free facile and rapid synthesis of two-dimensional MXenes as multifunctional energy materials, J. Am. Chem. Soc. 141 (2019) 9610–9616.

[91] Y. Wei, P. Zhang, R.A. Soomro, Q. Zhu, B. Xu, Advances in the synthesis of 2D MXenes, Adv. Mater. 33 (2021) 2103148.

[92] C. Xu, L. Wang, Z. Liu, L. Chen, J. Guo, N. Kang, X.-L. Ma, H.-M. Cheng, W. Ren, Large-area high-quality 2D ultrathin Mo2C superconducting crystals, Nat. Mater. 14 (2015) 1135–1141.

[93] F. Turker, O.R. Caylan, N. Mehmood, T.S. Kasirga, C. Sevik, G., Cambaz buke, CVD synthesis and characterization of thin Mo2C crystals, J. Am. Ceram. Soc. 103 (2020) 5586–5593.

[94] W. Bi, G. Gao, C. Li, G. Wu, G. Cao, Synthesis, properties, and applications of MXenes and their composites for electrical energy storage, Prog. Mater. Sci. 101227 (2023).

[95] D. Geng, X. Zhao, Z. Chen, W. Sun, W. Fu, J. Chen, W. Liu, W. Zhou, K.P. Loh, Direct synthesis of large-area 2D Mo2C on in situ grown graphene, Adv. Mater. 29 (2017) 1700072.

[96] D.D. Robertson, S.H. Tolbert, A direct and clean route to MXenes, Science (80-.). 379 (2023) 1189–1190.

[97] C. Yang, Q. Jiang, W. Li, H. He, L. Yang, Z. Lu, H. Huang, Ultrafine Pt nanoparticle-decorated 3D hybrid architectures built from reduced graphene oxide and MXene Nanosheets for methanol oxidation, Chem. Mater. 31 (2019) 9277–9287, https://doi.org/10.1021/acs.chemmater.9b02115.

[98] L. Tang, J. Tan, H. Nong, B. Liu, H.-M. Cheng, Chemical vapor deposition growth of two-dimensional compound materials: controllability, material quality, and growth mechanism, accounts, Mater. Res. 2 (2020) 36–47.

[99] X. Xiao, H. Yu, H. Jin, M. Wu, Y. Fang, J. Sun, Z. Hu, T. Li, J. Wu, L. Huang, Salt-templated synthesis of 2D metallic MoN and other nitrides, ACS Nano 11 (2017) 2180–2186.

[100] K. Li, M. Liang, H. Wang, X. Wang, Y. Huang, J. Coelho, S. Pinilla, Y. Zhang, F. Qi, V. Nicolosi, Y. Xu, 3D MXene architectures for efficient energy storage and conversion, Adv. Funct. Mater. 30 (2020), https://doi.org/10.1002/ adfm.202000842.

[101] T.A. Oyehan, B.A. Salami, A.A. Abdulrasheed, H.U. Hambali, A. Gbadamosi, E. Valsami-Jones, T.A. Saleh, MXenes: synthesis, properties, and applications for sustainable energy and environment, Appl. Mater. Today 35 (2023) 101993, https://doi.org/10.1016/j.apmt.2023.101993.

[102] S. Munir, A. Rasheed, T. Rasheed, I. Ayman, S. Ajmal, A. Rehman, I. Shakir, P. O. Agboola, M.F. Warsi, Exploring the influence of critical parameters for the effective synthesis of high-quality 2D MXene, ACS Omega 5 (2020) 26845–26854.

[103] R.P. Pandey, P.A. Rasheed, T. Gomez, K. Rasool, J. Ponraj, K. Prenger, M. Naguib, K.A. Mahmoud, Effect of sheet size and atomic structure on the antibacterial activity of Nb-MXene nanosheets, ACS Appl. Nano Mater. 3 (2020) 11372–11382.

[104] M. Shekhirev, C.E. Shuck, A. Sarycheva, Y. Gogotsi, Progress in Materials Science Characterization of MXenes at every step , from their precursors to single flakes and assembled films, Prog. Mater. Sci. 120 (2021) 100757. doi:https://doi.org/ 10.1016/j.pmatsci.2020.100757.

[105] O. Mashtalir, M.R. Lukatskaya, A.I. Kolesnikov, E. Raymundo-Pinero, M. Naguib, M.W. Barsoum, Y. Gogotsi, The effect of hydrazine intercalation on the structure and capacitance of 2D titanium carbide (MXene), Nanoscale 8 (2016) 9128–9133.

[106] Q. Tao, M. Dahlqvist, J. Lu, S. Kota, R. Meshkian, J. Halim, J. Palisaitis, L. Hultman, M.W. Barsoum, P.O.Å. Persson, Two-dimensional Mo1., 33C MXene with divacancy ordering prepared from parent 3D laminate with in-plane chemical ordering, Nat. Commun. 8 (2017) 14949.

[107] R. Syamsai, A.N. Grace, Ta4C3 MXene as supercapacitor electrodes, J. Alloys Compd. 792 (2019) 1230–1238.

[108] K. Zhu, Y. Jin, F. Du, S. Gao, Z. Gao, X. Meng, G. Chen, Y. Wei, Y. Gao, Synthesis of Ti 2 CT x MXene as electrode materials for symmetric supercapacitor with capable volumetric capacitance, J. Energy Chem. 31 (2019) 11–18, https://doi.org/10.1016/j.jechem.2018.03.010.

[109] X. Zhang, Y. Liu, S. Dong, J. Yang, X. Liu, Flexible electrode based on multi-scaled MXene (Ti3C2Tx) for supercapacitors, J. Alloys Compd. 790 (2019) 517–523, https://doi.org/10.1016/j.jallcom.2019.03.219.

[110] S.A. Zahra, E. Ceesay, S. Rizwan, Zirconia-decorated V2CTx MXene electrodes for supercapacitors, J. Energy Storage 55 (2022) 105721, https://doi.org/10.1016/j.est.2022.105721.

[111] A.S. Levitt, M. Alhabeb, C.B. Hatter, A. Sarycheva, G. Dion, Y. Gogotsi, Electrospun MXene/carbon nanofibers as supercapacitor electrodes, J. Mater. Chem. A 7 (2019) 269–277.

[112] Q. Yang, Z. Huang, X. Li, Z. Liu, H. Li, G. Liang, D. Wang, Q. Huang, S. Zhang, S. Chen, A wholly degradable, rechargeable Zn–Ti3C2 MXene capacitor with superior anti-self-discharge function, ACS Nano 13 (2019) 8275–8283.

[113] X. Xie, M.-Q. Zhao, B. Anasori, K. Maleski, C.E. Ren, J. Li, B.W. Byles, E. Pomerantseva, G. Wang, Y. Gogotsi, Porous heterostructured MXene/carbon nanotube composite paper with high volumetric capacity for sodium-based energy storage devices, Nano Energy 26 (2016) 513–523.

[114] T.-H. Chang, T. Zhang, H. Yang, K. Li, Y. Tian, J.Y. Lee, P.-Y. Chen, Controlled crumpling of two-dimensional titanium carbide (MXene) for highly stretchable, bendable, efficient supercapacitors, ACS Nano 12 (2018) 8048–8059.

[115] G. Wu, T. Li, Z. Wang, M. Li, B. Wang, A. Dong, Molecular ligand-mediated assembly of multicomponent nanosheet superlattices for compact capacitive energy storage, Angew. Chemie 132 (2020) 20809–20816.

[116] X. Wang, H. Li, H. Li, S. Lin, W. Ding, X. Zhu, Z. Sheng, H. Wang, X. Zhu, Y. Sun, 2D/2D 1T-MoS2/Ti3C2 MXene heterostructure with excellent supercapacitor performance, Adv. Funct. Mater. 30 (2020) 190302.

[117] M. Lai, K. Chen, D. Wang, P. Cai, L. Sun, K. Zhang, B. Li, C. Yuan, Y. Zou, Z. Wang, H. Peng, Protective hydrothermal treatment to improve ion pathway in Ti3C2Tx MXene for high-performance flexible supercapacitors, Mater. Today Nano 25 (2024) 100450, https://doi.org/10.1016/j.mtnano.2023.100450.

[118] Y. Liu, J. Gong, J. Wang, C. Hu, M. Xie, X. Jin, S. Wang, Y. Dai, Facile fabrication of MXene supported nickel-cobalt selenide ternary composite via one-step hydrothermal for high-performance asymmetric supercapacitors, J. Alloys Compd. 899 (2022) 163354, https://doi.org/10.1016/j.jallcom.2021.163354.

[119] P. Zhang, J. Li, D. Yang, R.A. Soomro, B. Xu, Flexible carbon dots-intercalated MXene film electrode with outstanding volumetric performance for supercapacitors, Adv. Funct. Mater. 33 (2023) 2209918.

[120] Y.Z. Cai, Y.S. Fang, W.Q. Cao, P. He, M.S. Cao, MXene-CNT/PANI ternary material with excellent supercapacitive performance driven by synergy, J. Alloys Compd. 868 (2021) 159159, https://doi.org/10.1016/j.jallcom.2021.159159.

[121] L. Shao, J. Xu, J. Ma, B. Zhai, Y. Li, R. Xu, Z. Ma, G. Zhang, C. Wang, J. Qiu, MXene/RGO composite aerogels with light and high-strength for supercapacitor electrode materials, Compos. Commun. 19 (2020) 108–113.

[122] J. Come, M. Naguib, P. Rozier, M.W. Barsoum, Y. Gogotsi, P.-L. Taberna, M. Morcrette, P. Simon, A non-aqueous asymmetric cell with a Ti2C-based Two-dimensional negative electrode, J. Electrochem. Soc. 159 (2012) A1368.

[123] X. Guo, X. Xie, S. Choi, Y. Zhao, H. Liu, C. Wang, S. Chang, G. Wang, Sb2O3/MXene(Ti3C2Tx) hybrid anode materials with enhanced performance for sodium-ion batteries, J. Mater. Chem. A 5 (2017) 12445–12452, https://doi.org/10.1039/c7ta02689g.

[124] Y. Xie, H. Zhang, H. Huang, Z. Wang, Z. Xu, H. Zhao, Y. Wang, N. Chen, W. Yang, High-voltage asymmetric MXene-based on-chip micro-supercapacitors, Nano Energy 74 (2020) 104928.

[125] Q. Yang, Z. Xu, B. Fang, T. Huang, S. Cai, H. Chen, Y. Liu, K. Gopalsamy, W. Gao, C. Gao, MXene/graphene hybrid fibers for high performance flexible supercapacitors, J. Mater. Chem. A 5 (2017) 22113–22119.

[126] M. Naguib, J. Halim, J. Lu, K.M. Cook, L. Hultman, Y. Gogotsi, M.W. Barsoum, New two-dimensional niobium and vanadium carbides as promising materials for li-ion batteries, J. Am. Chem. Soc. 135 (2013) 15966–15969, https://doi.org/10.1021/ja405735d.

[127] S. Zhao, X. Meng, K. Zhu, F. Du, G. Chen, Y. Wei, Y. Gogotsi, Y. Gao, Li-ion uptake and increase in interlayer spacing of Nb4C3 MXene, Energy Storage Mater. 8 (2017) 42–48.

[128] X. Zhu, K. Yang, Z. Zhang, S. He, Z. Shen, W. Jiang, Y. Huang, Y. Xu, Q. Jiang, L. Pan, Additive-free anode with high stability: Nb2CT x MXene prepared by HCl-LiF hydrothermal etching for Lithium-ion batteries, ACS Appl. Mater. Interfaces 16 (2024) 28709–28718.

[129] G. Zou, Z. Zhang, J. Guo, B. Liu, Q. Zhang, C. Fernandez, Q. Peng, Synthesis of MXene/ag composites for extraordinary long cycle lifetime lithium storage at high rates, ACS Appl. Mater. Interfaces 8 (2016) 22280–22286.

[130] H. Shi, C.J. Zhang, P. Lu, Y. Dong, P. Wen, Z.-S. Wu, Conducting and lithiophilic MXene/graphene framework for high-capacity, dendrite-free lithium–metal anodes, ACS Nano 13 (2019) 14308–14318.

[131] R. Gan, Y. Liu, N. Yang, C. Tong, M. Deng, Q. Dong, X. Tang, N. Fu, C. Li, Z. Wei, Lithium electrodeposited on lithiophilic LTO/Ti 3 C 2 substrate as a dendrite-free lithium metal anode, J. Mater. Chem. A 8 (2020) 20650–20657.

[132] X. Wang, J. Wang, J. Qin, X. Xie, R. Yang, M. Cao, Surface charge engineering for covalently assembling three-dimensional MXene network for all-climate sodium ion batteries, ACS Appl. Mater. Interfaces 12 (2020) 39181–39194.

[133] T. Zhang, X. Jiang, G. Li, Q. Yao, J.Y. Lee, A red-phosphorous-assisted ball-milling synthesis of few-layered Ti3C2Tx (MXene) Nanodot composite, ChemNanoMat 4 (2018) 56–60.

[134] Z. Xiao, Z. Li, P. Li, X. Meng, R. Wang, Ultrafine Ti3C2 MXene nanodots-interspersed nanosheet for high-energy-density lithium–sulfur batteries, ACS Nano 13 (2019) 3608–3617.

[135] Y. Dong, S. Zheng, J. Qin, X. Zhao, H. Shi, X. Wang, J. Chen, Z.-S. Wu, All-MXene-based integrated electrode constructed by Ti3C2 nanoribbon framework host and nanosheet interlayer for high-energy-density Li–S batteries, ACS Nano 12 (2018) 2381–2388.

[136] X. He, S. Jin, L. Miao, Y. Cai, Y. Hou, H. Li, K. Zhang, Z. Yan, J. Chen, A 3D hydroxylated MXene/carbon nanotubes composite as a scaffold for dendrite-free sodium-metal electrodes, Angew. Chemie Int. Ed. 59 (2020) 16705–16711.

[137] H. Tang, Q. Hu, M. Zheng, Y. Chi, X. Qin, H. Pang, Q. Xu, MXene–2D layered electrode materials for energy storage, Prog. Nat. Sci. Mater. Int. 28 (2018) 133–147.

[138] T. Song, H. Yun, Y. Kim, H.S. Jeon, K. Ha, H. Jung, H. Han, Y. Gogotsi, C.W. Ahn, Y. Lee, Vertically aligned nanopatterns of amine-functionalized Ti3C2 MXene via soft lithography, Adv. Mater. Interfaces 7 (2020) 2000424.

[139] Q. Zhang, R. Fan, W. Cheng, P. Ji, J. Sheng, Q. Liao, H. Lai, X. Fu, C. Zhang, H. Li, Synthesis of large-area MXenes with high yields through power-focused delamination utilizing Vortex kinetic energy, Adv. Sci. 9 (2022) 1–12, https://doi.org/10.1002/advs.202202748.

[140] X.H. Zha, J. Zhou, Y. Zhou, Q. Huang, J. He, J.S. Francisco, K. Luo, S. Du, Promising electron mobility and high thermal conductivity in Sc2CT2 (T = F, OH) MXenes, Nanoscale 8 (2016) 6110–6117, https://doi.org/10.1039/c5nr08639f.

[141] J. Zhang, N. Kong, S. Uzun, A. Levitt, S. Seyedin, P.A. Lynch, S. Qin, M. Han, W. Yang, J. Liu, X. Wang, Y. Gogotsi, J.M. Razal, Scalable manufacturing of free-standing, strong Ti3C2Tx MXene films with outstanding conductivity, Adv. Mater. 32 (2020) 1–9, https://doi.org/10.1002/adma.202001093.

[142] A. Lipatov, H. Lu, M. Alhabeb, B. Anasori, A. Gruverman, Y. Gogotsi, A. Sinitskii, Elastic properties of 2D Ti3C2T x MXene monolayers and bilayers, Sci. Adv. 4 (2018) eaat0491.

[143] A. Iqbal, F. Shahzad, K. Hantanasirisakul, M.K. Kim, J. Kwon, J. Hong, H. Kim, D. Kim, Y. Gogotsi, C.M. Koo, Anomalous absorption of electromagnetic waves by 2D transition metal carbonitride Ti3CNTx (MXene), MXenes From Discov. to Appl. Two-Dimensional Met. Carbides Nitrides 450 (2023) 1013–1027, https://doi.org/10.1201/9781003306511-51.

[144] J. Guo, Y. Zhao, T. Ma, Electrostatic self-assembly of 2D delaminated MXene (Ti3C2) onto Ni foam with superior electrochemical performance for supercapacitor, Electrochim. Acta 305 (2019) 164–174.

[145] J.T. Paul, A.K. Singh, Z. Dong, H. Zhuang, B.C. Revard, B. Rijal, M. Ashton, A. Linscheid, M. Blonsky, D. Gluhovic, Computational methods for 2D materials: discovery, property characterization, and application design, J. Phys. Condens. Matter 29 (2017) 473001.

[146] R. Verma, A. Sharma, V. Dutta, A. Chauhan, D. Pathak, S. Ghotekar, Recent trends in synthesis of 2D MXene-based materials for sustainable environmental applications, Emerg. Mater. 7 (2024) 35–62.

[147] T.L. Tan, H.M. Jin, M.B. Sullivan, B. Anasori, Y. Gogotsi, High-throughput survey of ordering configurations in MXene alloys across compositions and temperatures, ACS Nano 11 (2017) 4407–4418.

[148] Y.-W. Cheng, J.-H. Dai, Y.-M. Zhang, Y. Song, Two-dimensional, ordered, double transition metal carbides (MXenes): a new family of promising catalysts for the hydrogen evolution reaction, J. Phys. Chem. C 122 (2018) 28113–28122.

[149] A. Lipatov, M. Alhabeb, M.R. Lukatskaya, A. Boson, Y. Gogotsi, A. Sinitskii, Effect of synthesis on quality, electronic properties and environmental stability of individual monolayer Ti3C2 MXene flakes, Adv. Electron. Mater. 2 (2016) 1600255.

[150] K. Hantanasirisakul, Y. Gogotsi, Electronic and optical properties of 2D transition metal carbides and nitrides (MXenes), Adv. Mater. 30 (2018) 1804779.

[151] J. Pang, R.G. Mendes, A. Bachmatiuk, L. Zhao, H.Q. Ta, T. Gemming, H. Liu, Z. Liu, M.H. Rummeli, Applications of 2D MXenes in energy conversion and storage systems, Chem. Soc. Rev. 48 (2019) 72–133.

[153] S. Kumar, H.M. Park, T. Singh, M. Kumar, Y. Seo, Long-term stability studies and applications of Ti3C2Tx MXene, Int. J. Energy Res. 2023 (2023), https://doi.org/10.1155/2023/5275439.

[155] L. Zhou, Y. Zhang, Z. Zhuo, A.J. Neukirch, S. Tretiak, Interlayer-decoupled Sc-based MXene with high carrier mobility and strong light-harvesting ability, J. Phys. Chem. Lett. 9 (2018) 6915–6920.

[156] H. Lashgari, M.R. Abolhassani, A. Boochani, S.M. Elahi, J. Khodadadi, Electronic and optical properties of 2D graphene-like compounds titanium carbides and nitrides: DFT calculations, Solid State Commun. 195 (2014) 61–69, https://doi.org/10.1016/j.ssc.2014.06.008.

[157] M. Khazaei, M. Arai, T. Sasaki, A. Ranjbar, Y. Liang, S. Yunoki, OH terminated two-dimensional transition metal carbides and nitrides (MXenes) as ultralow work function materials, Adv. Funct. Mater. 23 (2013) 2185–2192.

[158] Z. Ling, C.E. Ren, M.Q. Zhao, J. Yang, J.M. Giammarco, J. Qiu, M.W. Barsoum, Y. Gogotsi, Flexible and conductive MXene films and nanocomposites with high capacitance, Proc. Natl. Acad. Sci. U. S. A. 111 (2014) 16676–16681, https://doi.org/10.1073/pnas.1414215111.

[159] F. Shahzad, M. Alhabeb, C.B. Hatter, B. Anasori, S.M. Hong, C.M. Koo, Y. Gogotsi, Electromagnetic interference shielding with 2D transition metal carbides, MXenes from Discov. To Appl, Two-Dimensional Met. Carbides Nitrides 353 (2023) 933–947, https://doi.org/10.1201/9781003306511-47.

[160] L.-X. Liu, W. Chen, H.-B. Zhang, L. Ye, Z. Wang, Y. Zhang, P. Min, Z.-Z. Yu, Super-Tough and Environmentally Stable Aramid. Nanofiber@MXene coaxial fibers

with outstanding electromagnetic interference shielding efficiency, Nano-Micro Lett. 14 (2022) 111, https://doi.org/10.1007/s40820-022-00853-1.

[161] A.N. Enyashin, A.L. Ivanovskii, Two-dimensional titanium carbonitrides and their hydroxylated derivatives: structural, electronic properties and stability of MXenes Ti3C2− xNx (OH) 2 from DFTB calculations, J. Solid State Chem. 207 (2013) 42–48.

[162] M.T. Hossaın, M.R. Repon, M.A. Shahid, A. Ali, T. Islam, Progress, prospects and challenges of MXene integrated optoelectronics devices, ChemElectroChem 202400008 (2024), https://doi.org/10.1002/celc.202400008.

[163] Y. Liu, H. Xiao, W.A. Goddard, Schottky-barrier-free contacts with Two-dimensional semiconductors by surface-engineered MXenes, J. Am. Chem. Soc. 138 (2016) 15853–15856, https://doi.org/10.1021/jacs.6b10834.

[164] X. Zhan, C. Si, J. Zhou, Z. Sun, MXene and MXene-based composites: synthesis, properties and environment-related applications, Nanoscale Horizons 5 (2020) 235–258, https://doi.org/10.1039/c9nh00571d.

[165] T.E. Song, H. Yun, Y.J. Kim, H.S. Jeon, K. Ha, H.T. Jung, H. Han, Y. Gogotsi, C. W. Ahn, Y. Lee, Vertically aligned Nanopatterns of amine-functionalized Ti3C2 MXene via soft lithography, Adv. Mater. Interfaces 7 (2020), https://doi.org/10.1002/admi.202000424.

[166] W. Tian, A. VahidMohammadi, M.S. Reid, Z. Wang, L. Ouyang, J. Erlandsson, T. Pettersson, L. Wågberg, M. Beidaghi, M.M. Hamedi, Multifunctional nanocomposites with high strength and capacitance using 2D MXene and 1D Nanocellulose, Adv. Mater. 31 (2019), https://doi.org/10.1002/adma.201902977.

[167] G. Commentary, De fi nitions for hydrophilicity, Hydrophobicity, and Superhydrophobicity: Getting the Basics Right (2014) 686–688.

[168] W.X. Huang, Z.P. Li, D.D. Li, Z.H. Hu, C. Wu, K. Le Lv, Q. Li, Ti3C2 MXene: recent progress in its fundamentals, synthesis, and applications, Rare Metals (2022), https://doi.org/10.1007/s12598-022-02058-2.

[169] M. Seredych, C.E. Shuck, D. Pinto, M. Alhabeb, E. Precetti, G. Deysher, B. Anasori, N. Kurra, Y. Gogotsi, High-temperature behavior and surface chemistry of carbide MXenes studied by thermal analysis, Chem. Mater. 31 (2019) 3324–3332, https://doi.org/10.1021/acs.chemmater.9b00397.

[170] Q. Wang, H. Zhang, J. Liu, S. Zhao, X. Xie, L. Liu, R. Yang, N. Koratkar, Z. Yu, Multifunctional and water-resistant MXene-decorated polyester textiles with outstanding electromagnetic interference shielding and joule heating performances, Adv. Funct. Mater. 29 (2019) 1806819.

[171] J. Liu, H. Zhang, R. Sun, Y. Liu, Z. Liu, A. Zhou, Z. Yu, Hydrophobic, flexible, and lightweight MXene foams for high-performance electromagnetic-interference shielding, Adv. Mater. 29 (2017) 1702367.

[172] D. Wang, D. Zhang, P. Li, Z. Yang, Q. Mi, L. Yu, Electrospinning of flexible poly (vinyl alcohol)/MXene nanofiber-based humidity sensor self-powered by monolayer molybdenum Diselenide piezoelectric Nanogenerator, Nano-Micro Lett. 13 (2021) 1–13, https://doi.org/10.1007/s40820-020-00580-5.

[173] Q. Peng, J. Guo, Q. Zhang, J. Xiang, B. Liu, A. Zhou, R. Liu, Y. Tian, Unique lead adsorption behavior of activated hydroxyl group in two-dimensional titanium carbide, J. Am. Chem. Soc. 136 (2014) 4113–4116, https://doi.org/10.1021/ja500506k.

[174] S. Tian, K. Zhou, C.-Q. Huang, C. Qian, Z. Gao, Y. Liu, Investigation and understanding of the mechanical properties of MXene by high-throughput computations and interpretable machine learning, Extrem. Mech. Lett. 57 (2022) 101921.

[175] M.A.A.M. Abdah, H.T.A. Awan, M. Mehar, M.N. Mustafa, R. Walvekar, M. W. Alam, M. Khalid, R. Umapathi, V. Chaudhary, Advancements in MXene-polymer composites for high-performance supercapacitor applications, J. Energy Storage 63 (2023) 106942.

[176] A.M. Aravind, M. Tomy, A. Kuttapan, A.M. Kakkassery Aippunny, X.T. Suryabai, Progress of 2D MXene as an electrode architecture for advanced supercapacitors: a comprehensive review, ACS, Omega 8 (2023) 44375–44394, https://doi.org/10.1021/acsomega.3c02002.

[177] J. Zhang, N. Kong, S. Uzun, A. Levitt, S. Seyedin, P.A. Lynch, S. Qin, M. Han, W. Yang, J. Liu, Scalable manufacturing of free-standing, strong Ti3C2Tx MXene films with outstanding conductivity, Adv. Mater. 32 (2020) 2001093.

[178] K.L. Firestein, J.E. von Treifeldt, D.G. Kvashnin, J.F.S. Fernando, C. Zhang, A. G. Kvashnin, E.V. Podryabinkin, A.V. Shapeev, D.P. Siriwardena, P.B. Sorokin, Young's modulus and tensile strength of Ti3C2 MXene nanosheets as revealed by in situ TEM probing, AFM nanomechanical mapping, and theoretical calculations, Nano Lett. 20 (2020) 5900–5908.

[179] Y. Xue, J. Feng, S. Huo, P. Song, B. Yu, L. Liu, H. Wang, Polyphosphoramide-intercalated MXene for simultaneously enhancing thermal stability, flame retardancy and mechanical properties of polylactide, Chem. Eng. J. 397 (2020) 125336.

[180] C. Rong, T. Su, Z. Li, T. Chu, M. Zhu, Y. Yan, B. Zhang, F.Z. Xuan, Elastic properties and tensile strength of 2D Ti3C2Tx MXene monolayers, Nat. Commun. 15 (2024), https://doi.org/10.1038/s41467-024-45657-6.

[181] A. Lipatov, M. Alhabeb, H. Lu, S. Zhao, M.J. Loes, N.S. Vorobeva, Y. Dall'Agnese, Y. Gao, A. Gruverman, Y. Gogotsi, A. Sinitskii, Electrical and elastic properties of individual single-layer Nb4C3Tx MXene flakes, Adv. Electron. Mater. 6 (2020) 1–10, https://doi.org/10.1002/aelm.201901382.

[182] C. Lee, X. Wei, J.W. Kysar, J. Hone, Measurement of the elastic properties and intrinsic strength of monolayer graphene, Science (80-.). 321 (2008) 385–388, https://doi.org/10.1126/science.1157996.

[183] S. Bertolazzi, J. Brivio, A. Kis, Stretching and breaking of ultrathin MoS2, ACS Nano 5 (2011) 9703.

[184] A. Falin, Q. Cai, E.J.G. Santos, D. Scullion, D. Qian, R. Zhang, Z. Yang, S. Huang, K. Watanabe, T. Taniguchi, M.R. Barnett, Y. Chen, R.S. Ruoff, L.H. Li, Mechanical

properties of atomically thin boron nitride and the role of interlayer interactions, Nat. Commun. 8 (2017) 1–9, https://doi.org/10.1038/ncomms15815.

[185] A. Falin, M. Holwill, H. Lv, W. Gan, J. Cheng, R. Zhang, D. Qian, M.R. Barnett, E.J. G. Santos, K.S. Novoselov, T. Tao, X. Wu, L.H. Li, Mechanical properties of atomically thin tungsten Dichalcogenides: WS2, WSe2, and WTe2, ACS Nano 15 (2021) 2600–2610, https://doi.org/10.1021/acsnano.0c07430.

[186] H. Wang, E.J. Sandoz-Rosado, S.H. Tsang, J. Lin, M. Zhu, G. Mallick, Z. Liu, E.H. T. Teo, Elastic properties of 2D ultrathin tungsten nitride crystals grown by chemical vapor deposition, Adv. Funct. Mater. 29 (2019) 1–7, https://doi.org/10.1002/adfm.201902663.

[187] A. Mikhaylov, N. Moiseev, K. Aleshin, T. Burkhardt, Global climate change and greenhouse effect, Entrep. Sustain. Issues 7 (2020) 2897.

[188] M.F. Bashir, M. Shahbaz, B. Ma, K. Alam, Evaluating the roles of energy innovation, fossil fuel costs and environmental compliance towards energy transition in advanced industrial economies, J. Environ. Manage. 351 (2024) 119709.

[189] G.O. Atedhor, Greenhouse gases emissions and their reduction strategies: perspectives of Africa's largest economy, Sci. African 20 (2023) e01705.

[190] G. Nalcaci, N. Yarar, G.W. Weber, Potential sources of renewable energy in smart grids: opportunities and challenges, Adv. Renew. Energy Green Hydrog. (2024) 1–26.

[191] M.Z. Al Mahmud, Investigating Eco-Friendly Materials as Energy Storage Solutions, Available SSRN 4743342 (n.d.).

[192] A.A. Nkembi, M. Simonazzi, D. Santoro, P. Cova, N. Delmonte, Comprehensive review of energy storage systems characteristics and models for automotive applications, Batteries 10 (2024) 88.

[193] O. Gohar, M.Z. Khan, I. Bibi, N. Bashir, U. Tariq, M. Bakhtiar, M.R.A. Karim, F. Ali, M.B. Hanif, M. Motola, Nanomaterials for advanced energy applications: recent advancements and future trends, Mater. Des. 241 (2024) 112930.

[194] A. Agarwala, T. Tahsin, M.F. Ali, S.K. Sarker, S.H. Abhi, S.K. Das, P. Das, M. M. Hasan, Z. Tasneem, M.M. Islam, Towards next generation power grid transformer for renewables: technology review, Eng. Reports 6 (2024) e12848.

[195] X. Tang, X. Guo, W. Wu, G. Wang, 2D metal carbides and nitrides (MXenes) as high-performance electrode materials for Lithium-based batteries, Adv. Energy Mater. 8 (2018) 1801897.

[196] Y. Zhou, L. Yin, S. Xiang, S. Yu, H.M. Johnson, S. Wang, J. Yin, J. Zhao, Y. Luo, P. K. Chu, Unleashing the potential of MXene-based flexible materials for high-performance energy storage devices, Adv. Sci. 11 (2024) 2304874.

[197] D. Ponnalagar, D.-R. Hang, C.-T. Liang, M.M.C. Chou, Recent advances and future prospects of low-dimensional Mo2C MXene-based electrode for flexible electrochemical energy storage devices, Prog. Mater. Sci. 101308 (2024).

[198] J. Nan, X. Guo, J. Xiao, X. Li, W. Chen, W. Wu, H. Liu, Y. Wang, M. Wu, G. Wang, Nanoengineering of 2D MXene-based materials for energy storage applications, Small 17 (2021), https://doi.org/10.1002/smll.201902085.

[199] I. Hussain, S. Sahoo, T. Hussain, M. Ahmad, M.S. Javed, C. Lamiel, S. Gu, T. Kaewmaraya, M.S. Sayed, K. Zhang, Theoretical and experimental investigation of In situ grown MOF-derived oriented Zr-Mn-oxide and solution-free CuO as hybrid electrode for supercapacitors, Adv. Funct. Mater. 33 (2023) 2210002.

[200] I. Hussain, M.Z. Ansari, M. Ahmad, A. Ali, T. Nawaz, T. Hussain, C. Lamiel, M. Sufyan Javed, X. Chen, M. Sajjad, Understanding the diffusion-dominated properties of MOF-derived Ni–co–se/C on CuO scaffold electrode using experimental and first principle study, Adv. Funct. Mater. 33 (2023) 2302888.

[201] S.B. Devi, S. Sekar, S. Sathish, S. Dhanasekaran, R. Nirmala, D.Y. Kim, Y. Lee, S. Lee, R. Navamathavan, Recent advancements in MXene with Two-dimensional transition metal chalcogenides/oxides nanocomposites for supercapacitor application-a topical review, J. Alloys Compd. 173481 (2024).

[202] K. Sharma, A. Arora, S.K. Tripathi, Review of supercapacitors: materials and devices, J. Energy Storage 21 (2019) 801–825.

[203] I. Hussain, C. Lamiel, M.S. Javed, M. Ahmad, S. Sahoo, X. Chen, N. Qin, S. Iqbal, S. Gu, Y. Li, MXene-based heterostructures: current trend and development in electrochemical energy storage devices, Prog. Energy Combust. Sci. 97 (2023) 101097.

[204] X. Jiang, J. Jia, Y. Zhu, J. Li, H. Jia, C. Liu, G. Zhao, L. Yu, G. Zhu, Beyond conventional limits: advancements and insights in broadening operating temperature ranges of supercapacitors, Energy Storage Mater. 103462 (2024).

[205] J. Yang, W. Bao, P. Jaumaux, S. Zhang, C. Wang, G. Wang, MXene-based composites: synthesis and applications in rechargeable batteries and supercapacitors, Adv. Mater. Interfaces 6 (2019) 1802004.

[206] I. Hussain, U. Amara, F. Bibi, A. Hanan, M.N. Lakhan, I.A. Soomro, A. Khan, I. Shaheen, U. Sajjad, G. Mohana Rani, M.S. Javed, K. Khan, M.B. Hanif, M. A. Assiri, S. Sahoo, W. Al Zoubi, D. Mohapatra, K. Zhang, Mo-based MXenes: synthesis, properties, and applications, Adv. Colloid Interface Sci. 324 (2024) 103077, https://doi.org/10.1016/j.cis.2023.103077.

[207] Q. Zhu, J. Li, P. Simon, B. Xu, Two-dimensional MXenes for electrochemical capacitor applications: Progress, challenges and perspectives, Energy Storage Mater. 35 (2021) 630–660, https://doi.org/10.1016/j.ensm.2020.11.035.

[208] Y. Yu, Q. Fan, Z. Li, P. Fu, MXene-based electrode materials for supercapacitors: synthesis, properties, and optimization strategies, Mater. Today Sustain. 24 (2023), https://doi.org/10.1016/j.mtsust.2023.100551.

[209] L. Sun, Q. Fu, C. Pan, Hierarchical porous "skin/skeleton"-like MXene/biomass derived carbon fibers heterostructure for self-supporting, flexible all solid-state supercapacitors, J. Hazard. Mater. 410 (2021) 124565, https://doi.org/10.1016/j.jhazmat.2020.124565.

[210] L. Yu, L. Hu, B. Anasori, Y.T. Liu, Q. Zhu, P. Zhang, Y. Gogotsi, B. Xu, MXene-bonded activated carbon as a flexible electrode for high-performance

supercapacitors, ACS Energy Lett. 3 (2018) 1597–1603, https://doi.org/10.1021/acsenergylett.8b00718.

[211] Y. Li, C. Pan, P. Kamdem, X.-J. Jin, Binder-free Two-dimensional MXene/acid activated carbon for high-performance supercapacitors and methylene blue adsorption, Energy Fuel 34 (2020) 10120–10130, https://doi.org/10.1021/acs.energyfuels.0c01352.

[212] A. Sangili, B. Unnikrishnan, A. Nain, Y.-J. Hsu, R.-S. Wu, C.-C. Huang, H.-T. Chang, Stable carbon encapsulated titanium carbide MXene aqueous ink for fabricating high-performance supercapacitors, Energy Storage Mater. 53 (2022) 51–61, https://doi.org/10.1016/j.ensm.2022.08.038.

[213] J. Zhang, D. Jiang, L. Liao, L. Cui, R. Zheng, J. Liu, Ti3C2Tx MXene based hybrid electrodes for wearable supercapacitors with varied deformation capabilities, Chem. Eng. J. 429 (2022) 132232, https://doi.org/10.1016/j.cej.2021.132232.

[214] M.-Q. Zhao, C.E. Ren, Z. Ling, M.R. Lukatskaya, C. Zhang, K.L. Van Aken, M. W. Barsoum, Y. Gogotsi, Flexible MXene/carbon nanotube composite paper with high volumetric capacitance, Adv. Mater. 27 (2014).

[215] Q. Fu, X. Wang, N. Zhang, J. Wen, L. Li, H. Gao, X. Zhang, Self-assembled Ti3C2Tx/SCNT composite electrode with improved electrochemical performance for supercapacitor, J. Colloid Interface Sci. 511 (2018) 128–134.

[216] J. Yan, C.E. Ren, K. Maleski, C.B. Hatter, B. Anasori, P. Urbankowski, A. Sarycheva, Y. Gogotsi, Flexible MXene/graphene films for ultrafast supercapacitors with outstanding volumetric capacitance, Adv. Funct. Mater. 27 (2017) 1–10, https://doi.org/10.1002/adfm.201701264.

[217] S. Kumar, P. Rugvedi, K. Mani, A. Gupta, Evaluation of anti-inflammatory and immunomodulatory activity of Chyawanprash on particulate matter-induced pulmonary disease in mice, J. Ayurveda Integr. Med. 12 (2021) 649–656, https://doi.org/10.1016/j.jaim.2021.06.022.

[218] S. Yuan, X. Duan, J. Liu, Y. Ye, F. Lv, T. Liu, Q. Wang, X. Zhang, Recent progress on transition metal oxides as advanced materials for energy conversion and storage, Energy Storage Mater. 42 (2021) 317–369.

[219] Z. Otgonbayar, S. Yang, I.-J. Kim, W.-C. Oh, Recent advances in Two-dimensional MXene for supercapacitor applications: Progress, Challenges, and Perspectives, Nanomaterials 13 (2023) 919.

[220] J. Zhu, Y. Tang, C. Yang, F. Wang, M. Cao, Composites of TiO 2 nanoparticles deposited on Ti 3 C 2 MXene Nanosheets with enhanced electrochemical performance, J. Electrochem. Soc. 163 (2016) A785–A791, https://doi.org/10.1149/2.0981605jes.

[221] V.A. Online, M. Cao, Y. Qin, J. Zhu, L. Wang, T. Yi, RSC Adv. (2016), https://doi.org/10.1039/C6RA15384D.

[222] H. Zhou, Y. Lu, F. Wu, L. Fang, H.J. Luo, Y.X. Zhang, M. Zhou, MnO2 nanorods/MXene/CC composite electrode for flexible supercapacitors with enhanced electrochemical performance, J. Alloys Compd. 802 (2019) 259–268, https://doi.org/10.1016/j.jallcom.2019.06.173.

[223] S. Liu, T. Zeng, Y. Zhang, Q. Wan, N. Yang, Coupling W18O49/Ti3C2Tx MXene Pseudocapacitive electrodes with redox electrolytes to construct high-performance asymmetric supercapacitors, Small 18 (2022) 2204829.

[224] R.A. Chavan, G.P. Kamble, S.B. Dhavale, A.S. Rasal, S.S. Kolekar, J.-Y. Chang, A. V. Ghule, NiO@MXene nanocomposite as an anode with enhanced energy density for asymmetric supercapacitors, Energy Fuel 37 (2023) 4658–4670, https://doi.org/10.1021/acs.energyfuels.2c04206.

[225] H. Mustafa, A. Rasheed, S. Ajmal, N. Sarwar, U. Falak, S.G. Lee, A. Sattar, Investigation of electrical and electrochemical properties of ascorbic acid-treated SnO2/MXene Heterostructures for hybrid supercapacitors, Energy Fuel 37 (2023) 2410–2419, https://doi.org/10.1021/acs.energyfuels.2c03878.

[226] M.G. Tadesse, A.S. Ahmmed, J.F. Lübben, Review on conductive polymer composites for supercapacitor applications, J. Compos. Sci. 8 (2024) 53.

[227] W. Wei, M. Zhang, J. Ren, K. Wang, Two-Dimensional Nanosheet Stacking Structure Films for Li/Na/K-Ion Batteries and Supercapacitors, ACS Appl, Nano Mater, 2024.

[228] A. VahidMohammadi, J. Moncada, H. Chen, E. Kayali, J. Orangi, C.A. Carrero, M. Beidaghi, Thick and freestanding MXene/PANI pseudocapacitive electrodes with ultrahigh specific capacitance, J. Mater. Chem. A 6 (2018) 22123–22133.

[229] W. Wu, D. Wei, J. Zhu, D. Niu, F. Wang, L. Wang, L. Yang, P. Yang, C. Wang, Enhanced electrochemical performances of organ-like Ti3C2 MXenes/polypyrrole composites as supercapacitors electrode materials, Ceram. Int. 45 (2019) 7328–7337.

[230] H. Wang, L. Li, C. Zhu, S. Lin, J. Wen, Q. Jin, X. Zhang, In situ polymerized Ti3C2Tx/PDA electrode with superior areal capacitance for supercapacitors, J. Alloys Compd. 778 (2019) 858–865.

[231] M. Boota, M. Pasini, F. Galeotti, W. Porzio, M.-Q. Zhao, J. Halim, Y. Gogotsi, Interaction of polar and nonpolar polyfluorenes with layers of two-dimensional titanium carbide (MXene): intercalation and pseudocapacitance, Chem. Mater. 29 (2017) 2731–2738.

[232] M.S. Iyer, P. Rajkumar, B. Sanghavi, G. Parvathy, K. Aravinth, J. Kim, Elevating energy storage performance of bismuth antimonate coupled with MXene and graphitic nanofibers in advanced supercapacitors, J. Power Sources 602 (2024) 234379.

[233] Y. Cai, X. Chen, Y. Xu, Y. Zhang, H. Liu, H. Zhang, J. Tang, Ti3C2Tx MXene/carbon composites for advanced supercapacitors: synthesis, progress, and perspectives, Carbon Energy 6 (2024) e501.

[234] M.S. Javed, A. Mateen, I. Hussain, A. Ahmad, M. Mubashir, S. Khan, M.A. Assiri, S.M. Eldin, S.S.A. Shah, W. Han, Recent progress in the design of advanced MXene/metal oxides-hybrid materials for energy storage devices, Energy Storage Mater. 53 (2022) 827–872.

[235] W. Bai, C. Li, F. Pan, Y. Luo, T. Gao, D. Yu, X. Wang, H. Sun, S. Wang, High stability supercapacitors based on MXene/spherical g-PPy composite electrodes, Electrochim. Acta 144300 (2024).

[236] Y. Cai, X. Chen, Y. Xu, Y. Zhang, H. Liu, H. Zhang, J. Tang, Ti3C2Tx MXene/carbon composites for advanced supercapacitors: synthesis, progress, and perspectives, Carbon Energy 6 (2024) e501.

[237] T. Xu, Y. Wang, K. Liu, Q. Zhao, Q. Liang, M. Zhang, C. Si, Ultralight MXene/carbon nanotube composite aerogel for high-performance flexible supercapacitor, Adv. Compos. Hybrid Mater. 6 (2023) 1–9.

[238] A. Qian, Y. Pang, G. Wang, Y. Hao, Y. Liu, H. Shi, C.-H. Chung, Z. Du, F. Cheng, Pseudocapacitive charge storage in MXene–V2O5 for asymmetric flexible energy storage devices, ACS Appl. Mater. Interfaces 12 (2020) 54791–54797.

[239] S.M. Varghese, V.V. Mohan, S. Suresh, E.B. Gowd, R.B. Rakhi, Synergistically modified Ti3C2Tx MXene conducting polymer nanocomposites as efficient electrode materials for supercapacitors, J. Alloys Compd. 973 (2024) 172923.

[240] A.C. Ezika, E.R. Sadiku, C.I. Idumah, S.S. Ray, G.J. Adekoya, R.S. Odera, Recently emerging trends in MXene hybrid conductive polymer energy storage nanoarchitectures, Polym. Technol. Mater. 61 (2022) 861–887.

[241] M. Cao, F. Wang, L. Wang, W. Wu, W. Lv, J. Zhu, Room temperature oxidation of Ti 3 C 2 MXene for supercapacitor electrodes, J. Electrochem. Soc. 164 (2017) A3933–A3942, https://doi.org/10.1149/2.1541714jes.

[242] Y. Wen, T.E. Rufford, X. Chen, N. Li, M. Lyu, L. Dai, L. Wang, Nitrogen-doped Ti3C2Tx MXene electrodes for high-performance supercapacitors, Nano Energy 38 (2017) 368–376, https://doi.org/10.1016/j.nanoen.2017.06.009.

[243] Y. Deng, T. Shang, Z. Wu, Y. Tao, C. Luo, J. Liang, D. Han, R. Lyu, C. Qi, W. Lv, Fast gelation of Ti3C2Tx MXene initiated by metal ions, Adv. Mater. 31 (2019) 1902432.

[244] X. Wang, D. Zhang, H. Zhang, L. Gong, Y. Yang, W. Zhao, S. Yu, Y. Yin, D. Sun, In situ polymerized polyaniline/MXene (V2C) as building blocks of supercapacitor and ammonia sensor self-powered by electromagnetic-triboelectric hybrid generator, Nano Energy 88 (2021) 106242, https://doi.org/10.1016/j.nanoen.2021.106242.

[245] L. Shen, X. Zhou, X. Zhang, Y. Zhang, Y. Liu, W. Wang, W. Si, X. Dong, Carbon-intercalated Ti 3 C 2 T x MXene for high-performance electrochemical energy storage, J. Mater. Chem. A 6 (2018) 23513–23520.

[246] J. Yan, C.E. Ren, K. Maleski, C.B. Hatter, B. Anasori, P. Urbankowski, A. Sarycheva, Y. Gogotsi, Flexible MXene/graphene films for ultrafast supercapacitors with outstanding volumetric capacitance, Adv. Funct. Mater. 27 (2017) 1701264.

[247] L. Yu, L. Hu, B. Anasori, Y.-T. Liu, Q. Zhu, P. Zhang, Y. Gogotsi, B. Xu, MXene-bonded activated carbon as a flexible electrode for high-performance supercapacitors, ACS Energy Lett. 3 (2018) 1597–1603.

[248] Z. Tan, W. Wang, M. Zhu, Y. Liu, Y. Yang, X. Ji, Z. He, Ti3C2Tx MXene@ carbon dots hybrid microflowers as a binder-free electrode material toward high capacity capacitive deionization, Desalination 548 (2023) 116267.

[249] L. Li, F. Wang, J. Zhu, W. Wu, The facile synthesis of layered Ti 2 C MXene/carbon nanotube composite paper with enhanced electrochemical properties, Dalt. Trans. 46 (2017) 14880–14887.

[250] Q. Liu, J. Yang, X. Luo, Y. Miao, Y. Zhang, W. Xu, L. Yang, Y. Liang, W. Weng, M. Zhu, Fabrication of a fibrous MnO2@MXene/CNT electrode for high-performance flexible supercapacitor, Ceram. Int. 46 (2020) 11874–11881, https://doi.org/10.1016/j.ceramint.2020.01.222.

[251] Y. Wei, W. Luo, Z. Zhuang, B. Dai, J. Ding, T. Li, M. Ma, X. Yin, Y. Ma, Fabrication of ternary MXene/MnO2/polyaniline nanostructure with good electrochemical performances, Adv. Compos. Hybrid Mater. 4 (2021) 1082–1091, https://doi.org/10.1007/s42114-021-00323-z.

[252] Y. Ma, H. Sheng, W. Dou, Q. Su, J. Zhou, E. Xie, W. Lan, Fe2O3 nanoparticles anchored on the Ti3C2T x MXene paper for flexible supercapacitors with ultrahigh volumetric capacitance, ACS Appl. Mater. Interfaces 12 (2020) 41410–41418.

[253] W. Luo, Y. Sun, Z. Lin, X. Li, Y. Han, J. Ding, T. Li, C. Hou, Y. Ma, Flexible Ti3C2Tx MXene/V2O5 composite films for high-performance all-solid supercapacitors, J. Energy Storage 62 (2023) 106807.

[254] Y. Wang, X. Wang, X. Li, R. Liu, Y. Bai, H. Xiao, Y. Liu, G. Yuan, Intercalating ultrathin MoO3 Nanobelts into MXene film with ultrahigh volumetric capacitance and excellent deformation for high-energy-density devices, Nano-Micro Lett. 12 (2020) 1–14, https://doi.org/10.1007/s40820-020-00450-0.

[255] H. Jiang, Z. Wang, Q. Yang, M. Hanif, Z. Wang, L. Dong, M. Dong, A novel MnO2/Ti3C2Tx MXene nanocomposite as high performance electrode materials for flexible supercapacitors, Electrochim. Acta 290 (2018) 695–703, https://doi.org/10.1016/j.electacta.2018.08.096.

[256] H. Tang, R. Chen, Q. Huang, W. Ge, X. Zhang, Y. Yang, X. Wang, Scalable manufacturing of leaf-like MXene/ag NWs/cellulose composite paper electrode for all-solid-state supercapacitor, EcoMat 4 (2022) e12247.

[258] S.B. Ambade, R.B. Ambade, W. Eom, S.H. Noh, S.H. Kim, T.H. Han, 2D Ti3C2 MXene/WO3 hybrid architectures for high-rate supercapacitors, Adv. Mater. Interfaces 5 (2018) 1801361.

[260] Z. Zheng, W. Wu, T. Yang, E. Wang, Z. Du, X. Hou, T. Liang, H. Wang, In situ reduced MXene/AuNPs composite toward enhanced charging/discharging and specific capacitance, J. Adv. Ceram. 10 (2021) 1061–1071, https://doi.org/10.1007/s40145-021-0491-0.

[261] H. Zhou, Y. Lu, F. Wu, L. Fang, H. Luo, Y. Zhang, M. Zhou, MnO2 nanorods/MXene/CC composite electrode for flexible supercapacitors with enhanced electrochemical performance, J. Alloys Compd. 802 (2019) 259–268.

[262] C. Li, S. Wang, Y. Cui, X. Wang, Z. Yong, D. Liang, Y. Chi, Z. Wang, Sandwich-like high-load MXene/polyaniline film electrodes with ultrahigh volumetric

capacitance for flexible supercapacitors, J. Colloid Interface Sci. 620 (2022) 35–46.

[263] W. Wu, C. Wang, C. Zhao, D. Wei, J. Zhu, Y. Xu, Facile strategy of hollow polyaniline nanotubes supported on Ti3C2-MXene nanosheets for high-performance symmetric supercapacitors, J. Colloid Interface Sci. 580 (2020) 601–613.

[264] Y. Li, P. Kamdem, X.-J. Jin, Hierarchical architecture of MXene/PANI hybrid electrode for advanced asymmetric supercapacitors, J. Alloys Compd. 850 (2021) 156608.

[265] L. Tong, C. Jiang, K. Cai, P. Wei, High-performance and freestanding PPy/ Ti3C2Tx composite film for flexible all-solid-state supercapacitors, J. Power Sources 465 (2020) 228267, https://doi.org/10.1016/j.jpowsour.2020.228267.

[266] X. Lu, J. Zhu, W. Wu, B. Zhang, Hierarchical architecture of PANI@ TiO2/ Ti3C2Tx ternary composite electrode for enhanced electrochemical performance, Electrochim. Acta 228 (2017) 282–289.

[267] S. Ali, A. Ahmad, I. Hussain, S.S.A. Shah, M. Sufyan Javed, S. Ali, A. Ali, M. S. Javed, Experimental and theoretical aspects of MXenes-based energy storage and energy conversion devices, J. Chem. Environ. 2 (2023) 54–81, https://doi. org/10.56946/jce.v2i2.214.

[268] C. Wei, B. Xi, P. Wang, Z. Wang, X. An, K. Tian, J. Feng, S. Xiong, In situ growth engineering on 2D MXenes for next-generation rechargeable batteries, Adv. Energy Sustain. Res. 4 (2023), https://doi.org/10.1002/aesr.202300103.

[269] L. Chen, Y. Sun, X. Wei, L. Song, G. Tao, X. Cao, D. Wang, G. Zhou, Y. Song, Dual-functional V2C MXene assembly in facilitating sulfur evolution kinetics and Li-ion sieving toward practical lithium–sulfur batteries, Adv. Mater. 35 (2023) 2300771.

[270] Y. Song, Z. Sun, Z. Fan, W. Cai, Y. Shao, G. Sheng, M. Wang, L. Song, Z. Liu, Q. Zhang, Rational design of porous nitrogen-doped Ti3C2 MXene as a multifunctional electrocatalyst for Li–S chemistry, Nano Energy 70 (2020) 104555.

[271] J. Ma, Y. Li, N.S. Grundish, J.B. Goodenough, Y. Chen, L. Guo, Z. Peng, X. Qi, F. Yang, L. Qie, C.A. Wang, B. Huang, Z. Huang, L. Chen, D. Su, G. Wang, X. Peng, Z. Chen, J. Yang, S. He, X. Zhang, H. Yu, C. Fu, M. Jiang, W. Deng, C.F. Sun, Q. Pan, Y. Tang, X. Li, X. Ji, F. Wan, Z. Niu, F. Lian, C. Wang, G.G. Wallace, M. Fan, Q. Meng, S. Xin, Y.G. Guo, L.J. Wan, The 2021 battery technology roadmap, J. Phys. D Appl. Phys. 54 (2021), https://doi.org/10.1088/1361-6463/ abd353.

[272] Y. Xie, M. Naguib, V.N. Mochalin, M.W. Barsoum, Y. Gogotsi, X. Yu, K.-W. Nam, X.-Q. Yang, A.I. Kolesnikov, P.R.C. Kent, Role of surface structure on Li-ion energy storage capacity of two-dimensional transition-metal carbides, J. Am. Chem. Soc. 136 (2014) 6385–6394.

[273] Q. Tang, Z. Zhou, P. Shen, Are MXenes promising anode materials for Li ion batteries? Computational studies on electronic properties and Li storage capability of Ti3C2 and Ti3C2X2 (X= F, OH) monolayer, J. Am. Chem. Soc. 134 (2012) 16909–16916.

[274] B. Ahmed, D.H. Anjum, M.N. Hedhili, Y. Gogotsi, H.N. Alshareef, H 2 O 2 assisted room temperature oxidation of Ti 2 C MXene for Li-ion battery anodes, Nanoscale 8 (2016) 7580–7587.

[275] J. Zhou, X. Zha, X. Zhou, F. Chen, G. Gao, S. Wang, C. Shen, T. Chen, C. Zhi, P. Eklund, Synthesis and electrochemical properties of two-dimensional hafnium carbide, ACS Nano 11 (2017) 3841–3850.

[276] L. Huang, T. Li, Q. Liu, J. Gu, Fluorine-free Ti3C2Tx as anode materials for Li-ion batteries, Electrochem. Commun. 104 (2019) 106472, https://doi.org/10.1016/j. elecom.2019.05.021.

[277] A. Byeon, M.-Q. Zhao, C.E. Ren, J. Halim, S. Kota, P. Urbankowski, B. Anasori, M. W. Barsoum, Y. Gogotsi, Two-dimensional titanium carbide MXene as a cathode material for hybrid magnesium/lithium-ion batteries, ACS Appl. Mater. Interfaces 9 (2017) 4296–4300.

[278] O. Mashtalir, M.R. Lukatskaya, M. Zhao, M.W. Barsoum, Y. Gogotsi, Amine-assisted delamination of Nb2C MXene for Li-ion energy storage devices, Adv. Mater. 27 (2015) 3501–3506.

[279] J. Luo, W. Zhang, H. Yuan, C. Jin, L. Zhang, H. Huang, C. Liang, Y. Xia, J. Zhang, Y. Gan, X. Tao, Pillared structure design of MXene with Ultralarge interlayer spacing for high-performance Lithium-ion capacitors, ACS Nano 11 (2017) 2459–2469, https://doi.org/10.1021/acsnano.6b07668.

[280] S. Kim, D. Seo, X. Ma, G. Ceder, K. Kang, Electrode materials for rechargeable sodium-ion batteries: potential alternatives to current lithium-ion batteries, Adv. Energy Mater. 2 (2012) 710–721.

[281] Y. Wen, K. He, Y. Zhu, F. Han, Y. Xu, I. Matsuda, Y. Ishii, J. Cumings, C. Wang, Expanded graphite as superior anode for sodium-ion batteries, Nat. Commun. 5 (2014) 4033.

[282] Synthesisandnano-engineeringofMXene...erspectives_ElsevierEnhancedReader, (n.d.).

[283] F. Wu, Y. Jiang, Z. Ye, Y. Huang, Z. Wang, S. Li, Y. Mei, M. Xie, L. Li, R. Chen, A 3D flower-like VO 2/MXene hybrid architecture with superior anode performance for sodium ion batteries, J. Mater. Chem. A 7 (2019) 1315–1322.

[284] S. Sun, Z. Xie, Y. Yan, S. Wu, Hybrid energy storage mechanisms for sulfur-decorated Ti3C2 MXene anode material for high-rate and long-life sodium-ion batteries, Chem. Eng. J. 366 (2019) 460–467, https://doi.org/10.1016/j. cej.2019.01.185.

[285] C. Zhang, H. Pan, L. Sun, F. Xu, Y. Ouyang, F. Rosei, Progress and perspectives of 2D materials as anodes for potassium-ion batteries, Energy Storage Mater. 38 (2021) 354–378, https://doi.org/10.1016/j.ensm.2021.03.007.

[286] P. Wang, X. Lu, Y. Boyjoo, X. Wei, Y. Zhang, D. Guo, S. Sun, J. Liu, Pillar-free TiO2/Ti3C2 composite with expanded interlayer spacing for high-capacity sodium ion batteries, J. Power Sources 451 (2020) 227756.

[287] P. Lian, Y. Dong, Z.-S. Wu, S. Zheng, X. Wang, S. Wang, C. Sun, J. Qin, X. Shi, X. Bao, Alkalized Ti3C2 MXene nanoribbons with expanded interlayer spacing for high-capacity sodium and potassium ion batteries, Nano Energy 40 (2017) 1–8.

[288] D. Sun, M. Wang, Z. Li, G. Fan, L.Z. Fan, A. Zhou, Two-dimensional Ti3C2 as anode material for Li-ion batteries, Electrochem. Commun. 47 (2014) 80–83, https://doi.org/10.1016/j.elecom.2014.07.026.

[289] M. Naguib, J. Halim, J. Lu, K.M. Cook, L. Hultman, Y. Gogotsi, M.W. Barsoum, New Two-dimensional niobium and vanadium carbides as promising materials for Li-ion batteries, J. Am. Chem. Soc. 135 (2013) 15966.

[290] M.-Q. Zhao, M. Torelli, C.E. Ren, M. Ghidiu, Z. Ling, B. Anasori, M.W. Barsoum, Y. Gogotsi, 2D titanium carbide and transition metal oxides hybrid electrodes for Li-ion storage, Nano Energy 30 (2016) 603–613.

[291] Y. Wang, Y. Li, Z. Qiu, X. Wu, P. Zhou, T. Zhou, J. Zhao, Z. Miao, J. Zhou, S. Zhuo, Fe3O4@Ti3C2 MXene hybrids with ultrahigh volumetric capacity as an anode material for lithium-ion batteries, J. Mater. Chem. A 6 (2018) 11189–11197, https://doi.org/10.1039/c8ta00122g.

[292] C. Shen, L. Wang, A. Zhou, B. Wang, X. Wang, W. Lian, Q. Hu, G. Qin, X. Liu, Synthesis and electrochemical properties of two-dimensional RGO/Ti3 C2 Tx nanocomposites, Nanomaterials 8 (2018) 1–11, https://doi.org/10.3390/ nano8020080.

[293] M. Zheng, R. Guo, Z. Liu, B. Wang, L. Meng, F. Li, T. Li, Y. Luo, MoS2 intercalated p-Ti3C2 anode materials with sandwich-like three dimensional conductive networks for lithium-ion batteries, J. Alloys Compd. 735 (2018) 1262–1270, https://doi.org/10.1016/j.jallcom.2017.11.250.

[294] Y. Zhang, B. Guo, L. Hu, Q. Xu, Y. Li, D. Liu, M. Xu, Synthesis of SnS nanoparticle-modified MXene (Ti3C2Tx) composites for enhanced sodium storage, J. Alloys Compd. 732 (2018) 448–453, https://doi.org/10.1016/j.jallcom.2017.10.223.

[295] Y. Dall'Agnese, P.-L. Taberna, Y. Gogotsi, P. Simon, Two-dimensional vanadium carbide (MXene) as positive electrode for sodium-ion capacitors, J. Phys. Chem. Lett. 6 (2015) 2305–2309.

[296] J. Zhou, X. Zha, X. Zhou, F. Chen, G. Gao, S. Wang, C. Shen, T. Chen, C. Zhi, P. Eklund, S. Du, J. Xue, W. Shi, Z. Chai, Q. Huang, Synthesis and electrochemical properties of Two-dimensional hafnium carbide, ACS Nano 11 (2017) 3841–3850, https://doi.org/10.1021/acsnano.7b00030.

[298] C.-F. Du, Q. Liang, Y. Zheng, Y. Luo, H. Mao, Q. Yan, Porous MXene frameworks support pyrite nanodots toward high-rate pseudocapacitive Li/Na-ion storage, ACS Appl. Mater. Interfaces 10 (2018) 33779–33784.

[299] M. Naguib, R.A. Adams, Y. Zhao, D. Zemlyanov, A. Varma, J. Nanda, V.G. Pol, Electrochemical performance of MXenes as K-ion battery anodes, Chem. Commun. 53 (2017) 6883–6886.

[300] J. Li, B. Rui, W. Wei, P. Nie, L. Chang, Z. Le, M. Liu, H. Wang, L. Wang, X. Zhang, Nanosheets assembled layered MoS2/MXene as high performance anode materials for potassium ion batteries, J. Power Sources 449 (2020) 227481.

[301] H. Huang, J. Cui, G. Liu, R. Bi, L. Zhang, Carbon-coated MoSe2/MXene hybrid nanosheets for superior potassium storage, ACS Nano 13 (2019) 3448–3456.

[302] Y. Dong, Z.-S. Wu, S. Zheng, X. Wang, J. Qin, S. Wang, X. Shi, X. Bao, Ti3C2 MXene-derived sodium/potassium titanate nanoribbons for high-performance sodium/potassium ion batteries with enhanced capacities, ACS Nano 11 (2017) 4792–4800.

[303] R. Jana, S. Ghosh, R. Bhunia, A. Chowdhury, Recent developments in the state-of-the-art optoelectronic synaptic devices premised on 2D materials: a review, J. Mater. Chem. C (2024).

[304] M.S. Javed, X. Zhang, T. Ahmad, M. Usman, S.S.A. Shah, A. Ahmad, I. Hussain, S. Majeed, M.R. Khawar, D. Choi, MXenes to MBenes: Latest Development and Opportunities for Energy Storage Devices, Mater, Today, 2024.

[305] S. Bansal, P. Chaudhary, B.B. Sharma, S. Saini, A. Joshi, Review of MXenes and their composites for energy storage applications, J. Energy Storage 87 (2024) 111420.

[306] L.-H. Yu, X. Tao, S.-R. Feng, J.-T. Liu, L.-L. Zhang, G.-Z. Zhao, G. Zhu, Recent development of three-dimension printed graphene oxide and MXene-based energy storage devices, Tungsten 6 (2024) 196–211.

[307] K.H. Tan, M.A. Zaed, R. Saidur, N. Abdullah, N.A.I.M. Ishak, J. Cherusseri, Strategic Insights for Bulk Production of MXene: A Review, in: E3S Web Conf., EDP Sciences, 2024: p. 1003.

[308] S. Nahirniak, A. Ray, B. Saruhan, Challenges and future prospects of the MXene-based materials for energy storage applications, Batteries 9 (2023), https://doi. org/10.3390/batteries9020126.

[309] H.T. Mathew, A. Kumar, S.S. Vhatkar, R. Oraon, Headway towards contemporary 2D MXene-based hybrid electrodes for alkali-ion batteries, Energy Adv. (2022) 950–979, https://doi.org/10.1039/d2ya00212d.

[310] F. Jamil, H.M. Ali, M.M. Janjua, MXene based advanced materials for thermal energy storage: a recent review, J. Energy Storage 35 (2021) 102322.

[311] S. Nahirniak, A. Ray, B. Saruhan, Challenges and future prospects of the MXene-based materials for energy storage applications, Batteries 9 (2023) 0–22. doi: https://doi.org/10.3390/batteries9020126.

[312] S. Sun, C. Liao, A.M. Hafez, H. Zhu, S. Wu, Two-dimensional MXenes for energy storage, Chem. Eng. J. 338 (2018) 27–45, https://doi.org/10.1016/j. cej.2017.12.155.

[313] C. Lamiel, I. Hussain, J.H. Warner, K. Zhang, Beyond Ti-Based MXenes: A Review of Emerging Non-Ti Based Metal-MXene Structure, Properties, and Applications, Mater, Today, 2023.

[314] P. Ma, D. Fang, Y. Liu, Y. Shang, Y. Shi, H.Y. Yang, MXene-based materials for electrochemical sodium-ion storage, Adv. Sci. 8 (2021) 1–25, https://doi.org/10.1002/advs.202003185.

[315] K. Shahzad, A.I. Mardare, A.W. Hassel, Accelerating materials discovery: combinatorial synthesis, high-throughput characterization, and computational advances, Sci. Technol. Adv. Mater. Methods 4 (2024) 2292486.

[316] N. Thakur, P. Kumar, D.C. Sati, R. Neffati, P. Sharma, Recent advances in two-dimensional MXenes for power and smart energy systems, J. Energy Storage 50 (2022) 104604, https://doi.org/10.1016/j.est.2022.104604.